Opportunity and challenges of Device-to-Device relaying for IoT connectivity in cellular networks

Cesar Augusto Vargas Anamuro

DOCTORAT BRETAGNE LOIRE / MATHSTIC

IMT Atlantique
Bretagne-Pays de la Loire
École Mines-Télécom

THESE DE DOCTORAT DE

L'ÉCOLE NATIONALE SUPERIEURE MINES-TELECOM ATLANTIQUE
BRETAGNE PAYS DE LA LOIRE - IMT ATLANTIQUE

ECOLE DOCTORALE N° 601
Mathématiques et Sciences et Technologies de l'Information et de la Communication
Spécialité : *Informatique*

Par

Cesar Augusto VARGAS ANAMURO

Etude du relayage entre terminaux pour la connectivité des objets dans les réseaux 5G

Thèse présentée et soutenue à Rennes, le 25/06/2020
Unité de recherche : IRISA
Thèse N° : 2020IMTA0196

Rapporteurs avant soutenance :

Philippe Martins	Professeur, Télécom Paris
Mohamad Assaad	Professeur, CentraleSupélec

Composition du Jury :

Président :	Martin Heusse	Professeur, ENSIMAG, Grenoble
Examinateurs :	Fabrice Valois	Professeur, INSA Lyon
	Philippe Martins	Professeur, Télécom Paris
	Mohamad Assaad	Professeur, CentraleSupélec
Dir. de thèse :	Xavier Lagrange	Professeur, IMT Atlantique, Rennes
Encadrante :	Nadège Varsier	Ingénieure Experte, Orange Labs, Meylan

Invité :

Jean Schwoerer	Ingénieur Expert, Orange Labs, Meylan

Acknowledgements

I address my sincere thanks to my supervisors: Dr. Nadège Varsier and Dr. Jean Schwoerer, not only for giving me the opportunity to work on this thesis but also for their invaluable support and guidance throughout the development of this research work. I also deeply thank my thesis director, Professor Xavier Lagrange. His knowledge and experience were essential for the development of this research work. I especially appreciate his remarks, recommendations, and rigor during my investigation.

A special thanks to the reviewers: Professor Philippe Martins and Professor Mohamad Assaad for spending time to review my manuscript and for their comments. Also, I would like to express my gratitude to Professor Martin Heusse and Professor Fabrice Valois for being members of the jury in my thesis defense and for their questions and feedback.

I cannot fail to mention my thanks to all the members of the CITY team at Orange Labs Meylan, especially to Juan Carlos for his collaboration in my research. Being part of this research team during the development of my thesis was pleasant and professionally enriching. I also thank the members of the European project ONE5G of which I was a member.

The most important source of emotional support during this time was my family. I am infinitely grateful to my parents Luzmila and Eusebio; my brothers Joel, Jose, and Christian; and my girlfriend Gabriella. They were always by my side despite the thousands of kilometers that separate France and Peru. Finally, I thank my friends and all those people with whom I was able to share pleasant moments throughout these three years in Grenoble.

Abstract

Massive Machine-Type Communication (mMTC) is one of the main services delivered by the fifth Generation (5G) mobile network. mMTC represents a major challenge for 5G network since it is characterized by a large number of low complexity devices that send small data packets. Moreover, mMTC devices are often battery-powered, and the battery is expected to operate for long periods without being recharged or replaced. Traditional cellular networks, which are designed for human communications, are not energy efficient for this type of service. To address this problem, in this thesis, we study the use of Device-to-Device (D2D) relaying as a complementary transmission. In this approach, the mMTC device can transmit its data using a nearby user equipment (UE) as a relay.

First, we calculate the energy consumed in each phase of the communication process for a device located at the cell border that uses Long-Term Evolution for MTC (LTE-M) technology. Then, using a simple model, we compare the energy consumption of cellular and D2D transmission modes, and we determine the optimal relay location. Using stochastic geometry, we analyze the performance of D2D communication with Automatic Repeat reQuest (ARQ) and Hybrid ARQ with Chase Combining (CC-HARQ) with regard to the transmission success probability, the average number of transmissions, and the energy consumption. Finally, we propose an energy-efficient D2D relaying mechanism suitable for mMTC applications thanks to its easy implementation. This mechanism uses a distributed relay selection approach, which prioritizes the selection of the UEs with the best channel qualities. Moreover, we provide an analytical framework to evaluate the performance of our mechanism.

Table of contents

List of figures

List of tables

Nomenclature

Acronyms / Abbreviations

3GPP 3rd Generation Partnership Project

8-PSK 8-ary Phase Shift Keying

ACK Acknowledgement

ARQ Automatic Repeat Request

AWGN Additive White Gaussian Noise

BLER Block Error Rate

BS Base Station

CDF Cumulative distribution function

CIoT Cellular Internet of Things

CP Control Plane

CTS Clear-to-Send

D2D Device-to-Device

DRX Discontinuous reception

EC-GSM-IoT Extended Coverage-GSM-IoT

eDRX Extended Discontinued Reception

eMBB Enhanced Mobile Broadband

EPC Evolved Packet Core

FDD Frequency-division duplex

FEC Forward Error Correction

GMSK Gaussian Minimum Shift Keying

GSM Global System for Mobile

H-PPP Homogeneous Poisson Point Process

H2H Human-to-Human

HARQ Hybrid Automatic Repeat reQuest

IoT Internet of Things

IP Internet Protocol

ISD Inter-site Distance

ISM Industrial, Scientific and Medical

SIC Successive Interference Cancellation

ITU International Telecommunication Union

LPWAN Low-Power Wide Area Networks

LTE-M Long-Term Evolution for Machine-Type Communications

M2M Machine-to-Machine

MAC Medium Access Control

MAR Mobile Autonomous Reporting

MCL Maximum Coupling Loss

MCS Modulation and Coding Schemes

MIB Master Information Block

MME Mobility Management Entity

mMTC massive Machine-Type Communication

MRC Maximum Ratio Combining

MTC Machine-Type Communication

MTD Machine-Type Devices

NB-IoT Narrowband Internet of Things

NLoS Non-line-of-sight

OFDMA Orthogonal frequency-division multiple access

PDF Probability density function

PDSCH Physical Downlink Shared Channel

PGW Packet data network gateway

PMF Probability Mass Function

PPP Poisson Point Process

PRACH Physical Random Access Channel

PRB Physical Resource Block

PSM Power-saving mode

PSS Primary synchronization signal

PUSCH Physical Uplink Shared Channel

QAM Quadrature Amplitude Modulation

QoS Quality of Service

RA Random Access

RC Relay-Candidate

RF Radio Frequency

RR Request-for-Relay

RRC Radio Resource Control

RTS Request-to-Send

SC-FDMA Single Carrier Frequency Division Multiple Access

SCEF Service Capability Exposure Function

SGW Serving gateway

SIB System Information Block

SIR Signal to Interference Ratio

SMS Short Message Service

SSS Secondary synchronization signal

TAU Tracking Area Update

uMTC ultra-reliable Machine-Type Communication

UP User Plane

uRLLC ultra-Reliable Low Latency Communication

V2V Vehicle-to-vehicle

Chapter 1

Introduction

1.1 Context and Motivations

The era of fifth-Generation (5G) cellular network has arrived to meet the growing demand for new wireless communication services as well as to improve existing ones. The International Telecommunication Union (ITU) has classified the 5G services into three main categories [10]: (i) enhanced mobile broadband (eMBB), (ii) ultra-reliable low latency communication (uRLLC), and (iii) massive machine-type communication (mMTC). eMBB groups the traditional services currently supported by cellular networks as well as the new applications that require a high data rate across a wide coverage area such as ultra-high-definition video, virtual reality. uRLLC groups the applications that require critical communications, with extremely high reactivity and reliability such as remote surgery, 3D gaming. mMTC applications, also known as massive Internet of Things (IoT), is characterized by a massive number of battery-powered and low-complexity devices that sporadically transmit small data packets, for example, wearables, smart meters, parking sensors, waste management, and many other use cases. Devices in this third category are called Machine-Type Devices (MTD) [1].

Due to the huge number of potential mMTC applications, Cisco [11] and Ericsson [1] projections indicate exponential growth of the number of connections associated with these applications. There are currently different wireless technologies to cope with this growth, each connectivity technology having advantages and drawbacks depending on the use case. For short ranges, the most used technologies are Bluetooth [12], ZigBee [13], and Wi-Fi [14], which operate in unlicensed bands and have limitations in terms of Quality of Service (QoS) and security. There are other wireless technologies for mMTC applications, also known as Low-Power Wide Area Networks (LPWAN), which are specially designed

[1] The name MTD is used to refer to any MTC device, including those of the critical MTC applications. However, we will use the designation MTD to refer only to the devices of mMTC applications.

to provide long-range connectivity. These technologies can be grouped into unlicensed LPWAN (or non-cellular LPWAN) and cellular IoT (CIoT) technologies. Unlicensed LPWAN technologies, such as LoRaWAN [15] and Sigfox [16], have been designed exclusively for long-range mMTC applications. The deployment of these technologies began a few years ago, and today they are important players of the IoT market. On the other hand, the 3rd Generation Partnership Project (3GPP) has proposed three CIoT technologies, namely, Extended Coverage-GSM-IoT (EC-GSM-IoT), Narrowband IoT (NB-IoT), and Long-Term Evolution for MTC (LTE-M). Each of the CIoT technologies was designed for specific use cases, while EC-GSM-IoT is compatible with GSM networks, LTE-M and NB-IoT are based on the fundamentals of LTE. Ericsson estimates that the global number of CIoT connections supported by NB-IoT and LTE-M will overgrow in the coming years, from 100 million in 2019 to 2.5 billion in 2025, i.e., half of the total number of IoT connections projected for that year (see Fig. 1.1).

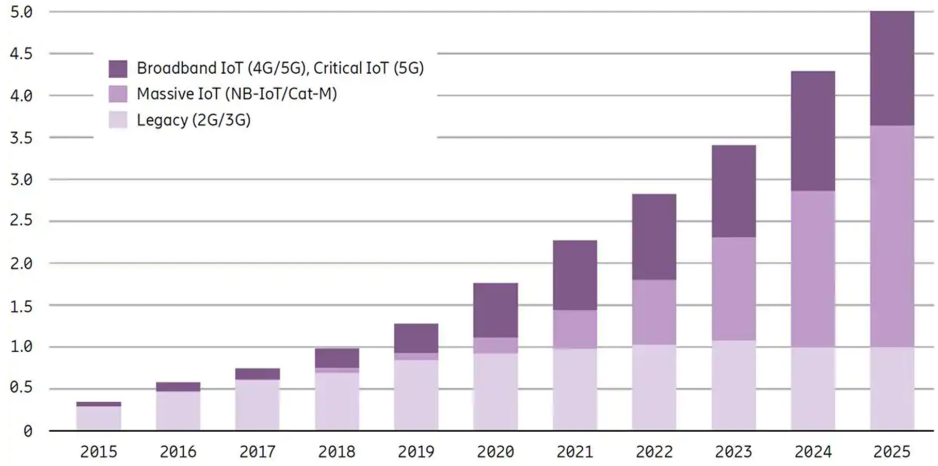

Fig. 1.1 Expected growth of massive IoT connections (billion) [1].

One of the requirements related to mMTC applications is long battery life since it is often not viable to recharge or replace the batteries due to the considerable number of MTDs and their locations. Many MTDs are placed in locations with poor coverage, such as smart utility meters installed in the building basements, other devices are deployed in deep indoor scenarios suffering an extra penetration loss, such as smoke detectors. The method most used by CIoT technologies to improve coverage is the repetition technique [17], which consists of repeating the same transmission several times; for example, LTE-M supports up to 2048 repetitions [18]. However, the cost of this technique is the increase in both the use of radio resources and MTD energy consumption. The latter being a big issue for these kinds of applications since they require a long battery life, as mentioned above.

In traditional cellular communications, all the devices involved in the communication have to establish a connection with the base station (BS). This approach, in some cases, is not the most efficient, especially when the communicating devices are located close to each other. LTE Device-to-Device (D2D) communication is a new approach that takes advantage of the proximity of the devices; it consists of the establishment of direct communication between nearby devices, i.e., the data transmitted does not pass through the base station. D2D communication is one of the key enablers for a variety of 5G services [19], including public safety services, content sharing, coverage extension, vehicle-to-vehicle (V2V) communication, D2D relaying, etc.

In this thesis, we are particularly interested in D2D relaying, which consists of using a device as a relay to help another device that is in poor coverage. The idea is that an MTD with an unfavorable MTD-BS link budget can use a nearby UE (e.g., a smartphone) as a relay instead of transmitting its data directly to the base station wasting radio resources and energy. This new approach involves many challenges such as the allocation of resources for D2D communications, determining when it is convenient to use a relay instead of a direct transmission to the base station, the criteria for selecting a relay, the security of the D2D communication. We will show the advantages of using D2D technology for mMTC applications instead of traditional cellular communication. Our analysis focuses on the energy consumption of MTDs since we consider that this performance metric is one of the most critical requirements to take into account for these types of applications. A part of the work done in this thesis has contributed to the H2020 European project ONE5G [20].

1.2 Contributions

As mentioned before, this thesis focuses on the use of D2D relaying mechanisms to reduce MTD energy consumption. This approach considers that an MTD uses a nearby UE as a relay, establishing a D2D link between both devices. In order to have a tractable analytical model, we consider that the locations of MTDs and UEs form two independent Poisson point processes (PPPs), and then by using the stochastic geometry, we evaluate the performance of D2D communication and compare it with traditional cellular communication. The main contributions of this thesis are summarized as follows:

- Through simulations, we calculate the amount of energy consumed in each phase of the communication process for an MTD at 164 dB Maximum Coupling Loss (MCL) that uses LTE-M technology. In this analysis, we consider the parameters proposed by the 3GPP as well as the repetition mechanism.

- Using a simple model, we compare the energy consumption in cellular mode and the global energy consumption in D2D mode (i.e., the energy consumed by both the MTD and the relay). Based on this analysis, we determine the optimal location of the relay to minimize global energy consumption.
- In a scenario where the MTDs autonomously select the radio resources to be used for the D2D link, we analyze the performance of D2D communication with Hybrid Automatic Repeat reQuest with Chase Combining (CC-HARQ). Using stochastic geometry, we derive formulas for the transmission success probability, the average number of transmissions, and the MTD energy consumption. The performance of the Automatic Repeat reQuest (ARQ) is also analyzed as a reference.
- Considering that the MTD selects the best UE as a relay during the discovery phase, we analyze the performance of both ARQ and CC-HARQ. Then, we compare the performance of both retransmission schemes in terms of energy consumption for different modulation and coding schemes (MCS) levels and considering a target loss probability of 10%.
- We propose a D2D relaying mechanism suitable for mMTC applications thanks to its easy implementation and the amount of energy that it could save. This mechanism uses a distributed relay selection approach (i.e., without the participation of the base station), which prioritizes the selection of the UEs with the best channel qualities.
- Using stochastic geometry, we provide an analytical framework to evaluate the performance of our D2D relaying mechanism. We derive formulas for the relay discovery probability, the average number of time slots used in the contention process, the probability density function (PDF) of the MTD-relay distance, and the total MTD energy consumption. These formulas are useful for determining the optimal values of the key parameters of our relay selection protocol.

1.3 Thesis outline

The remainder of this thesis is organized as follows:

In Chapter 2, we provide an overview of mMTC applications, including the key 5G requirements, the new cellular IoT technologies, the traffic models, and the energy consumption model. We also study the energy consumed by an MTD when sending an uplink report, according to the LTE-M specifications.

In Chapter 3, we give background information about LTE D2D communication focusing on D2D relaying. Furthermore, in this chapter, we conduct a comparative analysis, in terms of global energy consumption, between traditional cellular communication and an approach that uses a D2D relaying mechanism for data transmission.

In Chapter 4, we show a performance comparison between ARQ and CC-HARQ in terms of the transmission success probability, the average number of transmissions, and MTD energy consumption in D2D communications. Then the analytical results are validated by simulations. As a particular case, we study a scenario where the MTDs select the best UEs as relays. Based on this analysis, we then compare both retransmission mechanisms as a function of the UE density.

In Chapter 5, we propose an energy-efficient D2D relaying mechanism. Through analytical models, we study the performance of our relay mechanism based on the relay discovery probability, the average number of time slots used in the contention process, the probability to select a close relay, and the MTD energy consumption. Simulations validate the analytical results and then we discuss how the key parameter of our relay selection protocol affects performance metrics. Finally, we compare energy consumption when the MTD uses our relaying mechanism and when it uses a cellular transmission.

Chapter 2

Massive Machine-type Communication Overview

2.1 Introduction

In 2007 the 3GPP initiated the studies related to the feasibility of Machine-Type Communication (MTC) [21]. This group defined the MTC as a form of communication involving one or more entities that do not necessarily need human interaction [22].

MTC applications are varied and have specific QoS features depending on the use case. They are often grouped into two categories [23], namely, ultra-reliable MTC (uMTC) and massive MTC (mMTC). uMTC applications are characterized by very low latency, high reliability and availability, and in fact, such applications are also part of URLLC 5G category defined in [10]. On the other hand, mMTC applications are characterized by a large number of devices, low mobility, small and infrequent data transmission, long battery life (e.g., smart meters or smart buildings). In this thesis, we focus on connectivity technologies for mMTC applications. Most MTDs are low complexity devices and must operate for many years entirely depending on a low-cost battery [24]. Furthermore, these devices are usually located in places where they suffer a considerable building penetration loss (up to 50 dB [25]) like deep inside buildings or basements. In other words, they generally have an unfavorable link budget. Therefore, the main challenges in mMTC applications are to ensure the connectivity of a massive number of MTDs without degrading the network performance and to reduce the energy consumed by the MTD without increasing the device complexity.

As new connectivity technologies dedicated to mMTC applications, LPWAN technologies are distinguished by their ability to provide high coverage while using low energy consumption. These technologies may operate in licensed bands, also known as CIoT tech-

nologies such as EC-GSM-IoT, NB-IoT, and LTE-M or in unlicensed bands such as Sigfox, LoRa, and Ingenu [24].

The rest of this chapter is organized as follows: Section 2.2 presents the requirements of mMTC applications. The existing cellular IoT technologies designed for mMTC applications are compared in Section 2.3. The traffic model for MTC is shown in Section 2.4. Section 2.5 provides an overview of the MTC energy consumption, including the energy consumption model, an energy consumption analysis of LTE-M, and a survey about energy-efficiency for MTC. Finally, conclusions are drawn in Section 2.6.

2.2 mMTC 5G Requirements

From their inception with the traditional services (e.g., voice and SMS) to the most recent services (e.g., video calls and high-speed internet access), the requirements associated with cellular technologies were centered on humans. As a consequence, the complexity of UEs has evolved over the years; nowadays, one of the most used devices is the smartphone, which has a powerful processor and a high storage capacity. Nevertheless, with the emergence of MTC, many of these requirements become more relaxed, while others become more restrictive compared to human-centered cellular technologies.

MTDs usually perform a specific task and send a data report to the network; for example, smart utility meters send a monthly report. Due to the wide variety of use cases, the 3GPP considers that the network can support up to one million devices per square kilometer. Another characteristic of mMTC applications is the location of the MTDs; many of them are located in places of poor cellular coverage such as deep inside buildings or basements. For this reason, the coverage of the cellular network must be extended; the target for coverage is 164 dB of MCL for a data rate of 160 bps at the application layer [3]. Unlike human applications where the UEs are close to users, many MTDs are located in places of difficult access for humans. Therefore, an essential requirement to maintain low operating costs is the long battery life since recharging the device batteries or changing them would be a complicated task due to the location of the MTDs. For a daily data transfer of 200 bytes in uplink followed by 20 bytes in downlink at an MCL of 164 dB, the battery life must be more than 10 years (15 years is desirable) for a device battery of 5 Wh. MTDs are low-cost devices; this requirement is directly related to the low complexity device. Finally, a requirement less restrictive compared to human applications is the latency, mMTC applications can tolerate a delay of up to 10 seconds in uplink for a 20 bytes application packet (with uncompressed IP header) at 164 dB MCL. Table 2.1 presents a summary of the main requirements of mMTC applications based on [3, 26].

Table 2.1 5G requirements for mMTC

Requirement	**Objective**
Connection density	The target for connection density in the urban environment is one million devices/km^2
Coverage	164 dB of MCL for a data rate of 160 bps at the application layer
UE battery life	At least 10 years for a battery of 5 Wh, a daily data transfer of 200 bytes uplink followed by 20 bytes downlink at 164 dB MCL
Latency	Less than 10 seconds on the uplink for a 20 bytes application packet (with uncompressed IP header) at an MCL of 164 dB
Complexity	Ultra-low device complexity

Enhanced coverage is one of the key features of CIoT technologies. One of the main techniques used for this purpose is repetitions. This technique consists of repeating the same transmission several times, and then all transmissions are combined on the reception side. Ideally, doubling the number of repetitions a 3 dB gain is expected but also doubling the latency while reducing by half the throughput and spectral efficiency.

Regarding battery life, CIoT technologies propose the use of power-saving modes (PSM) and extended Discontinued Reception (eDRX) techniques to save energy when the IoT device is in inactivity periods. However, when the device is in an active state (Tx or Rx state), the coverage has a significant impact on the energy consumed by the device. For example, if the device is located in deep indoor, it will need large numbers of repetitions to successfully transmit its data. The greater is the number of repetitions, the higher is the energy consumption, and the shorter is the lifetime of the battery.

CIoT technologies introduce a series of features that reduce device complexity. Among the most important, we can mention the following ones: the limited frequency bandwidth (1.4 MHz for LTE-M and 200 kHz for EC-GSM-IoT and NB-IoT), only one antenna chain, half-duplex operation in frequency-division duplex (FDD) bands.

2.3 Cellular Internet of Things

Nowadays, cellular networks are widely deployed worldwide. They are formed by cells and base stations. A base station covers a particular area, providing connections to devices located within this area. Cellular networks were optimized for Human-to-Human (H2H) communication, but with the emergence of new applications, they are expected to become

the most attractive technology to support IoT services. They offer scalability, reliability, large coverage, low-cost deployment (reuse of the installed cellular network infrastructure), security, dedicated spectrum, and simplicity of management [27].

CIoT can support IP and non-IP data packets [28]. This hybrid solution allows data communication without any overhead for specific applications that do not need IP connectivity. The network architecture of the CIoT is based on the LTE architecture (see Fig. 2.1). The Control Plane (CP) and User Plane (UP) optimization mechanisms for CIoT are implemented on the Mobility Management Entity (MME), serving gateway (SGW), and packet data network gateway (PGW) entities. The standard also considers a new network entity, the Service Capability Exposure Function (SCEF). The interface between MME and SCEF is called T6a and is based on the DIAMETER protocol, which is adapted to transmit small amounts of non-IP data packets over the CP. As shown in the figure, on the new control plane CIoT, the radio access network switches the data between the UE and the MME. Then, the data is transmitted to the PGW via the SGW (IP data) or to the SCEF (non-IP data). With the user plane, both IP (legacy LTE) and non-IP data can be transferred via the SGW and PGW to the CIoT application server.

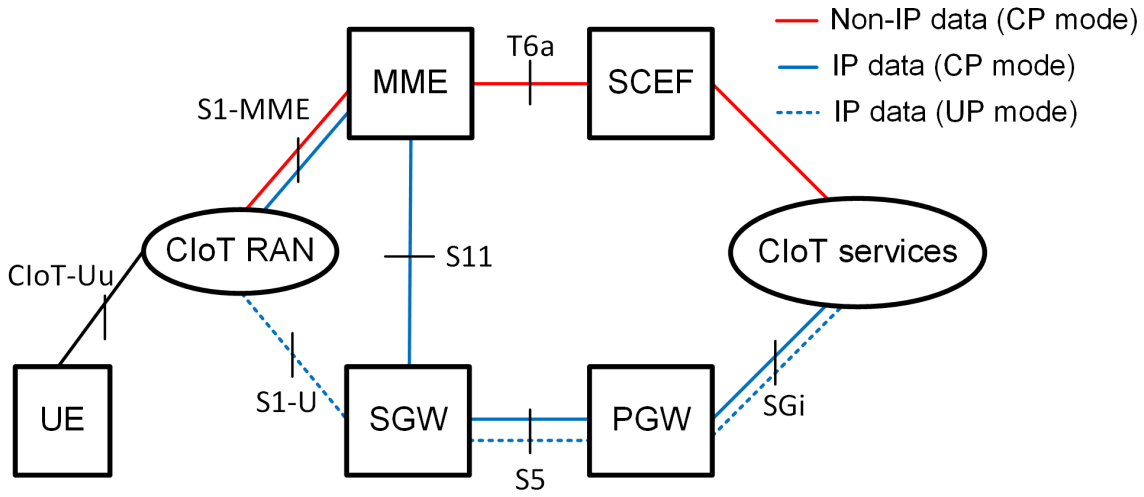

Fig. 2.1 CIoT network architecture (based on [2]).

3GPP standards developed three new technologies (EC-GSM-IoT, NB-IoT, LTE-M) dedicated to providing cellular services for mMTC applications.

2.3.1 LTE-M

LTE-M extends LTE technology with features to support mMTC applications requiring low to medium data rate [24]. It may provide low complexity, extended coverage, and improved

battery life while reusing the existing LTE cellular infrastructure. LTE-M operates on a lower system bandwidth of 1.4 MHz and provides bi-directional communication with a data rate of 1 Mbps. It uses single-carrier Frequency Division Multiple Access (SC-FDMA) with 15 kHz tone spacing for the uplink and orthogonal frequency-division multiple access (OFDMA) with 15 kHz subcarrier spacing and 16-QAM modulation for the downlink. LTE-M device is restricted to a maximum transport block size of 1000 bits and typically operates in half-duplex mode. Moreover, it supports PSM and eDRX to extend battery life.

2.3.2 EC-GSM-IoT

The EC-GSM-IoT is a new radio access technology for IoT [3]. It is compatible with existing GSM technologies and uses a system bandwidth of 2.4 MHz and 200 kHz per channel. Two modulation techniques for data transmission are considered, the Gaussian Minimum Shift Keying (GMSK) and 8-ary Phase Shift Keying (8-PSK), achieving a peak data rate of 10 kbps and 240 kbps, receptively. EC-GSM-IoT extends the coverage of the typical GSM by 20 dB using the repetition techniques. Moreover, this technology improves battery lifetime by using PSM and eDRX techniques. The maximum transmission power level of an EC-GSM-IoT device is either 33 dBm or 23 dBm.

2.3.3 NB-IoT

NB-IoT is one of the new cellular technologies proposed by the 3GPP [3]. This technology reuse some LTE technical components to facilitate the deployment in the existing LTE networks. The downlink is based on OFDMA with a system bandwidth of 180 kHz, i.e., one LTE Physical Resource Blocks (PRBs). In the uplink, it uses SC-FDMA with 3.75 and 15 kHz subcarrier spacing. NB-IoT may operate in three different modes: guard-band, in-band, and stand-alone. In guard-band mode, it uses an LTE carrier in the LTE guard-band. In-band mode, it uses one LTE PRB. In stand-alone mode, it may be deployed as a dedicated carrier using a bandwidth larger than 180 kHz (e.g., using one GSM channel of 200 kHz). NB-IoT may use battery-saving features such as PSM and eDRX. The maximum transmission power can be 20 dBm or 23 dBm.

A summary of the specifications of these three cellular technologies is shown in Table 2.2.

2.4 MTC Traffic Model

The 3GPP defines four different application traffic models for mMTC applications [3]:

Table 2.2 3GPP cellular IoT specifications

	EC-GSM-IoT	**NB-IoT**	**LTE-M**
Deployment	In-band GSM	In-band, guard-band, standalone	In-band LTE
Coverage (dB)	164	164	155.7
Bandwidth	200 kHz per channel	180 kHz	1.08 MHz
Duplexing	HD, FDD	HD, FDD	FD/HD, FDD/TDD
Power class	33 dBm, 23 dBm	23 dBm	20 dBm, 23 dBm
Power saving	PSM, eDRX	PSM, eDRX	PSM, eDRX

2.4.1 Mobile Autonomous Reporting (MAR) Periodic Reports

The MAR periodic reports model is the most common traffic model in mMTC applications; it is used when the device periodically sends a report to the server. This report is self-triggered by the MTD based on its configuration. In this model, it is assumed that the server responds with an acknowledgment (ACK) in 50% of cases. The application payload size distribution is modeled as a Pareto distribution with shape parameter $\alpha = 2.5$, the minimum payload size of 20 bytes, and the cut-off is 200 bytes. The payload size does not include the header size of the higher layers. The periodic inter-arrival time of this model is divided into four groups, which are shown in Table 2.3.

Table 2.3 Periodicity of inter-arrival time

Periodicity	**Percentage**
1 day	40%
2 hours	40%
1 hour	15%
30 minutes	5%

2.4.2 MAR Exception Reports

The MAR exception reports model is used when the MTD is programmed to send a report when an exceptional event is detected (these events are expected to be rare). It is assumed an uplink application payload of 20 bytes and a latency target of 10 seconds.

2.4.3 Network Command

The network command traffic model is used to model the traffic triggered by the server, either by requesting a report from the MTD or when sending commands to the MTD to perform an action. The size of the command (downlink) is 20 bytes, and its periodicity is similar to the MAR periodic reporting. For the uplink, the device responds with an ACK with zero bytes in 50% of cases, and in the remaining 50%, it responds with an uplink report with a payload size similar to the MAR periodic report.

2.4.4 Software Update/Reconfiguration

It is assumed that the device requires a software update/reconfiguration with a periodicity of 180 days. The application payload size distribution is modeled as a Pareto distribution with shape parameter $\alpha = 1.5$ and a minimum payload size of 200 bytes with a cut-off of 2000 bytes.

Unlike human-centered applications, most mMTC applications are focused on uplink communications [29, 30]. In the network simulations, MAR exception reports and software update/reconfiguration traffic models are usually not considered since the frequency of occurrence is rare. It is considered that 80% of the cases the traffic is MAR periodic reports and 20% network command [31]. Therefore in this thesis, we will conduct a performance analysis of the uplink reports, i.e., when the MTD sends its data packets to the network. In [3], it is assumed 65 bytes for header size without IP header compression and 29 bytes with IP header compression. Therefore, the packet size of the MAR periodic reports, including the headers, varies from 85 bytes to 265 bytes for uncompressed headers, and from 49 bytes to 229 bytes for compressed headers. By using the formula of the truncated Pareto distribution given in [32], the cumulative distribution function (CDF) of the packet sizes of the uplink reports, including the header size, is shown in Fig. 2.2. As it can be observed from the figure, 50% of the reports have a packet size greater than 65 bytes and 110 bytes for compressed headers and uncompressed headers, respectively.

2.5 MTC Energy Consumption

2.5.1 Energy Consumption Model

The energy consumption is a crucial parameter to evaluate the performance of a CIoT technology. The 3GPP proposes a simplified energy state model to compute the total energy

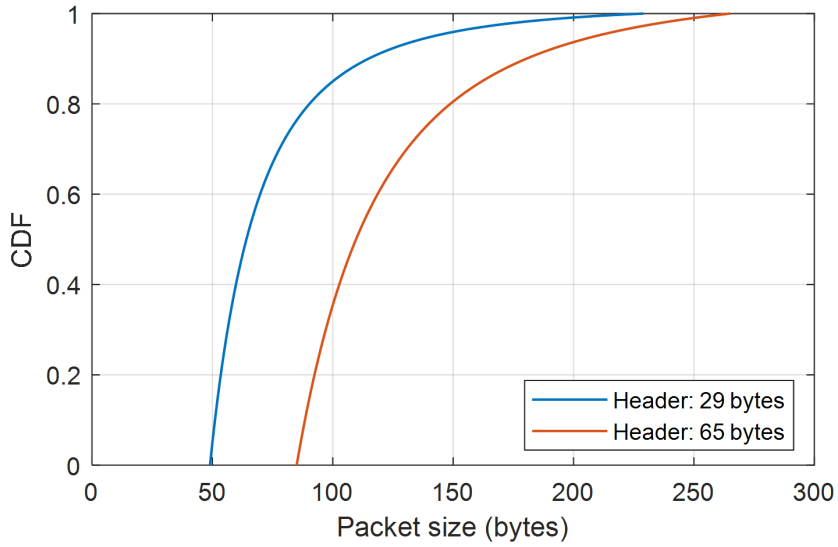

Fig. 2.2 CDF of the packet size of uplink reports.

consumption [3]. This model consists of four states, and at a given time, the device operate in one of these states:

- **Active Rx state:** The MTD is actively receiving or attempting to receive a signal.
- **Active Tx state:** The MTD is actively transmitting a signal.
- **Idle state:** The MTD maintains the accurate timing by keeping RF frequency reference active. In this state, the device wakes up to receive paging messages from the network so that it can be reached from the network.
- **Power Saving state (Sleep):** The MTD releases all radio connections; only the sleep clock is expected to be running. In this state the device is not monitoring paging, so it becomes unreachable from the network.

The MTD operating states, as well as the transitions, are shown in Fig. 2.3. The MTD in the sleep state is programmed to wake-up periodically and to switch to the idle state to read the paging channel. The MTD remains in the idle state for a specific time; if there is no new message to be transmitted, it goes into the sleep state (activity complete). The MTD moves from the idle state to the active state when it has uplink data to transmit (connection request). In the idle state, the MTD periodically moves to the active state to check whether there is any paging message for it from the network (paging). This periodicity is also known as the eDRX cycle. When the MTD has finished the transmission or reception of some information, it changes to the idle state (connection release) so that the base station can still reach it.

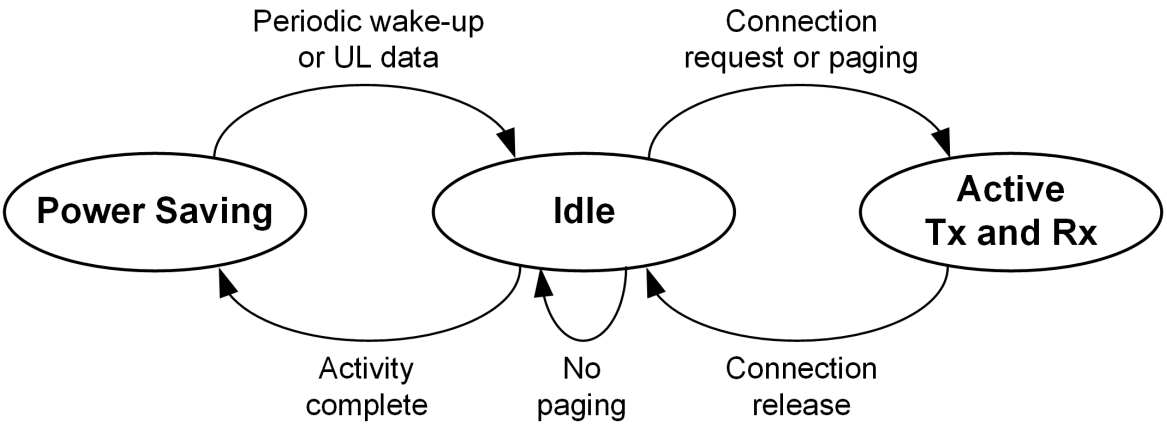

Fig. 2.3 MTD operating states.

In order to calculate the total MTD energy consumption, it is necessary to estimate the proportion of time spent by the MTD in each state during a reporting cycle. A reporting cycle is defined as the time between the transmission of two consecutive data reports, as illustrated in Fig. 2.4. During this cycle, there is an exchange of messages between the MTD and the network. When the device has no data to transmit, it remains in the sleep state, and it wakes up periodically to perform a tracking area update (TAU), i.e., it moves to the idle state to monitor the paging channel in order to check whether there is data for it from the network. At the end of the idle phase, it returns to the sleep state until the next TAU. When the MTD has some data to transmit, it moves to the active state starting with the synchronization phase (system information) and then the connection establishment phase (Random Access procedure). Once the device establishes a connection with the network, it transmits its data and waits for an ACK. Finally, there is an idle phase before the device returns to the sleep state. In the example shown in the figure, we assume that all messages are successfully transmitted to the base station, i.e., the repetition technique is not used.

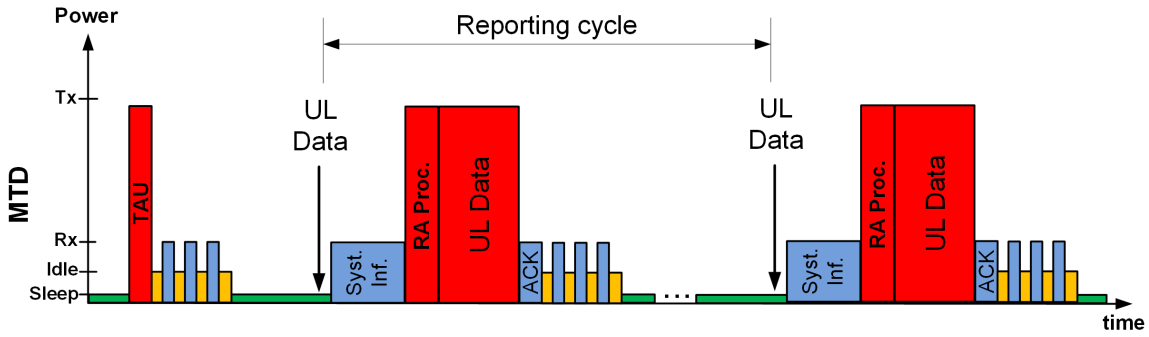

Fig. 2.4 Reporting cycle (based on [3, 4]).

In the energy consumption model, each operating state has a specific and constant power requirement. When the MTD is in Tx state, the power consumption (energy consumption per unit time) is $P_{m,T} = P_{\text{circ}} + P_{tx}/A_{\text{eff}}$, where P_{circ} represents the power consumption due to the circuitry, P_{tx} denotes the transmission power, and A_{eff} is the power amplifier efficiency. In [3], the 3GPP gives the parameters to be used in the energy consumption analysis. It is assumed a transmission power of 23 dBm, a power amplifier efficiency of 44%, and 90 mW for other analog and baseband circuitry. When the MTD is in Rx state, the Radio Frequency (RF) receiver circuit is active; in this state, the power consumption $P_{m,R}$ is considered constant. Let P_{idle} and P_{sleep} respectively be the power consumption during the idle, and sleep states. Thus, the total energy consumed by the device is computed as:

$$E_{\text{total}} = P_{m,T}t_{m,T} + P_{m,R}t_{m,R} + P_{\text{idle}}t_{\text{idle}} + P_{\text{sleep}}t_{\text{sleep}}, \tag{2.1}$$

where $t_{m,T}$, $t_{m,R}$, t_{idle}, and t_{sleep} are the proportion of time spent by the device in Tx, Rx, idle, and sleep states, respectively. The power consumption assumptions are given in Table 2.4.

Table 2.4 Power consumption assumptions [3]

MTD state	Power consumption (mW)
Tx active	545
Rx active	90
Idle	3
Power saving (Sleep)	0.015

2.5.2 Energy Consumption Analysis for LTE-M

2.5.2.1 MTD Energy Consumption

As a complementary part of my thesis, in my research team at Orange Labs, an internship[1] was carried out whose first objective was to develop link-level simulations for evaluating the performance of LTE-M, especially the data rate and MTD energy consumption. Appendix C shows more details about this work, including the simulation parameters. In this study, it is considered a scenario where the MTD is at 164 dB MCL and transmits a data packet of 200 bytes. The device is in coverage, and therefore, it is synchronized with the base station. In this study, it is shown that to guarantee a Block Error Rate (BLER) lower than 10%, the number of retransmissions for Physical Uplink Shared Channel (PUSCH) and Physical

[1] I was co-advisor of this internship.

Downlink Shared Channel (PDSCH), are respectively 512 and 256. As a consequence, the data rate for PUSCH and PDSCH, are respectively 608 bps and 3364 bps. However, to determine the time of each message, we use the formula given by (C.2).

The energy consumption analysis includes all messages exchanged between the MTD and the base station from the Physical Random Access Channel (PRACH) preamble transmission to the connection release message. All the sequences of messages considered in the analysis are shown in Fig. 2.5.

When the MTD wakes up, it listens to the synchronization messages sent by the base station. After that, it starts the random access procedure by sending the *Random Access Preamble* (message 1); 64 repetitions are necessary to guarantee a PRACH detection probability of 99% (see Fig. C.3 in the Appendix C). The base station replies with a *Random Access Response* (message 2) which contains scheduling information such as the radio resources to be used by the MTD to transmit a *RRC Connection Resume Request* (message 3). The base station sends the *RRC Connection Resume* (message 4). The MTD transmits later the *RRC Connection Resume Complete* and the *RLC ACK* for message 4 (message 5a); in the same message, the *Uplink Data* is transmitted (message 5b). After transmitting its data, the MTD receives the *RLC ACK for Uplink Data* (message 6) and the *Application Downlink* (message 7) and the MTD responds with *RLC ACK Downlink Data* (message 8). The base station sends the *RRC Connection Release* (message 9) and finally, the MTD responds with an *RLC ACK for Connection Realease* (message 10).

Table 2.5 shows a summary of the energy consumed by the MTD for each message exchanged with the base station. The sizes of all messages and the power consumption in each state are similar to those used in [25]. From the table, we can see that message 5 (uplink data) consumes a little more than half of the total energy consumption. Besides, the random access procedure (from message 1 to message 5a) consumes almost a quarter of the total energy consumption. Fig. 2.6 illustrates how energy consumption increases with each message transmitted, reaching up to 2830 mJ at the end of the communication.

2.5.2.2 LTE-M Battery Lifetime

In this section, we estimate the number of years that an MTD at 164 dB MCL powered by a 5 Wh battery remains operational, assuming that it sends a 200 bytes uplink report and receives 65 bytes downlink acknowledgment. First, we calculate the energy consumed to send one report and then the daily energy consumption considering the MAR periodic report models. Before the sequence of messages illustrated in Fig. 2.5, the MTD executes a synchronization process, which includes the Primary Synchronization Signal (PSS), the Secondary Synchronization Signal (SSS), the Master Information Block (MIB) and the

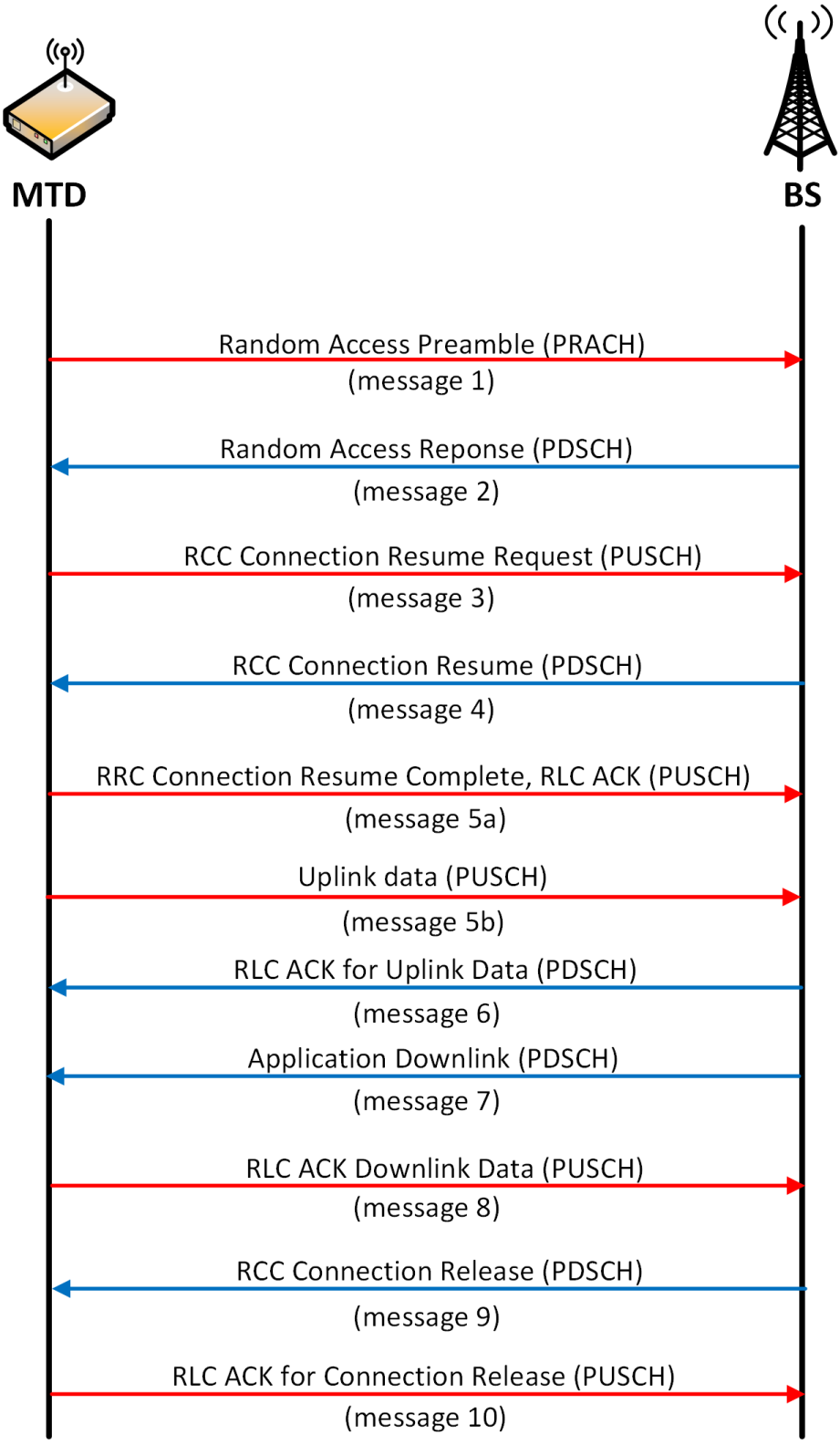

Fig. 2.5 Message sequence for LTE-M energy consumption analysis.

Table 2.5 LTE-M energy consumption at 164 dB MCL

Message	Size (bytes)	Time (ms)	Energy (mJ)	Percentage
1		64	36,8	1.30%
2	7	256	20,48	0.72%
3	7	512	294,4	10.40%
4	20	256	20,48	0.72%
5a	22	512	294,4	10.40%
5b	200	2631,6	1513,2	53.47%
6	3	256	20,48	0.72%
7	65	256	20,48	0.72%
8	3	512	294,4	10,40%
9	8	256	20,48	0,72%
10	3	512	294,4	10,40%

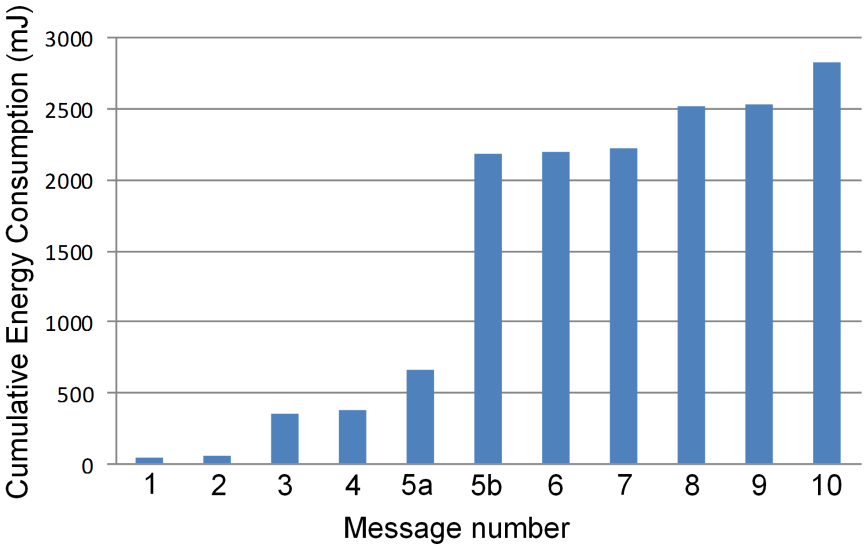

Fig. 2.6 Cumulative LTE-M energy consumption at 164 dB MCL.

System Information Blocks (SIB). In addition to these messages, it will also be considered one second of waiting time in light sleep between the uplink transmission and the downlink ACK, twenty seconds in light sleep after the release in case the eNB sends more information, and the rest of the time PSM. The duration of all these messages is given in [25]. Table 2.6 summarizes the energy consumption of all messages exchanged between the MTD and the base station for the transmission of a report. In total, the MTD consumed 3035.4 mJ per report and remains active for 28.8 seconds.

Table 2.6 Total LTE-M energy consumption at 164 dB MCL

Procedures	**Time (s)**	**Power (mW)**	**Energy (mJ)**
PSS/SSS	0.88	80	70.4
MIB	0.25	80	20
SIB	0.65	80	52
Waiting DL ACK	1	3	3
Waiting before PSM	20	3	60
Message sequence (Fig. 2.5)	6.02		2830
Total	**28.8**		**3035.4**

To determine the battery life, we consider the same inter-arrival time periodicity given in Table 2.3. First, we determine the daily reports N_{report} and then the daily MTD energy consumption in active state E_{active}, which can be computed as $E_{\text{active}} = N_{\text{report}} E_{\text{report}}$, where $E_{\text{report}} = 3035.4$ mJ is the total energy consumption per report. The daily energy consumption when the MTD sleeps can be derived as $E_{\text{sleep}} = t_{\text{PSM}} E_{\text{PSM}}$, where t_{PSM} is the time the device sleeps during the day; it can be computed as $t_{\text{PSM}} = 86400 - 28.8 N_{\text{report}}$ seconds. Thus, the total daily energy consumption can be computed as $E_{\text{total}} = E_{\text{active}} + E_{\text{sleep}}$. Then, we can determine the number of years that the MTD powered by a 5 Wh battery can remain operative. Table 2.7 resumes these calculations. From the table, we can see that the battery lifetime requirement (greater than ten years) is met only when the period is one message per day.

2.5.3 Related Studies on Energy-Efficient MTC

Optimization of energy consumption is one of the main challenges for mMTC applications. In this section, we present how some authors address this problem in a cellular IoT context.

Typically MTDs transmit or receive data sporadically. Taking advantage of the fact that MTDs are inactive for a long time, 3GPP introduces two new techniques to improve the

Table 2.7 Battery Life for LTE-M at 164 dB MCL

Periodicity	Daily reports	Total energy (J)	Battery life (years)
1 day	1	3.035	11.39
2 hours	12	36.425	1.31
1 hour	24	72.850	0.67
30 minutes	48	145.699	0.34

battery life of these devices: the PSM and the eDRX. Fig 2.7 illustrates both PSM and eDRX techniques.

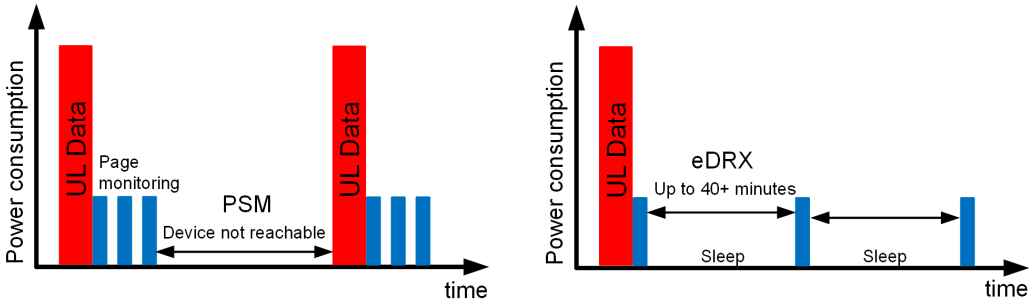

Fig. 2.7 PSM and eDRX techniques (based on [5]).

2.5.3.1 Power Saving Mode

Power Saving Mode is specified by the 3GPP Release 12 [28]. This mode allows to improve the battery life of MTDs since the device sleeps for long periods. The power consumption is significantly minimized while the device is not transmitting or receiving anything. When the device is dormant, it is unreachable for the network since it is not monitoring the paging messages sent by the base station; however, it remains registered with the network. The device using PSM wakes up for data transmission or a periodic TAU. After that, the device remains reachable for a short time before it goes back to sleep.

2.5.3.2 Extended Discontinued Reception

The discontinuous reception (DRX) technique consists of periods of sleep and wake-up to check whether the device has a paging message from the base station. The device must be synchronized with the base station, and it has to read the control messages every specific period. The eDRX technique [33], proposed by the 3GPP Release 13, allows a greater

reduction of MTD energy consumption. This technique extends the DRX cycles up to 40 minutes to allow an MTD to stay longer in sleep state between paging occasions.

In [34], the authors propose an Enhanced PSS (ePSS) and a novel DRX mechanism. The objective is to reduce the re-synchronization time and thus the device energy consumption. This ePSS can also be used to reduce the paging message processing time when there is no paging message for the MTD. In [35], the authors combine the mechanisms of relaying and DRX and propose an energy-efficient relay selection scheme. The results show that when the relays use the DRX, they can significantly reduce their energy consumption

The general objective of an MTD is to transmit some information to the network so it must establish communication with the base station. Nevertheless, it must first synchronize with the base station and then start the random access procedure before transmitting its data. The goal of many studies in the literature is to minimize the energy consumption of the synchronization and random access procedure.

2.5.3.3 Energy-Efficient Synchronization

Synchronization is the first step that a cellular device must perform in order to transmit or receive some information. In the case of MTDs, the fundamental issue is the longer synchronization acquisition time, which occurs due to the long period that these devices remain sleeping. This problem was addressed in [36, 37].

Some studies seek to save energy by reducing the computational complexity of the synchronization. In [36], the authors propose two low complexity algorithms for SSS detection to resynchronize quickly. The computational complexity and energy consumption are reduced while maintaining performance similar to the conventional method. In [37], the authors propose the use of simply-differential correlation-based timing synchronization based on Zadoff-Chu sequences. They suggest reducing the computational complexity using a recursive implementation simply differential metric.

In [34], the authors show that in the synchronization process, the energy consumption due to computational calculations is negligible in comparison to the energy consumption when the device is in the active state. They propose a novel DRX scheme for fast re-synchronization and thus to reduce the MTD energy consumption in this phase.

2.5.3.4 Signaling Overhead Reduction

Once the device is synchronized, the second step is to try to establish a connection with the base station through a random access procedure. During this procedure, there is an exchange

of control messages between the MTD and the base station, consuming a significant amount of energy. Therefore some authors aim to optimize this procedure.

One solution is the Radio Resource Control (RRC) resume procedure [38]; in this procedure, the goal is to optimize the number of signaling messages that are needed to establish a connection in LTE. The authors in [39] propose the use of a Polling service with a wide range of periods. This proposition takes into account the periodicity of most MTC traffic. This solution reduces the signaling overhead avoiding the collision caused by the random access.

In [40], the authors propose that MTDs use a buffer for packet aggregation. The random access only triggers if the number of packets in the buffer reaches a certain threshold. The optimization of energy configures the threshold value. This method saves energy by reducing the number of random access procedures. However, the drawback would be additional access latency due to the accumulation of several packets in the buffer. An improvement to this technique is presented in [41]. In this study, a new packet generated by an MTD does not remain in its buffer, but it is transferred to a neighboring MTD that have the number of packets in its buffer close to a threshold value. Thus, the number of random access procedures and the waiting time of a packet in the buffer are reduced.

2.6 Conclusion

In this chapter, we give an overview of mMTC applications and a brief survey about energy efficiency for these applications. We summarize the main requirements and the new cellular technologies for mMTC applications. An essential section of this chapter is the model of energy consumption which will be used in later chapters.

Among the MTC requirements identified, the most challenging and that have received the most attention from the research communities are the coverage and the device battery life. In order to improve the device battery life, the 3GPP proposes the PSM and eDRX techniques, which allow the device to sleep for long periods; however, the disadvantage of these techniques is that the device remains reachable for a short time. To extend the coverage, the 3GPP proposes the use of techniques such as repetitions, which is simple but effective to meet the coverage requirement. However, the main disadvantage of this technique is the high energy consumption, especially when the device is in poor coverage and requires a large number of repetitions.

In order to reduce the energy consumed during the exchange of messages between the MTD and the base station, in the literature the authors address their research on two

objectives, the first approach is to reduce the energy consumed during synchronization and the second approach is to reduce the energy consumption due to the control messages.

Through simulations according to the LTE-M specifications, the energy consumed by an MTD located at the cell border that sends a 200 bytes uplink report has been calculated. The results show that the data message represents half of the total energy consumption and the rest of the energy consumed is due to the control messages. A percentage of the total energy consumption could be reduced by reducing the number of control messages. However, a greater reduction would be achieved by reducing energy consumption during data transmission. To reduce energy consumption in the data transmission phase, the path loss between the MTD and the base station must be reduced. In this sense, the idea of using a relay is an exciting alternative to reduce energy consumption and extend the coverage. This technique will be detailed in the next chapter.

Chapter 3

D2D Communications Overview

3.1 Introduction

In traditional cellular communications, all communications pass through the base station. This configuration is not very efficient in some cases like when the UE is far from the base station; as an alternative to solve this problem appears the idea of D2D communication in cellular networks. D2D communication in mobile networks (LTE-D2D) is defined as direct communication between nearby devices without going through the base station. It is a promising technology to improve the performance of cellular networks since it takes advantage of the proximity for efficient use of radio resources, improving data rates, reducing latency, and improving energy efficiency. For this reason, it is being considered as a key enabling technology in 5G cellular networks [42].

D2D communication is not a new technology; it has been used mainly in non-cellular technologies (in the unlicensed band) such as Bluetooth, Wi-Fi Direct, ZigBee. These non-cellular technologies can also establish direct communication between devices, but in general, they have low spectrum and energy efficiency, short communication distance, and vulnerability to interference [43]. These problems are addressed more efficiently by LTE-D2D technology [44].

Initially, D2D communication was proposed for public safety services [45]. However, as shown in many studies reported in the literature there are many other potential use cases such as extending network coverage [46], offloading network coverage [47, 48], social proximity services [49], D2D relaying [50–53], V2V communication [54], local multicasting [55]. The possible D2D use cases are summarized in Fig. 3.1.

Although in some new use cases, D2D communication has advantages over traditional cellular communications, there are still many challenges that this technology must overcome in order to be successfully implemented in the future mobile network. Some of these

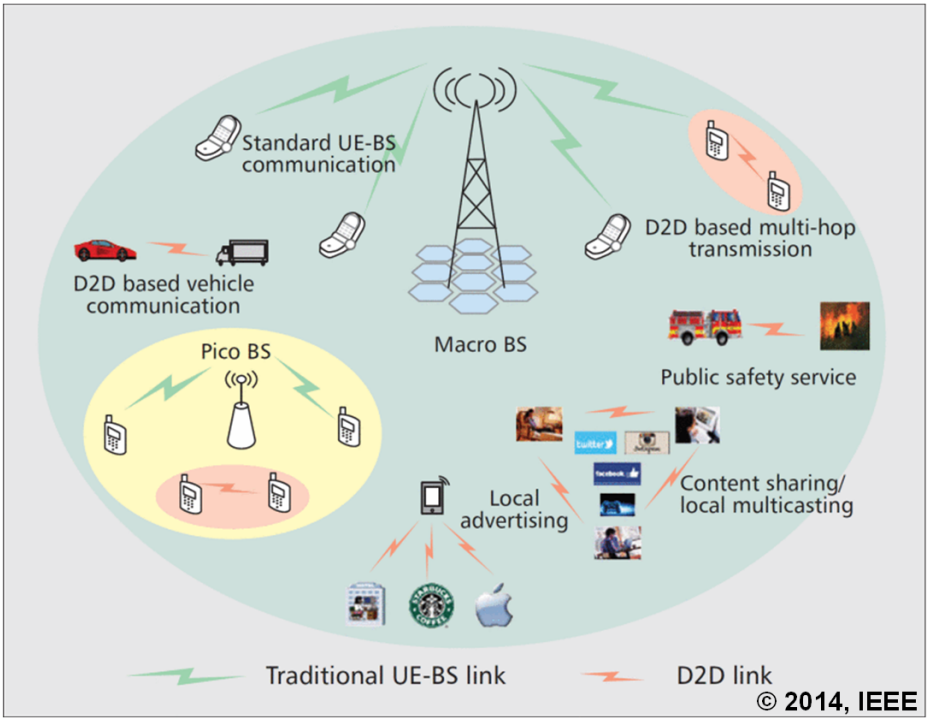

Fig. 3.1 D2D communications use cases [6].

challenges are efficient discovery, interference management, power allocation, resource allocation, and security.

The remainder of this chapter is organized as follows: Section 3.2 shows how D2D communication is categorized according to the use of the frequency spectrum. Section 3.3 describes the LTE D2D technology including the architecture, the functionalities, and the resource allocation modes. The D2D relaying technique is presented in Section 3.4. A survey about the D2D relaying for mMTC is given in Section 3.5. In Section 3.6, we present a comparative study that shows the interest of D2D for mMTC, the content of this section has been published in [56] and [57]. Finally, Section 3.7 concludes the chapter.

3.2 Spectrum Resource for D2D Communication

According to the use of the spectrum resource, D2D communication can be categorized into two groups [58]: inband D2D when it occurs on the cellular spectrum and outband D2D when it occurs on the unlicensed spectrum, usually on the industrial, scientific and medical (ISM) bands. In the case of inband, devices communicate directly using the cellular spectrum of their network provider, i.e., both cellular and D2D communications share the cellular spectrum. Inband D2D can be divided into two subgroups: underlay (non-orthogonal) and

overlay (orthogonal). In underlay inband D2D, the same resources are used in cellular and D2D communications, which could cause interference between both types of communication. In overlay inband D2D, a group of the cellular resources is dedicated to D2D communications which avoid interference. Fig. 3.2 illustrates the different categories of D2D communications according to the use of the spectrum. In this thesis, we will focus on LTE D2D technology in overlay inband in order to mitigate interference between D2D and cellular communications. In other words, we assume that the BS allocates dedicated resources for D2D links.

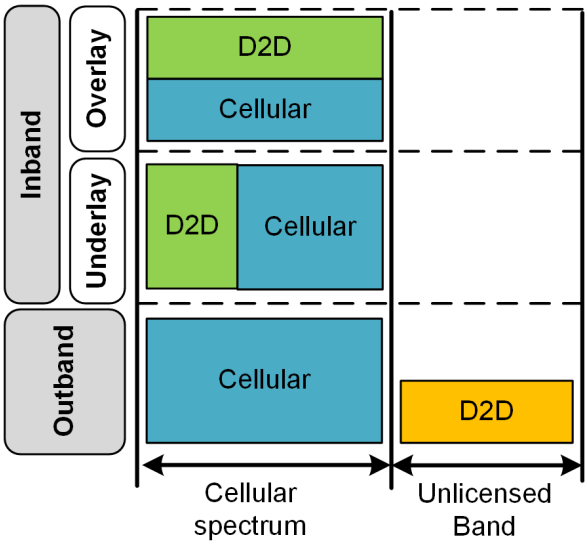

Fig. 3.2 Spectrum resource for D2D communication.

3.3 D2D LTE

3.3.1 Architecture

The 3GPP specifies the D2D architecture in [8]; it is based on the conventional LTE architecture, but introduces a new entity, called Proximity Services (ProSe) function, in the Evolved Packet Core (EPC) (see Fig. 3.3). The ProSe function is a logical function and its primary role is to provide configuration and authorization to UEs for discovery and direct communication and to manage the ProSe context of the UEs. Moreover, this function authorizes UE the use of a specific ProSe application.

Two new logical interfaces, PC3 and PC5, are introduced. A UE that wants to use a Prose application must first contact the ProSe function by exchanging messages via the PC3 interface. Once the UE is authorized, it can initiate the process of discovery or

communication with other UEs via the PC5 interface. Sidelink is the terminology to refer to the direct communication over PC5.

The uplink channel is reused for sidelink since (i) the interference from the D2D link to the base station is limited, and (ii) higher D2D energy efficiency is obtained adopting the SC-FDMA [43].

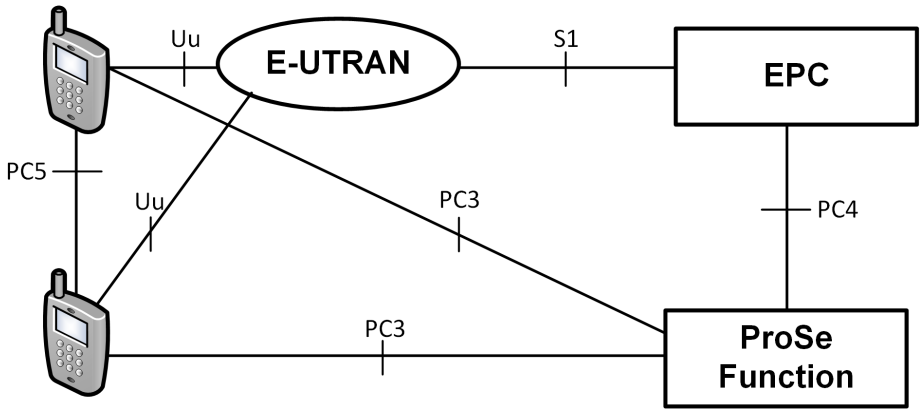

Fig. 3.3 Simplified D2D architecture (based on [7]).

3.3.2 Functionalities

The 3GPP defines two main functionalities for supporting LTE D2D, namely, discovery and communication. When the UEs are in-coverage, these functionalities can be network assisted, i.e., the base station can transmit configuration and control information to the UEs.

3.3.2.1 D2D Discovery

D2D discovery allows the detection of useful information provided by the UEs in physical proximity. The 3GPP specifies two direct proximity discovery protocols [8], namely, model A and model B, which are represented in Fig. 3.4. Model A ("I'm here") supports both open and restricted types of discovery. In this model, there are *announcing UEs* and *monitoring UEs* that monitor information of interest from announcing UEs. Model B ("Who is there?"), used mainly for restricted type. In this model, only the UEs willing or authorized to help the source UE will respond. Two roles are defined: the *discoverer UE*, which transmits a request containing information about what is interesting to discover, and the *discoveree UE*, which receives the request and can respond with information related to discoverer's request.

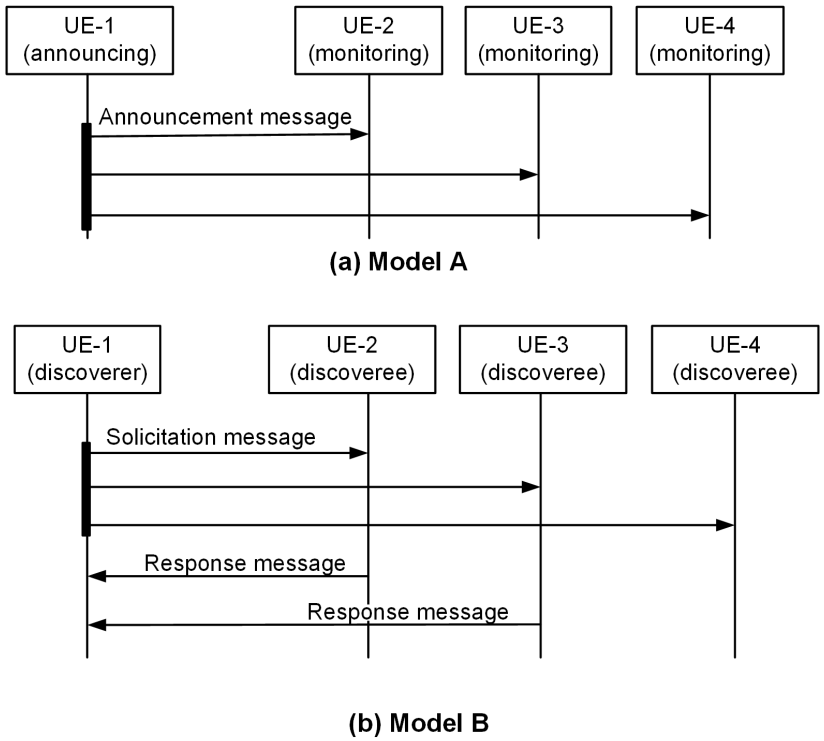

Fig. 3.4 Public safety direct discovery with Model A and Model B [8].

3.3.2.2 D2D Communication

D2D communication allows to establish direct communication between UEs without passing through the base station. However, before establishing communication between UEs, these devices must know in advance if they are close to each other. For this reason, it is often considered that D2D communication is preceded by a discovery phase.

3.3.3 Radio Resource Allocation for Sidelink

In D2D discovery and D2D communication, resource allocation can be performed in two modes: scheduled and autonomous.

3.3.3.1 Scheduled Mode

In this mode, the UE requests resources from the base station via radio resource control (RRC) signal; the base station assigns resources that the UE should use in the D2D link. This mode is similar to the allocation of resources in traditional cellular communications; therefore, it is feasible only when the UEs are in coverage. In the case of sidelink discovery,

this mode is also referred to as *Type 2*, while in the case of sidelink communication, this mode is referred to as *Mode 1*.

3.3.3.2 Autonomous Mode

In the autonomous mode, a device on its own randomly selects resources from a resource pool that is preconfigured or indicated by the base station if it is in coverage. This resource pool is dimensioned by the cellular operator depending on the traffic expectations. This mode is supported by the devices even if they are out-of-coverage. The main problem of this mode is interference since two or more devices could select the same radio resource. In the case of sidelink discovery, this mode is also known as *Type 1*, while in the case of sidelink communication it is also known as *Mode 2*. A resource pool is a set of resources assigned to the sidelink operation; it consists of a subframe pool and a subcarrier pool, as shown in Fig 3.5. The resource pool includes a bitmap, which indicates the subframes to be used for the sidelink. The configuration for the frequency domain depends on three parameters: PRB-Start, PRB-End, and PRB-Num. There are two bands, identified by the occupied PRBs. One band starts at PRB-Start and the other band ends at PRB-End, and both bands have a width of PRB-Num resource blocks.

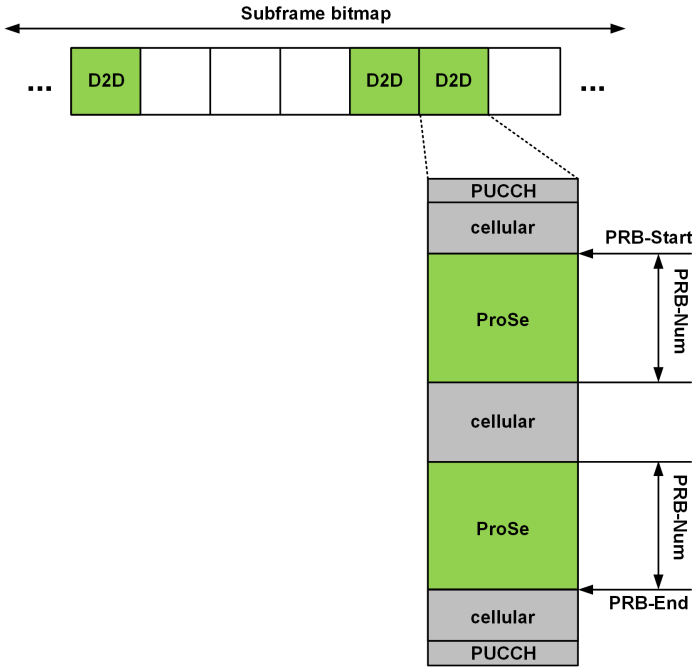

Fig. 3.5 Resource pool for sidelink (based on [9]).

3.4 D2D Relaying

D2D relaying is a technique that consists of using a UE as a relay to help another UE (source) to communicate with the base station. This UE-relay-BS configuration allows extending the base station coverage. Moreover, it exploits spatial diversity since the UEs form a virtual cellular infrastructure. Hence, the source UE can choose between establishing a direct link with the base station or establishing a link with a nearby UE that is used as a relay [59]. If the UE-relay link is better than the UE-BS link, the source UE could increase throughput and reduce energy consumption. Nevertheless, the cost would be paid by the selected relay, for example, increasing its energy consumption. For this reason, the cellular operator must encourage UEs to act as relays and give some compensation.

3.4.1 D2D Relaying Coverage Scenarios

We consider three different coverage scenarios in D2D relaying, which are shown in Fig. 3.6. In scenario 1, the relay and the source UE are in-coverage. Thus, both devices are synchronized and can establish a direct link with the base station. The relay can help to reduce energy consumption of the source UE if the source-relay path loss is less than the source-BS path loss. The main challenges of this scenario are the relay selection, the transmission mode selection (direct to the BS or indirect using a relay), and the radio resource allocation.

In scenario 2, the relay is in-coverage, and the source UE has only downlink coverage. Both devices acquire synchronization from the base station, but the source cannot transmit its data directly to the base station and thus, it must find a relay (indirect transmission mode). The main challenges of this scenario are the relay selection and radio resource allocation.

In scenario 3, the relay is in-coverage, and the source UE is out-of-coverage. The source UE does not receive any signal from the base station. Hence, the main challenges are the synchronization, the relay selection, and the radio resource allocation. One solution to the synchronization issue would be to use the relay UE as a synchronization source.

3.4.2 D2D Relaying Phases

The D2D relaying mechanism consists in three phases, which are shown in Fig. 3.7: synchronization, discovery, and data transmission.

3.4.2.1 Synchronization Phase

Before establishing discovery and direct communication, both devices have to be synchronized in time and frequency, i.e., they require to use the same synchronization reference.

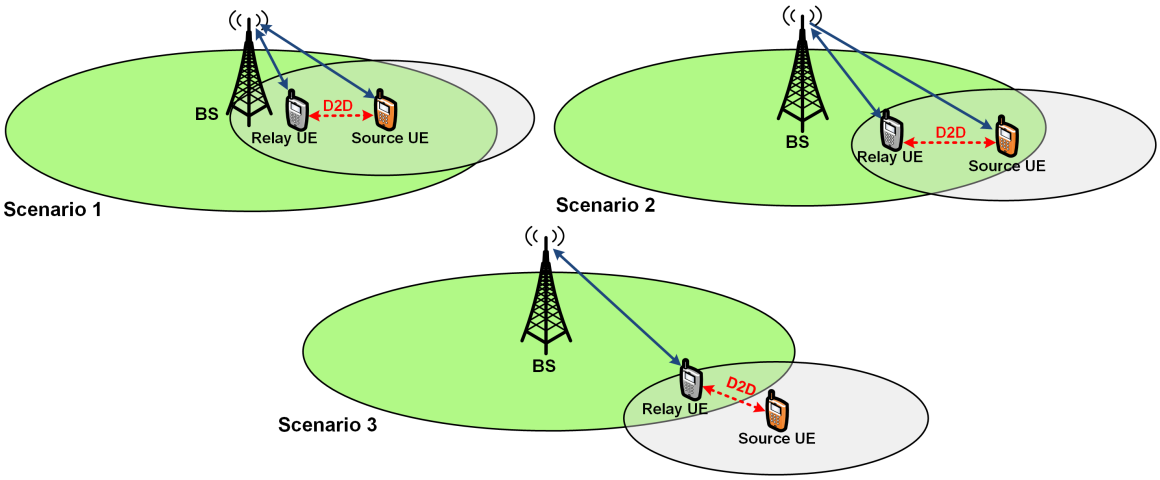

Fig. 3.6 Coverage scenarios for D2D relaying.

When they are in downlink coverage (scenarios 1 and 2), they can reuse the LTE synchronization signals PSS and SSS provided by the base station. PSS and SSS are generated from Zadoff-Chu sequences and M-sequences, respectively. They are broadcasted by the base station every 5 ms and are located in the center of the spectral band occupying a bandwidth of 1.4 MHz. On the other hand, when the source UE is out-of-coverage (scenario 3), the synchronization becomes more challenging because the relay UE has to transmit periodic synchronization signals.

When devices sleep for an extended period, they could lose synchronization. The time that a device can sleep without losing its synchronization depends on the amount of clock drift, which depends on the oscillator quality. The base station, UEs, and MTDs have oscillators with a specific accuracy. The MTDs have low-quality oscillators since they are devices of low complexity/cost. When they are in the sleep state, they easily lose the timing synchronization and require timing re-acquisition, increasing the time spent in the active state and thus energy consumption [34].

In the figure, the source UE is represented by an MTD and we consider a scenario where all devices are in-coverage. we also include the messages of the random access procedure.

3.4.2.2 Discovery Phase

In the discovery phase, the MTD searches for and selects a device that will be used as a relay. In the literature, there are multiple criteria to select a relay depending on the metrics to improve: the transmission rate [60], energy consumption [52, 61], the network lifetime [61, 62]. The relay selection can be performed in a centralized manner [63, 64, 53] or distributed manner [65, 66]. With the centralized approach, the base station selects the relay

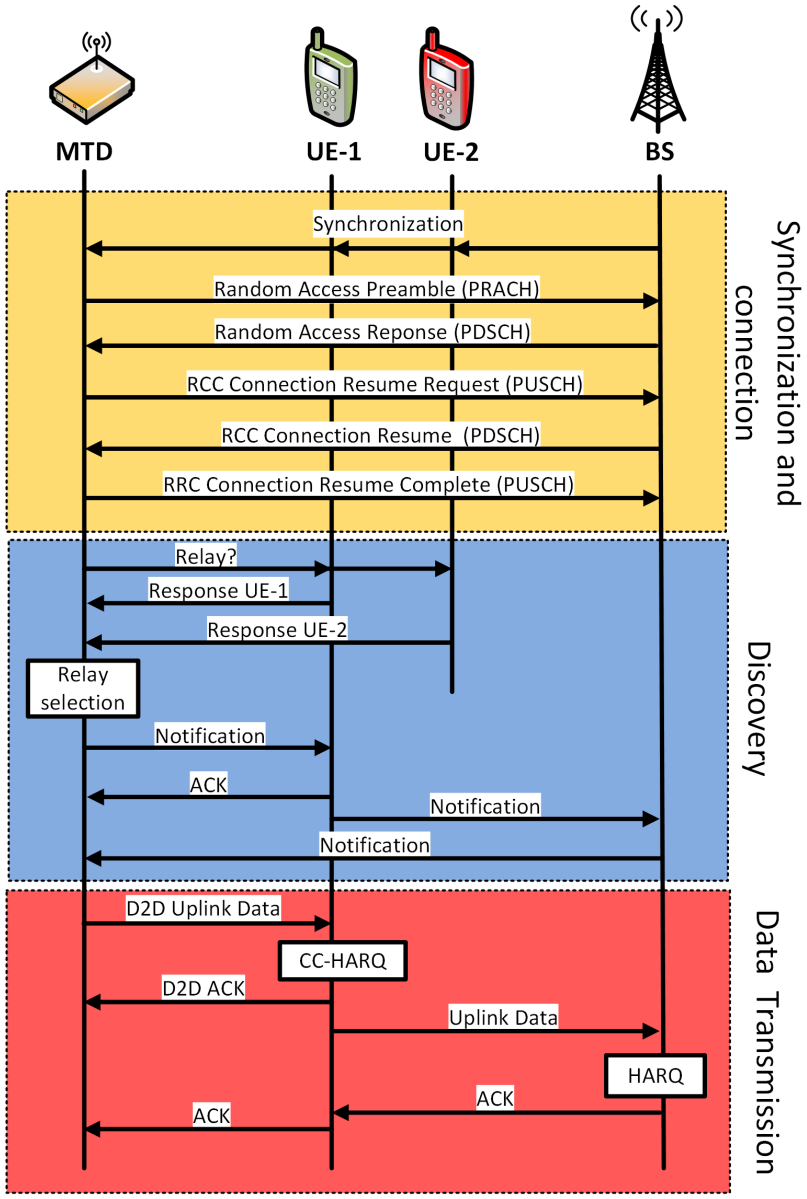

Fig. 3.7 D2D relaying phases.

that the MTD should use to transmit its data. The advantage of this approach is that the base station can select the optimal relay (e.g., the UE that minimizes energy consumption) since it has an overview of the network. Nevertheless, the base station needs to know all the information about the channel states, which requires more control signals. The latter can become a big problem, especially if there are a large number of devices as in mMTC applications [67]. On the other hand, with the distributed approach, the MTD itself selects the relay without the participation of the base station.

In Fig. 3.7, we represent the model B ("Who is there?") using a distributed approach. The MTD sends a request message and receive many responses from potential relays. Then it chooses the best relay using some relay selection criteria and sends a message specifying the identity (ID) of the selected relay. Finally, the selected relay responds with an ACK.

3.4.2.3 Data Transmission Phase

In the data transmission phase, the MTD transmits its data to the relay, establishing D2D communication. Once the relay has correctly received the data, it will retransmit them to the base station via a cellular link. When no relay is found during the discovery phase: in scenario 1, the MTD directly transmits its data to the base station, while in scenarios 2 and 3, it will retry the search for a relay later.

In order to increase the transmission reliability of the D2D link, a retransmission mechanism such as HARQ may be used. This mechanism, which exploits the temporal diversity of the channel, is especially beneficial when interference is severe.

3.4.3 Relay UE Density Scenarios

In the literature, authors assume different values of relay UE density. In [68], the authors consider that the UE density is fixed at 4.62×10^{-5} UE/m^2 for the urban macro scenario. In [69], the authors assume a relay density of 5×10^{-5} relays/m^2. In this section, we calculate the relay UE density considering the 3GPP evaluation assumptions [70]. There are two deployment scenarios:

- Scenario 1 (dense urban) with inter-site distance (ISD) of 500 meters and 10 UEs/cell.
- Scenario 2 (urban) with ISD of 1732 meters and 20 UEs/cell (40 UEs/cell is optional).

It is noteworthy that the number of UEs suggested by 3GPP is the number of UE devices intended explicitly for relaying. In this thesis, we consider that the location of the devices forms an H-PPP, where the number of UEs per cell specified in [70] is the mean number of UEs per cell. Now, we calculate the UE density for both scenarios. We assume hexagonal

cellular networks and 3-sector antenna as in [3], the relationship between ISD and cell site sector radius R is shown in Fig. 3.8. When the cell is a regular hexagon, $R = \text{ISD}/3$ and the area of a cell site sector can be calculated as follow:

$$A_{cell} = \frac{3R^2\sqrt{3}}{2} = \frac{\text{ISD}^2\sqrt{3}}{6}. \tag{3.1}$$

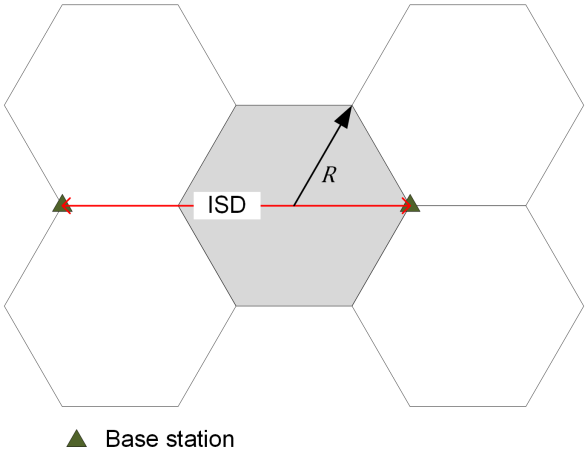

Fig. 3.8 Cell area and inter-site distance.

Table 3.1 summarizes the UE density for both low and high UE density scenarios. For practical purposes, these UE density values are approximate to 2.5×10^{-5} UE/m^2 and 14×10^{-5} UE/m^2 for low UE density and high UE density, respectively.

Table 3.1 UE densities considered in this work

Scenario	**ISD (m)**	**Cell area (m^2)**	**UEs/cell**	**UE density (UE/m^2)**
Low UE density	1732	865974	20	2.3×10^{-5}
High UE density	500	72168	10	13.8×10^{-5}

3.5 Related Studies on D2D Relaying for mMTC

Energy consumption due to data transmission represents a significant percentage of total energy consumption in the active state, especially when the MTD has an unfavorable link budget. In order to reduce this energy consumption, in recent years, the D2D relaying technique for mMTC applications has gained relevance. In this section, we present the studies related to D2D relaying for mMTC applications.

Two configurations could be considered when using a relay to connect MTDs. The first configuration is when the cellular operator specifically deploys the relays. The second configuration and the one that has been considered by 3GPP in [8] is the use of UE as relays to connect other devices such as wearables or MTDs.

3.5.1 Relays Deployed by the Operator

The relays are installed by the mobile operator in strategic places where there is a lack of coverage or unfavorable propagation conditions. These relays may be non-energy-constrained if they have a continuous source of energy, or energy-constrained devices using a battery with higher capacity than MTDs. The advantage of this configuration is that the relays do not change their location over time; thus, its coverage area is predictable. However, the biggest drawback of this configuration is the cost of deployment.

In the literature, few studies propose this configuration since the opportunistic side of D2D relaying using UEs as relays is lost. In [61], the authors assume that the relays are deployed by the operator; they study the relay positioning problem in order to minimize the total energy consumption satisfying the QoS constraints of MTDs.

3.5.2 UEs as Relays

In this configuration, the UEs that are close to the MTDs play the role of relays. The condition for a UE to be a relay is to have the D2D functionality enabled. The MTD transmits its data to a neighboring UE via a D2D link, and then the UE re-transmits the aggregated data to the base station via cellular communication. Like the MTDs, the UEs are energy-constrained devices but have less stringent energy constraints than MTDs since their batteries are frequently recharged by users.

The advantage of using UEs as relays is that it does not imply additional deployment costs. A drawback of this configuration is that it is difficult to determine the areas covered by UEs since they regularly change their location following the pattern of their owners. In the literature, several research studies have analyzed the interest of using a UE as a relay to connect MTDs via D2D links.

Regarding the sharing of radio resources between cellular links and D2D links, in [71] the authors introduce a multi-hop D2D communication scheme to minimize energy consumption and additional interference. In [72], the authors show that MTD can reuse the radio resources used by cellular devices. For which they propose the successive interference cancellation (SIC) mechanism.

Considering a UE as a cluster head, the authors of [73] propose two mechanisms, the first one to reduce the total energy consumption and the second one to reduce the delay. They use an optimization process. In [74], the authors propose a scheme in which the UE adds its data to the data recovered from the MTDs located inside a cluster. The results highlight a compromise between latency and energy consumption and show a significant difference in terms of energy consumption between the proposed scheme and traditional cellular communication. The authors of [75] present a complete analysis of the total energy consumption, taking into account the energy consumption of the cluster. The authors propose to reduce energy consumption through an optimization process. First, they calculate the optimal size of the cluster, then a cluster-head re-selection mechanism and a cluster reform are proposed.

Our results in [56] have shown the interest of a D2D relay mechanism compared to a direct link with an unfavorable link budget. We calculate the total D2D energy consumption (MTD and relay) and compare it with the consumption in a cellular transmission.

The selection of an optimal relay that minimizes the MTD energy consumption is studied in [76, 77, 53, 52]. The authors of [76] mathematically determine an energy-saving zone where the relays located inside this zone assist a D2D pair reducing the total energy consumption. The authors of [77] analyze and propose an optimal solution for energy-efficient issue using a joint optimization problem of relay selection, channel allocation, and power control. The authors of [53] propose an energy-efficient relay selection approach based on the double auction theory in cooperative cellular networks.

3.6 D2D Relaying Interest for mMTC

3.6.1 System Model

In this study, the MTD is in-coverage and has some data to transmit to the network; it can transmit its data directly to the base station (cellular mode) or use a UE as a relay (D2D mode) as shown in Fig. 3.9. The objective of this study is to compare the energy consumption in both transmission modes. We only calculate the energy consumption due to the transmission of data, i.e., in the cellular mode we do not consider the energy consumption due to the synchronization or the connection establishment, while in the D2D mode we do not consider the energy consumption due to the synchronization and discovery phases.

We consider the centralized D2D overlay mode, i.e., the base station allocates resources dedicated to D2D communications, avoiding interference between devices. The MTD transmits at a fixed transmission power (i.e., no power control) and it well knows the

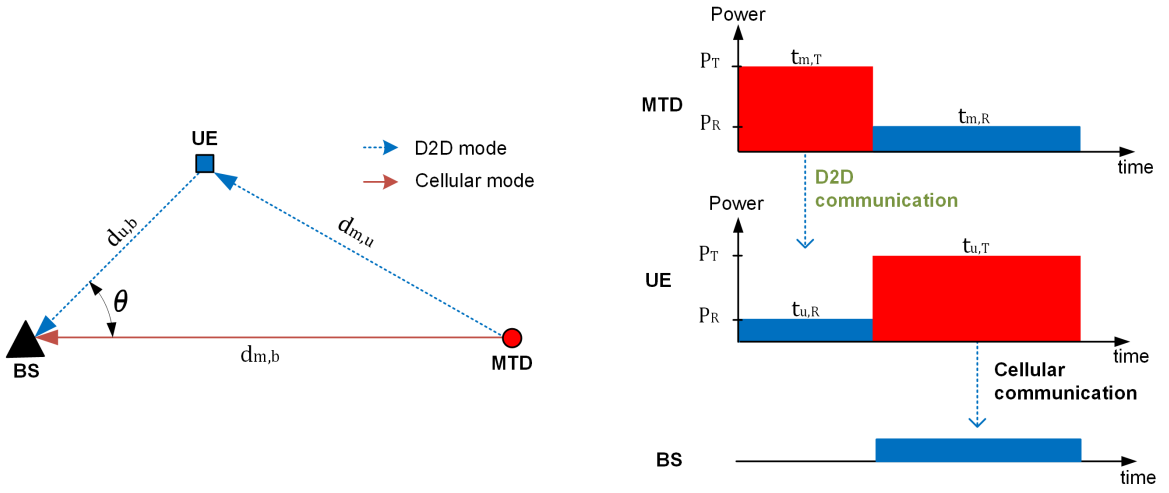

Fig. 3.9 D2D relaying process.

communication channel and thus use a perfect dynamic adaptation of the MCS. We consider only additive white Gaussian noise (AWGN) [75, 78]. From Shannon's capacity equation, the data rate R is derived as:

$$R = W \log_2 \left(1 + \frac{P_{rx}}{N_0 W}\right) \approx W \log_2 \left(\frac{P_{rx}}{N_0 W}\right), \tag{3.2}$$

where W is the transmission bandwidth, N_0 is the noise power spectral density, and P_{rx} is the received power which can be derived according to the Okumura-Hata model as $P_{rx} = K P_{tx} d^{-\alpha}$, where P_{tx} is the transmission power, K is the constant path loss factor, d is the distance between the transmitter and the receiver, and α is the path loss exponent. In order to simplify our analysis, we assume that both the MTD and the UE transmit at the same power and consume the same power when they are in the same state.

3.6.2 Energy Consumption Model

We use the energy consumption model shown in Section 2.5.1, but considering only the data transmission phase. The energy consumption in cellular mode is calculated as follows:

$$E_{m,\text{cell}} = P_T t_{m,T} + P_R t_{m,R}, \tag{3.3}$$

where P_T and P_R are the MTD power consumption in Tx state and Rx state, respectively; $t_{m,T}$ and $t_{m,R}$ are the duration of Tx state and Rx state, respectively. We consider that after transmitting its data, the MTD remains in Rx state $t_{m,R} = t_{m,T}$ waiting for an ACK from the base station. We have $t_{m,T} = L/R_{m,b}$, where L is the data packet size, and $R_{m,b}$ is the MTD

transmission rate in the MTD-BS link, which can be derived from (3.2) as follows:

$$R_{m,b} = W \log_2 \left(\frac{K P_{tx}}{N_0 W d_{m,b}^{\alpha}} \right), \tag{3.4}$$

where $d_{m,b}$ is the distance between the MTD and the BS. Then, we have:

$$E_{m,\text{cell}} = \frac{(P_T + P_R)L}{R_{m,b}}. \tag{3.5}$$

The total energy consumption in D2D mode $E_{T,\text{D2D}}$ can be calculated as the sum of the energy consumed by the MTD and the UE during the relaying process:

$$E_{T,\text{D2D}} = E_{m,\text{D2D}} + E_{u,\text{D2D}}, \tag{3.6}$$

where $E_{m,\text{D2D}}$ and $E_{u,\text{D2D}}$ are the energy consumption by the MTD and UE, respectively. The relaying process is shown in Fig. 3.9, the MTD first transmits its data to the UE while the UE remains in Rx state receiving and demodulating, i.e., $t_{m,T} = t_{u,R}$. Then, the UE retransmits the MTD data to the BS while the MTD stays listening (Rx state), i.e., $t_{m,R} = t_{u,T}$. Thus, the energy consumed by the MTD in D2D mode can be derived as follows:

$$E_{m,\text{D2D}} = P_T t_{m,T} + P_R t_{m,R}, \tag{3.7}$$

where P_T and P_R are the MTD power consumption in Tx state and Rx state, respectively; $t_{m,T}$ and $t_{m,R}$ are the duration of Tx state and Rx state, respectively. We have $t_{m,T} = L/R_{m,u}$ and $t_{m,R} = t_{u,T} = L/R_{u,b}$, where $R_{m,u}$ and $R_{u,b}$ are the transmission rate in the MTD-UE link and the UE-BS link, respectively.

Then, we have

$$E_{m,\text{D2D}} = \frac{P_T L}{R_{m,u}} + \frac{P_R L}{R_{u,b}}. \tag{3.8}$$

Similarly, we can obtain the energy consumed by the UE in D2D mode:

$$E_{u,\text{D2D}} = \frac{P_T L}{R_{u,b}} + \frac{P_R L}{R_{m,u}}. \tag{3.9}$$

The total energy consumption in D2D mode is obtained by substituting (3.8) and (3.9) into (3.6):

$$E_{T,\text{D2D}} = (P_T + P_R)L \left(\frac{1}{R_{u,b}} + \frac{1}{R_{m,u}} \right). \tag{3.10}$$

In order to simplify our analysis, let:

$$A = \frac{(P_T + P_R)L}{\alpha W}, \tag{3.11}$$

and

$$B = \frac{1}{\alpha}\log_2\left(\frac{KP_{tx}}{N_0 W}\right). \tag{3.12}$$

Thus, the total energy consumption in relaying mode is

$$E_{T,\mathrm{D2D}} = A\left(\frac{1}{B-\log_2(d_{u,b})} + \frac{1}{B-\log_2(d_{m,u})}\right). \tag{3.13}$$

3.6.3 Minimum-Energy Consumption in D2D Mode

In this section, we look for the UE location minimizing the total energy consumption in D2D mode. Without loss of generality, we consider a base station at the origin of coordinates $(0,0)$, the MTD at a fixed position $d_{m,b}$ on the x-axis, and a UE located anywhere with polar coordinates θ and $d_{u,b}$ (see Fig. 3.9). We normalize the UE-BS distance:

$$d_{u,b} = x d_{m,b},\ 0 < x < 1. \tag{3.14}$$

Then, the MTD-UE distance can be calculated as

$$d_{m,u} = d_{m,b}\sqrt{x^2 + 1 - 2x\cos(\theta)}. \tag{3.15}$$

Substituting (3.14) and (3.15) into (3.13) we have:

$$E_{T,\mathrm{D2D}} = A\left(\frac{1}{B-\log_2(x d_{m,b})} + \frac{1}{B-\log_2(d_{m,b}\sqrt{x^2+1-2x\cos(\theta)})}\right). \tag{3.16}$$

$E_{T,\mathrm{D2D}}$ has two variables, θ and x. Then, to minimize the total energy consumption, we calculate the partial derivatives with respect to θ and x and set it equal to zero searching for a minimum. The partial derivative with respect to θ is:

$$\frac{\partial E_{T,\mathrm{D2D}}}{\partial \theta} = \frac{A x d_{m,b}^2 \sin(\theta)}{\ln(2) d_{m,u}^2 \left(B-\log_2(d_{m,u})\right)^2}. \tag{3.17}$$

We set $\frac{\partial E_{T,\mathrm{D2D}}}{\partial \theta} = 0$, and we obtain $\theta = \{0, \pi\}$. Analyzing these values, $E_{T,\mathrm{D2D}}$ is a minimum when $\theta = 0$ and it is a maximum when $\theta = \pi$. Therefore, the total energy

consumption is minimal when the BS, UE, and MTD are aligned and the UE is located between the MTD and the BS. By substituting $\theta = 0$ into (3.16), we have:

$$E_{T,\mathrm{D2D}} = A\left(\frac{1}{B-\log_2(xd_{m,b})} + \frac{1}{B-\log_2((1-x)d_{m,b})}\right). \tag{3.18}$$

Using the first partial derivative criteria with respect to x, we can acquire the critical points solving $\frac{\partial E_{T,\mathrm{D2D}}}{\partial x} = 0$:

$$(1-x)(B-\log_2((1-x)d_{m,b}))^2 - x(B-\log_2(xd_{m,b}))^2 = 0, \tag{3.19}$$

we find a critical point at $x = 0.5$. To determine if this point is a local minimum or a local maximum, we have to calculate the second partial derivative with respect to x and evaluate it at $x = 0.5$:

$$\frac{\partial^2 E_{T,\mathrm{D2D}}}{\partial x^2}\Big|_{x=0.5} = \frac{8A(\log_2(e^2 d_{m,b}) - B - 1)}{\ln(2)(B+1-\log_2(d_{m,b}))^3}. \tag{3.20}$$

Using the second derivative criteria, if expression (3.20) is negative then $E_{T,\mathrm{D2D}}$ is concave around $x = 0.5$ (i.e., a local maximum), otherwise $E_{T,\mathrm{D2D}}$ is convex around $x = 0.5$ (i.e., a local minimum). One can easily verify that that $A > 0$ and $B > \log_2(d_{m,b})$. Therefore, in (3.20), $E_{T,\mathrm{D2D}}|_{x=0.5}$ is a local minimum when

$$\log_2(e^2 d_{m,b}) - B - 1 > 0, \tag{3.21}$$

Substituting (3.12) into (3.21):

$$d_{m,b} > \frac{2}{e^2}\left(\frac{KP_{tx}}{N_0 W}\right)^{1/\alpha}. \tag{3.22}$$

Therefore, $E_{T,\mathrm{D2D}}|_{x=0.5}$ is a local minimum when condition (3.22) is satisfied, otherwise it is a local maximum.

To find the total minimum of $E_{T,\mathrm{D2D}}$, we compare all possible local minima and determine which one is the minimum. $E_{T,\mathrm{D2D}}$ may have three local minima at $x = 0$, $x = 0.5$ and $x = 1$, by symmetry $E_{T,\mathrm{D2D}}|_{x=0} = E_{T,\mathrm{D2D}}|_{x=1}$. Therefore, we search for the total minimum comparing $E_{T,\mathrm{D2D}}|_{x=0.5}$ and $E_{T,\mathrm{D2D}}|_{x=1}$.

By substituting $x = 0.5$ into (3.18), we have:

$$E_{T,\mathrm{D2D}}|_{x=0.5} = \frac{2A}{B+1-\log_2(d_{m,b})}. \tag{3.23}$$

$E_{T,\mathrm{D2D}}|_{x=1}$ is obtained also using expression (3.18). Physically, $x = 1$ means that MTD and UE are in the same location. In other words, the receiving power must be equal to the transmission power in the MTD-UE link. Thus:

$$\lim_{x\to 1}(B - \log_2((1-x)d_{m,b})) = \frac{1}{\alpha}\log_2\left(\frac{P_{tx}}{N_0 W}\right). \tag{3.24}$$

Substituting (3.24) and $x = 1$ into (3.18):

$$E_{T,\mathrm{D2D}}|_{x=1} = \frac{A}{B - \log_2(d_{m,b})} + \frac{A}{C}, \tag{3.25}$$

where

$$C = \frac{1}{\alpha}\log_2\left(\frac{P_{tx}}{N_0 W}\right). \tag{3.26}$$

$E_{T,\mathrm{D2D}}|_{x=0.5}$ is the total minimum when:

$$E_{T,\mathrm{D2D}}|_{x=0.5} < E_{T,\mathrm{D2D}}|_{x=1}. \tag{3.27}$$

Substituting (3.23) and (3.25) into (3.27), we have

$$\frac{2A}{B + 1 - \log_2(d_{m,b})} < \frac{A}{B - \log_2(d_{m,b})} + \frac{A}{C}. \tag{3.28}$$

Equation (3.28) can be rewritten as

$$Q(\log_2(d_{m,b})) > 0, \tag{3.29}$$

where

$$Q(y) = y^2 + (C - 2B - 1)y + B^2 + B - CB + C. \tag{3.30}$$

We estimate the discriminant of $Q(y)$

$$\Delta = C^2 - 6C + 1. \tag{3.31}$$

If $\Delta < 0$, condition (3.29) is always satisfied for any value of $d_{m,b}$, otherwise it is satisfied for

$$d_{m,b} < 2^{\frac{2B+1-C-\sqrt{\Delta}}{2}} \tag{3.32}$$

or

$$d_{m,b} > 2^{\frac{2B+1-C+\sqrt{\Delta}}{2}}. \tag{3.33}$$

In conclusion, if $\Delta < 0$, the total minimum is always $E_{T,\mathrm{D2D}}|_{x=0.5}$ for any value of $d_{m,b}$. If $\Delta > 0$, then $E_{T,\mathrm{D2D}}|_{x=0.5}$ is the total minimum if and only if condition (3.32) or (3.33) is satisfied, otherwise the total minimum is $E_{T,\mathrm{D2D}}|_{x=1}$.

3.6.4 Comparison of Energy Consumption in Cellular and D2D Modes

In this section, we compare the minimum energy consumption in D2D mode and the energy consumption in cellular mode. We can rewrite expression (3.5) as

$$E_{m,\mathrm{cell}} = \frac{A}{B - \log_2(d_{m,b})}, \tag{3.34}$$

where A and B are given by (3.11) and (3.12), respectively.

The minimum energy consumption in D2D mode $\min(E_{T,\mathrm{D2D}})$ may be $E_{T,\mathrm{D2D}}|_{x=1}$ or $E_{T,\mathrm{D2D}}|_{x=0.5}$ depending on $d_{m,b}$ as shown in Section 3.6.3. However, we can easily show that $E_{T,\mathrm{D2D}}|_{x=1} > E_{m,\mathrm{cell}}$. Therefore, we compare only the scenario where $E_{T,\mathrm{D2D}}|_{x=0.5}$ is the minimum energy consumption in D2D mode, i.e.,

$$E_{T,\mathrm{D2D}}|_{x=0.5} < E_{m,\mathrm{cell}}. \tag{3.35}$$

By substituting (3.23) and (3.34) into (3.35), we have:

$$\frac{2A}{B - \log_2(0.5 d_{m,b})} < \frac{A}{B - \log_2(d_{m,b})}. \tag{3.36}$$

Simplifying

$$d_{m,b} > 2^{B-1}. \tag{3.37}$$

Substituting (3.12) into (3.37), we obtain the condition so that the minimum total energy consumption in D2D mode is less than the energy consumption in cellular mode:

$$d_{m,b} > \frac{1}{2}\left(\frac{KP_{tx}}{N_0 W}\right)^{1/\alpha}. \tag{3.38}$$

3.6.5 Numerical Results

In this section, we provide numerical results to verify our analytical results. We use MATLAB with parameters given in Table 5.1, which are chosen according to the 3GPP specifications. From (3.22), we deduce that $E_{T,\mathrm{D2D}}|_{x=0.5}$ is a local maximum when $d_{m,b} < 346$ meters and is a local minimum when $d_{m,b} > 346$ meters. From (3.32) and (3.33), we have $\min(E_{T,\mathrm{D2D}}) =$

$E_{T,\mathrm{D2D}}|_{x=0.5}$ if $d_{m,b} < 1$ meter or $d_{m,b} > 548$ meters, and $\min(E_{T,\mathrm{D2D}}) = E_{T,\mathrm{D2D}}|_{x=1}$ if $1 < d_{m,b} < 548$ meters.

Table 3.2 Parameters for the analysis

Parameter	**Value**
MTD transmission power (P_{tx})	23 dBm
MTD power consumption in Tx state (P_T)	545 mW
MTD power consumption in Rx state (P_R)	90 mW
MTD Bandwidth (W)	1.4 MHz
Noise Power Spectrum Density (N_0)	-174 dBm/Hz
Carrier Frequency (f_c)	900 MHz
Cellular path-loss exponent (α)	3.67
Cellular path-loss factor for a distance in meters (K)	0.0070

Fig. 3.10 shows the total energy consumption in D2D mode as a function of the normalized UE-BS distance when the BS, UE, and MTD are aligned. We observe the behavior of total energy consumption for five scenarios $d_{m,b} = \{200, 400, 600, 800, 1000\}$ meters. The total energy consumption is a concave curve when the MTD is close to the base station, while it is a convex curve when the MTD is far from the base station. As shown in this figure, $E_{T,\mathrm{D2D}}$ is minimum at $x = 0.5$ for $d_{m,b} = \{600, 800, 1000\}$ meters and it is a maximum for $d_{m,b} = \{200, 400\}$.

Fig. 3.11 compares the energy consumption of both cellular and D2D modes when the BS, UE, and MTD are aligned. We can observe that the energy consumption in D2D mode is lower than the energy consumption in cellular mode when the MTD is located far from the base station. From (3.38), the minimum energy consumption in D2D mode is less than in cellular mode when $d_{m,b} > 640$ meters, this condition deduced analytically is verified in the figure.

Now, for an MTD located at a certain distance from the base station, we compute the total energy consumption by varying the relay location in the whole cell. Fig. 3.12 shows the total energy consumption when the MTD-BS distance is 800 meters. The total energy consumption is minimal when the relay is located in the dark blue regions; on the contrary, it is maximum when the relay is in dark red regions. As a reference, we compute also the energy consumption in cellular mode (-35.74 dBJ for $d_{m,b} = 800$ meters), which is represented by a white oval in the figure. The region where the total energy consumption is the lowest is located at the midpoint between the BS and the MTD as shown in the figure. The energy consumption in relaying mode would be less than in direct mode if there were at least one

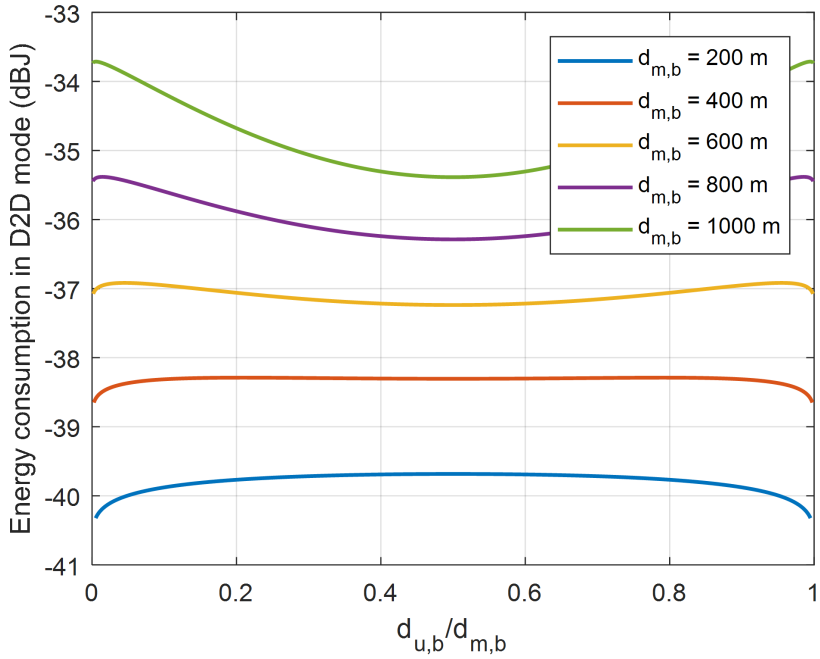

Fig. 3.10 Energy consumption in D2D mode versus normalized UE-BS distance, considering BS, UE and MTD aligned.

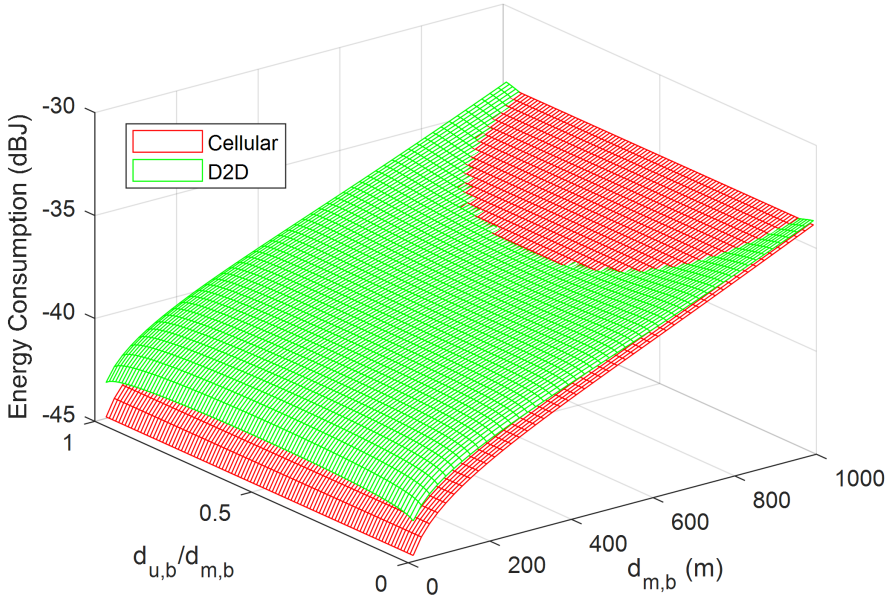

Fig. 3.11 Energy consumption comparison D2D mode versus cellular mode, the BS, the UE, and the MTD are aligned.

relay within the area enclosed by the white oval. This area tends to increase when $d_{m,b}$ increases, so the probability of finding a relay within this area will also increase as a function of $d_{m,b}$.

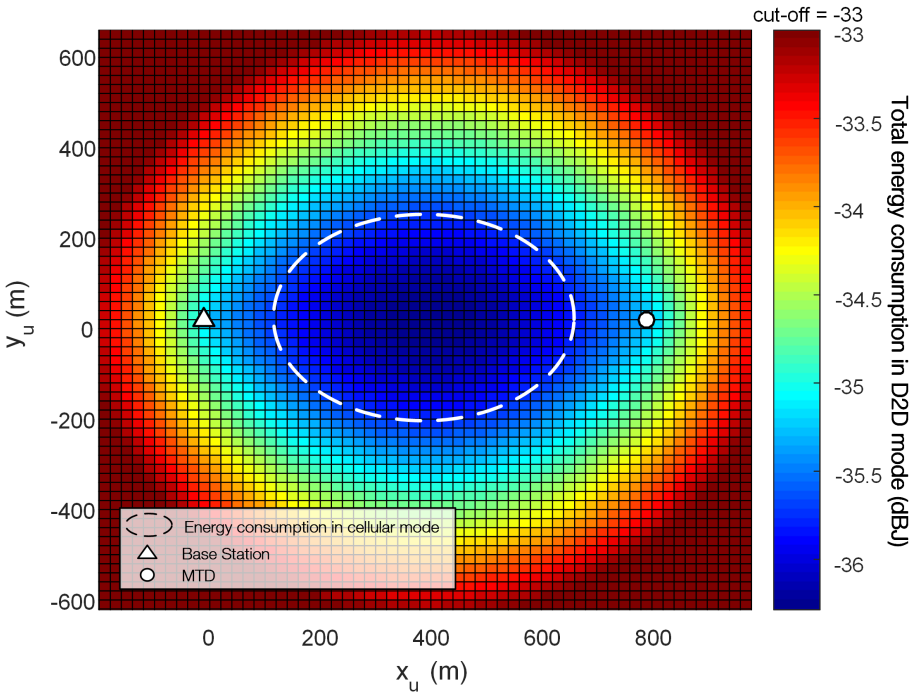

Fig. 3.12 Total energy consumption depending on the UE location, for $d_{m,b} = 800$ meters.

3.7 Conclusion

In this chapter, we present an overview of LTE D2D communication. We focus on the D2D relaying use case and its phases since it is an interesting alternative to meet the specific requirements of mMTC applications. We present three D2D relaying coverage scenarios, but in the following chapters we will only consider scenarios 1 and 2, i.e., the MTD is always in downlink coverage. Therefore, it is always synchronized with the base station and can receive control messages.

In the literature, the D2D communication has been extensively analyzed and the authors have shown the benefits of this technology. However, most studies focus on eMBB applications where the objectives are to reduce the transmission delay, to improve the throughput. Recently, some authors suggest the use of the D2D relaying mechanism for mMTC applications. The majority of these authors have been centered on the issue of energy consumption considering a centralized approach, i.e., the base station participates in the discovery and

communication process. Using a simple energy consumption model, we compare the MTD energy consumption of cellular and D2D communications and we find the optimal location of the relay to minimize global energy consumption (i.e., energy consumed by the MTD and the relay). However, since the objective is to reduce the MTD energy consumption in the following chapters, we only consider the energy consumed by the MTD as a key performance metric.

The major contribution of this thesis will be presented in the next chapters, we will analyze how D2D communications can be used to reduce the energy consumption of mMTC applications.

Chapter 4

Performance evaluation of D2D communications with CC-HARQ

4.1 Introduction

As mentioned in Chapter 2, D2D relaying is an interesting mechanism to reduce the energy consumed by the MTDs. In D2D communications, there are two possible resource allocation modes, namely, the scheduled mode and the autonomous mode (see Section 3.3.3). In the scheduled mode, the base station is responsible for the allocation of radio resources allowing devices to use either dedicated resources as traditional cellular communication or shared resources with other devices. For the sharing case, the radio resources are managed by the base station so as to minimizing interference. On the other hand, in the autonomous mode, the base station only indicates the pool of radio resources available for D2D communication, and each device autonomously selects the radio resource to be used for communication. The merit of doing so is the reuse of spectrum and avoidance of signaling overhead between the MTDs and the base station. However, as there is no central entity for controlling, the major problem of interference arises when two or more devices select the same radio resource.

High interference can cause unsuccessful transmissions. In order to deal with this critical issue, this chapter is focused on proposing the use of retransmission schemes to improve transmission reliability by exploiting the temporal diversity of the channel. In this study, we are therefore focused on exploiting retransmission schemes for reducing the impact of interference in D2D links for the scenario of autonomous resource allocation (i.e., MTDs share radio resources).

ARQ and HARQ have been widely used in communication systems as retransmission techniques. Indeed, ARQ simply consists of transmitting the same packet as many times as

necessary while on the receiver side the wrong packets are discarded. More complicated, HARQ combines ARQ and forward error correction (FEC) mechanisms. As opposed to ARQ, a packet received with errors is not discarded in HARQ but rather being stored in a buffer by the receiver, and when a new packet arrives, it will be combined with those stored in the buffer. Such mechanism is also known as HARQ with soft combining and in fact, it is classified into two types; namely, HARQ with Chase Combining (CC) [79] and HARQ with Incremental Redundancy (IR) [80]. While the same packet is sent in all transmission in CC-HARQ, the transmitter sends different packets[1] in consecutive rounds in IR-HARQ. The IR-HARQ scheme offers better performance than the CC-HARQ scheme but at the cost of greater transmitter complexity [81]. Therefore, ARQ and CC-HARQ would be suitable for mMTC applications to improve the transmission reliability without increasing the complexity of the MTDs.

This chapter is dedicated to analyze and draw a performance comparison between ARQ and CC-HARQ on the basis of transmission success probability, the average number of transmissions, and energy consumption in D2D communications. The content of this chapter has been published in [82].

4.1.1 Related Work

Energy-efficient communication has become the main challenge for mMTC applications and indeed, has been receiving growing attention from the research communities and industries. Energy efficiency of the resource allocation for HARQ has been carefully investigated in [83] and [84]. The authors in these research studies analyzed the problem from optimization perspectives by using numerical evaluations. Similarly, energy efficiency of CC-HARQ was addressed in [85] with an optimization approach. In this study, the analytical and simulation results showed the optimal values of payload length and average transmission energy per bit. The CC-HARQ scheme for sensor networks in a multi-hop context was considered in [86]. The authors derived analytical expressions for the outage probability and energy consumption and showed the trade-off between the number of relay nodes and the number of transmissions. Nevertheless, in all these studies, the impact of interference was never adequately considered.

The authors of [73] proposed a solution to reduce the MTD energy consumption using D2D communications. They presented an energy consumption model taking into account the effects of the interference due to the reuse of radio resources. However, only ARQ scheme was considered in such a study. We aim to complement this gap by considering both

[1] With different redundancy versions.

CC-HARQ and ARQ to draw a thorough performance comparison between both schemes. Moreover, our study goes beyond the existing work by providing a thorough analysis based on stochastic geometry to obtain analytical results rather than simply based on simulation.

4.1.2 Key Contributions and Organization

The main contributions of this chapter are the following:

1. Using stochastic geometry, we derive analytical expressions for the transmission success probability, the average number of transmissions, and the MTD energy consumption for both ARQ and CC-HARQ schemes used in D2D communications with autonomous resource allocation mode.

2. As a particular case, we analyze the performance of both retransmission schemes when the MTD selects the best UE as a relay during the discovery phase.

3. We compare the performance of the ARQ and CC-HARQ schemes in terms of energy consumption, considering a loss probability less than 10% for different MCS levels. Results show that the CC-HARQ scheme outperforms the ARQ scheme especially when the UE density is low.

The rest of this chapter is organized as follows: the system model is described in Section 4.2. The performance analysis is done in Section 4.3. The numerical results and discussion are presented in Section 4.4. Finally, the conclusions of this chapter are shown in Section 4.5.

4.2 System Model

4.2.1 Network Model

In this study, we consider a single cell in which the base station provides connectivity to the UEs and MTDs. All devices are in downlink coverage, and thus they are synchronized to the network. The UEs that have data to transmit always establish direct cellular communication with the base station. We assume that a subset of the UEs serve as relays to the MTDs so that they can connect to the network. These relay candidates are randomly distributed in $\mathbb{R}^2$ forming a homogeneous Poisson point process (H-PPP) Φ_U with density λ_U. An MTD with a data packet to transmit (i.e., an active MTD) uses a UE as a relay, establishing a D2D link. We assume that at a given time, the locations of active MTDs form an H-PPP Φ_M with density λ_M in $\mathbb{R}^2$.

We consider the autonomous resource allocation in D2D communications (see Section 3.3.3). Accordingly, a subset of radio resources, called resource pool, is dedicated to D2D communications, and thus there is no interference between cellular links and D2D links. The MTD randomly selects a radio resource (sub-channel) from a resource pool to transmit its data; therefore, D2D links can share the same sub-channel. In other words, a UE acting as a relay may suffer interference from other MTD-relay links, as shown in Fig. 4.1.

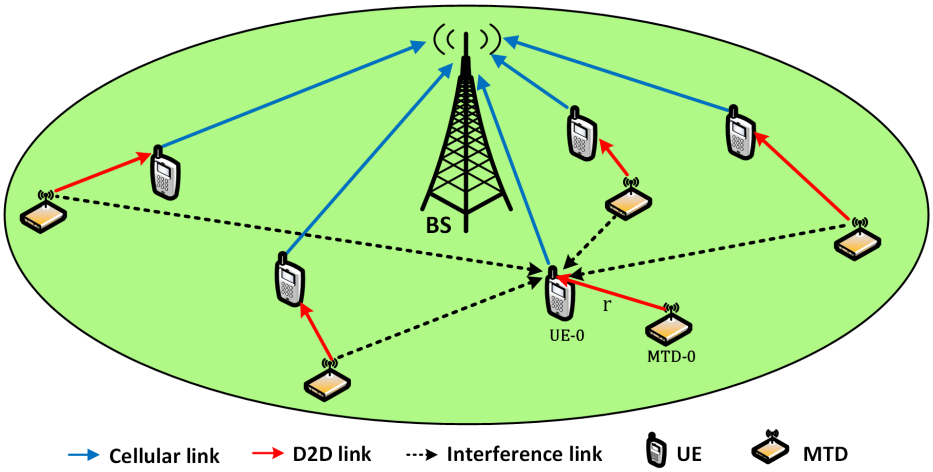

Fig. 4.1 Network model for D2D autonomous resource allocation.

In this study, we derive the energy consumed by the MTD only in the data transmission phase. We assume that the MTD has selected a UE as a relay during the discovery phase. The MTD uses this relay until one transmission is successful or until it reaches the maximum number of allowed attempts.

4.2.2 Propagation Model

The propagation model includes the path loss attenuation as a function of distance, the Rayleigh fading H, and the log-normal shadowing effect $\exp(\chi)$. We assume that MTDs transmit at fixed power P_{tx} and thus the received power at the relays can be derived as:

$$P_{rx} = P_{tx} K r_g^{-\alpha} H \exp(\chi), \tag{4.1}$$

where K and α are respectively the path loss factor and the path loss exponent of the D2D link; r_g is the Euclidean distance between the transmitter and the receiver; H is an exponentially distributed random variable with unit mean, and χ is zero-mean Gaussian random variable with variance σ^2. Log-normal shadowing is also defined in terms of its

dB-spread $\sigma_{dB} = 10\sigma/\ln(10)$. We consider that H and χ are constant during a data packet transmission and mutually independent for different D2D links.

Since the MTD-relay links are affected by shadowing, we use the displacement theorem [87, lemma 1] to simplify the analysis. Hence, the initial homogeneous PPP Φ_M with shadowing can be transformed into a homogeneous PPP Φ'_M with density $\lambda'_M = \lambda_M e^{2\sigma^2/\alpha^2}$ without shadowing but with modified distance $r = r_g \exp(-\chi/\alpha)$ [88]. Therefore, we can rewrite (4.1) as follows:

$$P_{rx} = P_{tx} K r^{-\alpha} H. \tag{4.2}$$

In order to ensure the analytical tractability, in the rest of this chapter, the analysis is based on the modified distance r.

4.2.3 Retransmission Schemes

A device that uses a retransmission scheme transmits a packet until it is successfully received (i.e., after T transmissions) or until a maximum number of transmissions N is reached. The relay answers with an ACK if the packet is received correctly or a negative acknowledgment (NACK) if the packet is received with errors, as shown in Fig. 4.2.

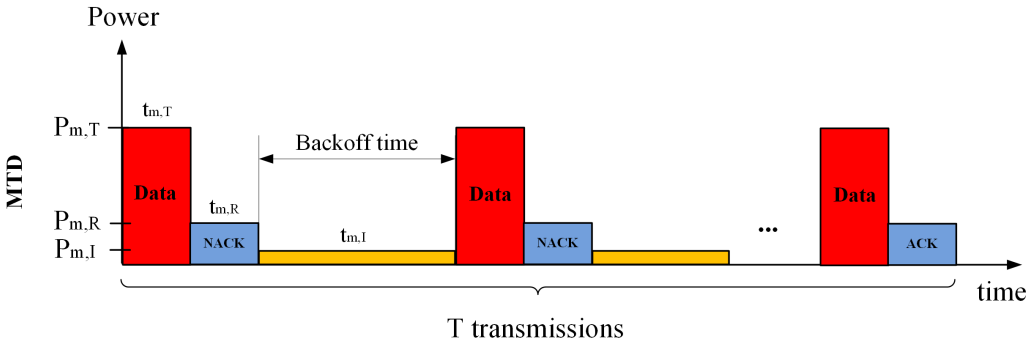

Fig. 4.2 Retransmission scheme.

In this work, we analyze energy consumption of the MTD only when it uses the ARQ and CC-HARQ retransmission mechanisms since, in both cases, the MTD does not need to increase its complexity. In ARQ, if a packet is received wrong, the relay discards it and sends a NACK to the MTD. When the MTD receives a NACK from the relay, it retransmits the same packet. The CC-HARQ scheme performs the same procedure as the ARQ scheme on the transmitter side (MTD). Nevertheless, on the receiver side, the operations a little more complex than in the ARQ, but this additional complexity is acceptable for the relay since it is a user equipment (e.g., a smartphone). In our model, the back-off time $t_{m,I}$ is a random time in which the MTD remains in the idle state, this time allows independent retransmission

in case two or more MTDs transmit at the same time. In other words, the MTDs that cause interference are different from those of the previous transmission. We consider that the ACK/NACK messages are always decoded without error.

4.3 Performance Analysis

In this section, we first analyze the success probability for a single transmission. After that, for a given MTD-relay distance, the global success probability and the average number of transmissions for ARQ and CC-HARQ are respectively derived in Section 4.3.2 and Section 4.3.3. In Section 4.3.4, we study the performance of both schemes when the best UE is selected as a relay. Finally, we provide the analytical expressions for energy consumption of both schemes in Section 4.3.5.

In this study, the global success probability is defined as the probability that the relay successfully receives a data packet after N transmissions, where N is the maximum number of transmissions. The number of transmissions is defined as the total number of transmissions carried out by the MTD, which is equal to the number of rounds until the relay successfully receives the data packet. In case all rounds fail, the number of transmissions is N.

4.3.1 Single Transmission Success Probability

In order to maintain calculation tractability, we consider that the noise power is negligible compared to cumulative interference. Therefore, for a fixed MCS level, a data packet is successfully received by the relay if and only if the signal-to-interference ratio (SIR) is higher than a certain threshold θ_{th}. It is worth mentioning that a threshold θ_{th} is defined for each MCS level. Let θ be the SIR at the relay, and the transmission success probability is thus:

$$P_s = \mathbb{P}(\theta \geq \theta_{th}). \tag{4.3}$$

Without loss of generality, we consider a reference relay (UE-0) located at the origin of coordinates $(0,0)$ and its MTD peer (MTD-0) located at a modified distance r from UE-0. Let S be the number of available sub-channels for D2D communications. An active MTD selects randomly and uniformly one of the available sub-channels to transmit its data, i.e., it selects a certain sub-channel with a probability of $1/S$. Therefore, the locations of the active MTDs that have chosen the same sub-channel as MTD-0 form a thinning PPP $\Phi_m = \{x_i\}$ from Φ'_M, with density $\lambda_m = \lambda'_M/S = \lambda_M \exp(2\sigma^2/\alpha^2)/S$ (Theorem A.1.3), where x_i refers to the location of MTD-i. According to (4.2), each MTD-i generates a certain interference level in the link between MTD-0 and UE-0. The cumulative interference at UE-0 can be

expressed as:

$$I = \sum_{x_i \in \Phi_m} P_{tx} K r_{x_i}^{-\alpha} H_{x_i}, \tag{4.4}$$

where r_{x_i} is the distance between UE-0 and MTD-i, all H_{x_i} are identical and independent distributed (i.i.d.) exponential random variables with unit mean.

Combining (4.2) and (4.4), we obtain the SIR at UE-0:

$$\theta = \frac{P_{rx}}{I} = \frac{P_{tx} K r^{-\alpha} H}{\sum_{x_i \in \Phi_m} P_{tx} K r_{x_i}^{-\alpha} H_{x_i}} = \frac{r^{-\alpha} H}{\sum_{x_i \in \Phi_m} r_{x_i}^{-\alpha} H_{x_i}}. \tag{4.5}$$

By substituting (4.5) into (4.3), we have:

$$P_s = \mathbb{P}\left(\frac{r^{-\alpha} H}{\sum_{x_i \in \Phi_m} r_{x_i}^{-\alpha} H_{x_i}} \geq \theta_{th} \right) = \mathbb{P}\left(H \geq \theta_{th} r^{\alpha} \sum_{x_i \in \Phi_m} r_{x_i}^{-\alpha} H_{x_i} \right). \tag{4.6}$$

The above expression is well investigated in the literature when $H \sim \exp(1)$ and Φ_m is a homogeneous PPP with density λ_m; a closed-form expression is derived in [89]:

$$P_s(r) = \exp(-\pi \lambda_m r^2 \theta_{th}^{2/\alpha} \Gamma(1+2/\alpha)\Gamma(1-2/\alpha)), \tag{4.7}$$

where $\Gamma(x) = \int_0^{\infty} t^{x-1} e^{-t} dt$ denotes the gamma function.

In our model $\lambda_m = \lambda_M \exp(2\sigma^2/\alpha^2)/S$, where λ_M is the density of active MTDs and S is the number of available sub-channels for D2D communications. Hence, we can rewrite (4.7) as follows:

$$P_s(r) = \exp\left(-\pi \lambda_M e^{2\sigma^2/\alpha^2} r^2 \theta_{th}^{2/\alpha} \Gamma\left(1+\frac{2}{\alpha}\right) \Gamma\left(1-\frac{2}{\alpha}\right) / S \right). \tag{4.8}$$

The CDF of the SIR at UE-0 can be derived as follows:

$$F_{\theta}(x) = 1 - \mathbb{P}(\theta \geq x) = 1 - \exp\left(-\pi \lambda_M e^{2\sigma^2/\alpha^2} r^2 x^{2/\alpha} \Gamma\left(1+\frac{2}{\alpha}\right) \Gamma\left(1-\frac{2}{\alpha}\right) / S \right). \tag{4.9}$$

We find the PDF of θ by deriving (4.9):

$$f_{\theta}(x) = \frac{dF_{\theta}(x)}{dx} = \frac{\beta}{\Omega} \left(\frac{x}{\Omega}\right)^{\beta-1} e^{-(x/\Omega)^{\beta}}, \tag{4.10}$$

where $\Omega = (\pi \lambda_M e^{2\sigma^2/\alpha^2} r^2 \Gamma(1+2/\alpha)\Gamma(1-2/\alpha)/S)^{-\alpha/2}$ and $\beta = 2/\alpha$.

Note that (4.10) is the PDF of a Weibull distribution of shape parameter β and scale parameter Ω. Therefore, θ follows a Weibull distribution with parameters β and Ω.

4.3.2 Performance of ARQ Scheme

In this section, we analyze the performance of ARQ in terms of the global success probability and the average number of transmissions. In the ARQ scheme, when the relay receives a packet with errors, it discards this packet and responds with a NACK. If the MTD receives a NACK, it attempts to send the same packet again after a random time.

4.3.2.1 Global Success Probability for a Given Distance

In a single transmission, a data packet is successfully received by the relay with a probability $P_s(r)$, which is given by (4.8). This event is independent of the previous transmissions [73]. Therefore, in the ARQ scheme, the global success probability after N transmissions can be derived as:

$$P_{s,\text{arq}}(r) = 1 - (1 - P_s(r))^N, \tag{4.11}$$

where r is the modified distance between the MTD and the relay.

4.3.2.2 Average Number of Transmissions for a Given Distance

Let T_{arq} be the number of transmissions performed by the MTD using the ARQ scheme. The MTD stops the transmissions when it receives an ACK or when the maximum number of transmissions N is reached. Therefore, T_{arq} is a discrete random variable with range $\{1,2,...,N\}$ and its average can be calculated as follows:

$$\overline{T}_{\text{arq}}(r) = \sum_{n=1}^{N} n\mathbb{P}(T_{\text{arq}} = n), \tag{4.12}$$

where $\mathbb{P}(T_{\text{arq}} = n)$ is the probability that the MTD transmits n times the same packet.

For $n \in \{1,2,...,N-1\}$, the MTD transmits n times a packet when the first (n-1) rounds fail and the nth round is successful. Since the consecutive transmissions are mutually independent, $\mathbb{P}(T_{\text{arq}} = n) = (1 - P_s(r))^{n-1} P_s(r)$. The probability that the MTD transmits N times is $(1 - P_s(r))^{N-1}$ whether the transmission is successful or unsuccessful since it is the maximum number of allowable attempts. Thus, we have:

$$\mathbb{P}(T_{\text{arq}} = n) = \begin{cases} (1 - P_s(r))^{n-1} P_s(r), & \text{if } n \in \{1,2,...,N-1\} \\ (1 - P_s(r))^{N-1}, & \text{if } n = N. \end{cases} \tag{4.13}$$

By substituting (4.13) into (4.12) and simplifying, the average number of transmissions in the ARQ scheme is:

$$\begin{aligned}\overline{T}_{\text{arq}}(r) &= \sum_{n=1}^{N-1} n(1-P_s(r))^{n-1}P_s(r) + N(1-P_s(r))^{N-1} \\ &= \frac{1-(1-P_s(r))^N}{P_s(r)},\end{aligned} \tag{4.14}$$

where $P_s(r)$ is given by (4.8).

From (4.11), we can also derive the z-th percentile number of transmissions for ARQ:

$$T_{z-th,arq}(r,z) = \min\left\{\frac{\ln(1-z/100)}{\ln(1-P_s(r))}, N\right\}. \tag{4.15}$$

4.3.3 Performance of CC-HARQ Scheme

4.3.3.1 Global Success Probability for a Given Distance

In the CC-HARQ scheme, when a new packet arrives, it is combined with the packets received in the previous rounds. The success probability in each new transmission depends on the previous transmissions. We assume that the relay uses the maximum ratio combining (MRC) technique [90]. In other words, the energy is accumulated in each round. Therefore, the global SIR after n transmissions Θ_n can be written as [91]:

$$\Theta_n = \sum_{i=1}^{n} \theta_i, \tag{4.16}$$

where θ_i is the SIR at the relay in transmission i. The SIR is i.i.d. for successive transmissions since we assume that at a given time, the locations of active MTDs form an H-PPP, and between two consecutive transmissions, the active devices are not the same.

Let φ_n be the probability that the transmission does not end at the nth transmission. In other words, φ_n is the probability that the first n transmissions fail, which can be expressed as:

$$\varphi_n = \mathbb{P}(\Theta_n < \theta_{th}) = \mathbb{P}(\sum_{i=1}^{n} \theta_i < \theta_{th}). \tag{4.17}$$

To provide an analytical expression of the global success probability, we first need to simplify (4.17). In Section 4.3.1, we have shown that θ_i follows a Weibull distribution with shape β and scale Ω parameters, which are given in (4.10). Therefore, the problem comes down to calculating φ_n, which is the CDF of the sum of n i.i.d. Weibull random variables. This was studied in depth in [92] where the authors present an approximate formula that

gives a result very close to the exact value; we use the same formula to rewrite analytically (4.17):

$$\varphi_n = 1 - \exp(-U_n(r)) \sum_{i=0}^{n-1} \frac{(U_n(r))^i}{i!} = 1 - \frac{\Gamma(n, U_n(r))}{(n-1)!}, \tag{4.18}$$

where $\Gamma(a,x) = \int_x^\infty t^{a-1}e^{-t}dt$ is the upper incomplete gamma function and

$$U_n(r) = \frac{\pi\lambda_M e^{2\sigma^2/\alpha^2} r^2}{S} \Gamma\left(1+\frac{2}{\alpha}\right) \Gamma\left(1-\frac{2}{\alpha}\right) \left(\frac{\Gamma(n+\alpha/2)\theta_{th}}{n!\Gamma(1+\alpha/2)}\right)^{2/\alpha}. \tag{4.19}$$

The global success probability after N transmissions can be expressed as follows:

$$P_{s,\text{harq}}(r) = 1 - \varphi_N = \frac{\Gamma(N, U_N(r))}{(N-1)!}. \tag{4.20}$$

4.3.3.2 Average Number of Transmissions for a Given Distance

Let T_{harq} be the number of transmission of a data packet in the CC-HARQ scheme. The average number of transmissions can be derived as in [93]. The transmission n is successful with probability $\varphi_{n-1} - \varphi_n$, for $n \in \{1,2,...,N\}$, where N is the maximum number of transmissions, φ_n is defined in (4.18), and $\varphi_0 = 1$. Recall that the number of transmissions is N in two cases: when the transmission is successful at the Nth round and when all transmissions are unsuccessful, the latter has a probability of φ_N. Hence, the average number of transmissions of a packet is:

$$\begin{aligned} \overline{T}_{\text{harq}}(r) &= \sum_{n=1}^{N} n(\varphi_{n-1} - \varphi_n) + N\varphi_N \\ &= 1 + \sum_{n=1}^{N-1} \varphi_n. \end{aligned} \tag{4.21}$$

By substituting (4.18) into (4.21), we obtain:

$$\overline{T}_{\text{harq}}(r) = N - \sum_{n=1}^{N-1} \frac{\Gamma(n, U_n(r))}{(n-1)!}, \tag{4.22}$$

where $U_n(r)$ is defined in (4.19).

For CC-HARQ, the z-th percentile number of transmissions $T_{z-th,\text{harq}}$ can be derived from (4.20):

$$T_{z-th,\text{harq}}(r,z) = \min\{n^*, N\}, \tag{4.23}$$

where n^* is the smallest integer value satisfying the following equation:

$$\frac{\Gamma(n^*, U_{n^*}(r))}{(n^*-1)!} \geq \frac{z}{100}. \tag{4.24}$$

We can use numerical computation to obtain n^*.

4.3.4 Best UE Selected as a Relay

In this section, we analyze a special case where the MTD-0 has selected the best UE as a relay during the discovery phase. According to a definition provided by [94], the best UE is the device for which the received power averaged over all fading realizations is the strongest. By using the displacement theorem as in Section 4.2.2, the initial PPP Φ_U is equivalent to a transformed PPP Φ'_U without shadowing, and the best UE in Φ_U is equivalent to the nearest UE (in terms of modified distance) in Φ'_U.

Let R be the distance between the MTD and the nearest UE in Φ'_U. As the locations of MTDs and UEs form two independent H-PPPs, the UE density λ_U is strongly related to R as shown in [95], the PDF of R is given by:

$$f_R(r) = 2\pi\lambda'_U \exp(-\pi\lambda'_U r^2) r,\ r \geq 0, \tag{4.25}$$

and the CDF of R is given by:

$$F_R(r) = \mathbb{P}(R \leq r) = 1 - \exp(-\pi\lambda'_U r^2),\ r \geq 0, \tag{4.26}$$

where $\lambda'_U = \lambda_U \exp(2\sigma^2/\alpha^2)$ is the UE density in the transformed PPP Φ'_U.

4.3.4.1 Performance of ARQ Scheme

For a given modified MTD-relay distance, the global success probability and the average number of transmissions for ARQ are derived in Section 4.3.2.1 and Section 4.3.2.2, respectively. When the best UE is selected as a relay, the modified MTD-relay distance R is a random variable whose PDF $f_R(r)$ given by (4.25). Thus, when the best UE is selected as a relay, the transmission success probability $P^{\text{best}}_{s,\text{arq}}$ for the ARQ scheme is derived by combining (4.11) and (4.25) as follows:

$$\begin{aligned} P^{\text{best}}_{s,\text{arq}}(\lambda_U) &= \int_0^{+\infty} P_{s,\text{arq}}(r) f_R(r) dr \\ &= \int_0^{+\infty} (1-(1-P_s(r))^N) 2\pi\lambda_U e^{2\sigma^2/\alpha^2} \exp(-\pi\lambda_U e^{2\sigma^2/\alpha^2} r^2) r dr, \end{aligned} \tag{4.27}$$

where $P_s(r) = \exp(-\pi\lambda_M e^{2\sigma^2/\alpha^2} r^2 \theta_{th}^{2/\alpha} \Gamma(1+\frac{2}{\alpha})\Gamma(1-\frac{2}{\alpha})/S)$.

Equation (4.27) is simplified as follows. The detailed steps are shown in Appendix B.1.1:

$$P_{s,\text{arq}}^{\text{best}}(\lambda_U) = \sum_{k=1}^{N} \binom{N}{k} (-1)^{k+1} \frac{1}{1+C_1 k}, \tag{4.28}$$

where $\binom{N}{k}$ is the binomial coefficient and

$$C_1 = \frac{\lambda_M}{S\lambda_U} \theta_{th}^{2/\alpha} \Gamma(1+2/\alpha)\Gamma(1-2/\alpha). \tag{4.29}$$

Let $\overline{T}_{\text{arq}}^{\text{best}}$ be the expected number of transmissions for ARQ when the best UE is selected as a relay. For a given distance r, the number of transmissions $\overline{T}_{\text{arq}}(r)$ of ARQ is given by (4.14). Thus, we have:

$$\begin{aligned} \overline{T}_{\text{arq}}^{\text{best}}(\lambda_U) &= \mathbb{E}_R[\overline{T}_{\text{arq}}(r)] \\ &= \int_0^{+\infty} \frac{1-(1-P_s(r))^N}{P_s(r)} 2\pi\lambda_U e^{2\sigma^2/\alpha^2} \exp(-\pi\lambda_U e^{2\sigma^2/\alpha^2} r^2) r dr. \end{aligned} \tag{4.30}$$

where $\mathbb{E}_R[\cdot]$ is the expectation operator with respect to R. Equation (4.30) is simplified as follows (more details are given in Appendix B.1.2):

$$\overline{T}_{\text{arq}}^{\text{best}}(\lambda_U) = \sum_{k=1}^{N} \binom{N}{k} (-1)^{k+1} \frac{1}{1+C_1(k-1)}, \tag{4.31}$$

where C_1 is given by (4.29).

4.3.4.2 Performance of CC-HARQ Scheme

For a given modified MTD-relay distance r, the global success probability and the average number of transmissions for CC-HARQ are derived in Section 4.3.3.1 and Section 4.3.3.2, respectively.

Similar to (4.27), the transmission success probability for CC-HARQ when the best UE is selected as a relay can be derived by combining (4.20) and (4.25) as follows:

$$\begin{aligned} P_{s,\text{harq}}^{\text{best}}(\lambda_U) &= \int_0^{+\infty} P_{s,\text{harq}}(r) f_R(r) dr \\ &= \int_0^{+\infty} \left(\frac{\Gamma(N, U_N(r))}{(N-1)!} \right) 2\pi\lambda_U e^{2\sigma^2/\alpha^2} \exp(-\pi\lambda_U e^{2\sigma^2/\alpha^2} r^2) r dr, \end{aligned} \tag{4.32}$$

where $U_N(r) = \pi\lambda_M e^{2\sigma^2/\alpha^2} r^2 \Gamma(1+2/\alpha)\Gamma(1-2/\alpha)/S\left(\frac{\Gamma(N+\alpha/2)\theta_{th}}{N!\Gamma(1+\alpha/2)}\right)^{2/\alpha}$.

Equation (4.32) is simplified as follows. A more detailed description of the steps can be seen in Appendix B.2.1:

$$P_{s,\text{harq}}^{\text{best}}(\lambda_U) = 1 - \frac{1}{(1+C_2)^W}, \tag{4.33}$$

where

$$C_2 = \frac{S\lambda_U(N!\Gamma(1+\alpha/2))^{2/\alpha}}{\lambda_M\Gamma(1+2/\alpha)\Gamma(1-2/\alpha)(\Gamma(N+\alpha/2)\theta_{th})^{2/\alpha}}. \tag{4.34}$$

Let $\overline{T}_{\text{harq}}^{\text{best}}$ be the expected number of transmissions for CC-HARQ when the best UE is selected as a relay. For a given distance r, the number of transmissions $\overline{T}_{\text{harq}}(r)$ of CC-HARQ is given by (4.14). Thus, similar to (4.30) we have:

$$\begin{aligned} \overline{T}_{\text{harq}}^{\text{best}}(\lambda_U) &= \mathbb{E}_R[\overline{T}_{\text{harq}}(r)] \qquad (4.35)\\ &= \int_0^{+\infty} \left(N - \sum_{n=1}^{N-1} \frac{\Gamma(n, U_n(r))}{(n-1)!}\right) 2\pi\lambda_U e^{2\sigma^2/\alpha^2} \exp(-\pi\lambda_U e^{2\sigma^2/\alpha^2} r^2) r dr. \end{aligned}$$

Equation (4.35) is simplified as follows (see Appendix B.2.2):

$$\overline{T}_{\text{harq}}^{\text{best}}(\lambda_U) = 1 + \sum_{n=1}^{N-1} \frac{1}{(1+C_3(n))^n}, \tag{4.36}$$

where

$$C_3(n) = \frac{S\lambda_U(n!\Gamma(1+\alpha/2))^{2/\alpha}}{\lambda_M\Gamma(1+2/\alpha)\Gamma(1-2/\alpha)(\Gamma(n+\alpha/2)\theta_{th})^{2/\alpha}}. \tag{4.37}$$

4.3.5 MTD Energy Consumption Modeling

In this section, we provide the analytical expressions for the energy consumed by the MTD in the data transmission phase. We use the energy consumption model given in Section 2.5.1, where the MTD transmits at a fixed power and each operating state has a constant power consumption. We know from Table 2.4 that the power consumption in the Idle state is insignificant compared to the power consumption in the active state (Tx and Rx). Therefore, to compute the total MTD energy consumption $E_{m,\text{total}}$, we only take into account energy consumption when the MTD is in the active state, i.e., we have:

$$E_{m,\text{total}} = (P_{m,T}t_{m,T} + P_{m,R}t_{m,R})T, \tag{4.38}$$

where T is the number of transmissions of a packet; $P_{m,T}$ and $P_{m,R}$ are the MTD power consumption in Tx state and Rx state, respectively; $t_{m,T}$ and $t_{m,R}$ are the duration of Tx state and Rx state, respectively.

We assume that the MTD transmits at a fixed MCS level (i.e., without link adaptation) during the data transmission phase. This parameter can be previously set, for example, after the discovery phase. Thus, we have $t_{m,T} = D/R_m$, where D is the data packet size and R_m is the MTD data rate (bits per second). In order to ensure that the acknowledgments have enough redundancy to be received correctly by the MTD, we consider that $t_{m,R} = t_{m,T}$. Hence, the average of the total MTD energy consumption can be derived as:

$$\overline{E}_{m,total}(r) = \frac{D(P_{m,T} + P_{m,R})}{R_m}\overline{T}, \tag{4.39}$$

where $\overline{T}$ denotes the average number of transmissions. When the MTD selects the best UE as a relay, $\overline{T}$ is given by (4.31) and (4.36) for ARQ and CC-HARQ, respectively.

4.4 Numerical Results and Discussion

In this section, the numerical results are presented from both the analytical model and simulations. The parameters used in the analysis are given in Section 4.4.1. The analytical results are validated by simulations in Section 4.4.2. Moreover, in this section, we compare the global success probability and the average number of transmission of ARQ and CC-HARQ. In Section 4.4.3, we compare the total MTD energy for both retransmission schemes for a target loss probability of 10%.

4.4.1 Parameters for the Analysis

Simulations are based on a Monte Carlo approach using MATLAB, where each point corresponds to the average value of 3000 iterations. In each iteration, the MTDs and UEs are distributed independently according to two H-PPPs in a square area of 3 km $\times$ 3 km, where UE-0 is located at the center of this area. The simulation parameters are specified in Table 4.1, where the values of the power consumption are according to the 3GPP specifications [3], and the values of the path loss parameters are taken from the path loss model for non-line-of-sight (NLoS) [96].

To compute energy consumption, we use the same MCS levels proposed in [97], as well as their respective SIR thresholds. These parameters are summarized in Table 4.2.

Table 4.1 Simulation parameters

Parameter	Value
MTD power consumption in Tx state ($P_{m,T}$)	545 mW
MTD power consumption in Rx state ($P_{m,R}$)	90 mW
MTD Bandwidth (B_w)	180 kHz
Data packet size (D)	1080 bits
Carrier frequency (f_c)	900 MHz
D2D path loss exponent (α)	4
Density of active MTDs (λ_M)	1.6×10^{-5} MTDs/m^2
Shadowing standard deviation (σ_{dB})	8 dB

Table 4.2 Transmission modes parameters

Mode	Modulation	Coding rate	Rate (bits/sym.)	SIR Threshold (dB)
MCS 1	BPSK	1/2	0.5	-1.5
MCS 2	QPSK	1/2	1.0	1
MCS 3	QPSK	3/4	1.5	4

4.4.2 Simulation versus Analytical Results

Fig. 4.3 compares the global success probability of ARQ and CC-HARQ as a function of the modified MTD-relay distance for $N = \{2,4,50\}$, where NARQ[2] represents the success probability of a single transmission. As can be seen from the figure, the analytical and simulation results match well; this confirms the correctness of (4.8), (4.11), and (4.20). As shown in the figure, in both retransmission schemes, there is a clear trend towards increasing the global success probability as the maximum number of transmissions N increases. Moreover, the CC-HARQ scheme becomes more advantageous than the ARQ scheme as N increases. The reason is that in CC-HARQ, the SIR increases as the number of transmissions increases while in ARQ, the SIR is independent of the number of transmissions.

Fig. 4.4 presents the average and the 95th percentile number of transmissions for the ARQ and CC-HARQ schemes as a function of the modified MTD-relay distance. We can see that the analytical and simulation results match well, which verifies the correctness of (4.14) and (4.22). This figure shows the advantage of CC-HARQ over ARQ in terms of the number of transmissions. This advantage increases significantly when the distance MTD-relay increases.

[2]The term NARQ refers to no ARQ.

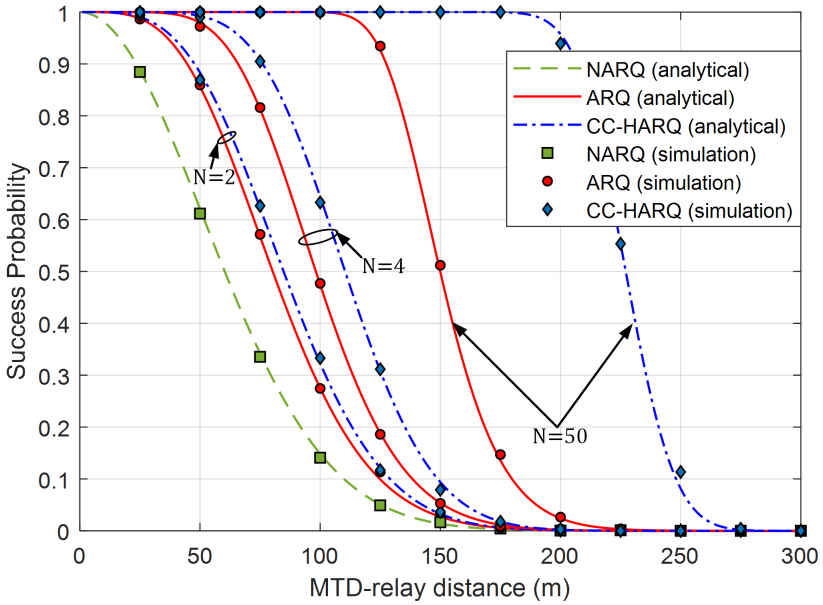

Fig. 4.3 Global success probability of ARQ and CC-HARQ as a function of the modified MTD-relay distance, considering MCS-3, maximum number of transmissions $N = \{2,4,50\}$, $\lambda_M = 16 \times 10^{-6}$ MTDs/m^2, and one sub-channel ($S = 1$).

From the figure, when the MTD-relay distance is 60 meters, 95% of the MTDs transmit successfully in less than 5 and 4 transmissions using ARQ and CC-HARQ, respectively. In contrast, if the distance is 120 meters, 95% of them transmit successfully in less than 47 and 13 transmissions using ARQ and CC-HARQ, respectively.

As mentioned in the previous chapter, the mMTC applications are characterized by their high connection density (MTDs/m^2). At the same time, one of the advantages of D2D relaying is the reuse of radio resources. When the number of MTDs that share a single sub-channel increases, the cumulative interference increases, and thus, the number of transmissions is high. Recall that we consider the autonomous mode, i.e., the base station does not participate in the allocation of radio resources, it only provides a pool of available radio resources (sub-channels). To limit the effects of interference, the base station can increase the number of available sub-channels, which decreases the density of MTDs that share a single sub-channel. In our analytical model, λ_M/S is the density of active MTDs sharing the same sub-channel, where λ_M and S denote the density of active MTDs and the number of available sub-channels, respectively. Note that the larger the S value, the lower the density of MTDs sharing the same sub-channel. Fig. 4.5 compares the average number of transmissions in both retransmission schemes ARQ and CC-HARQ as a function of the UE density and the number of available sub-channels $S = \{1,4,8\}$. As analytical and simulation

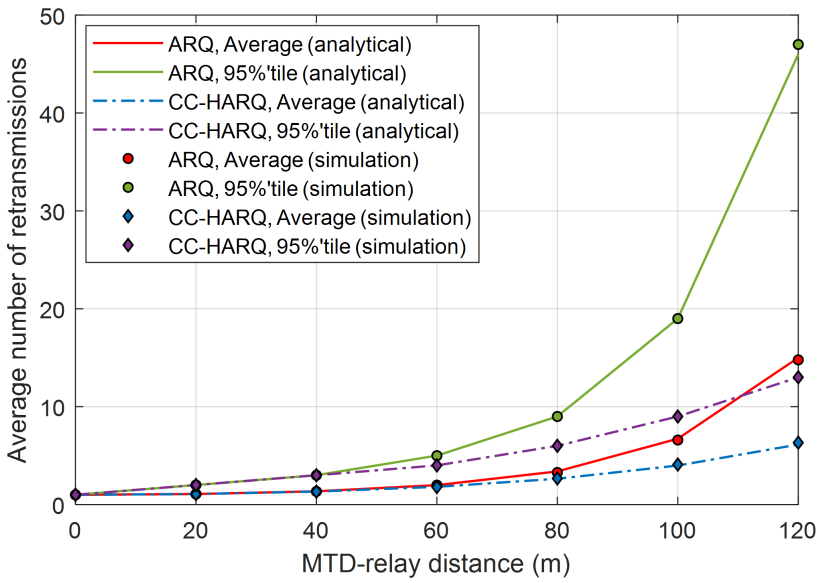

Fig. 4.4 Number of transmissions of ARQ and CC-HARQ as a function of the modified MTD-relay distance, considering MCS-3, maximum number of transmissions $N = 50$, and one sub-channel ($S = 1$).

results match well, we can verify the correctness of (4.31) and (4.36). We observe that CC-HARQ outperforms ARQ in terms of the number of transmissions, especially when the density of MTDs that share a sub-channel is high (e.g., $S = 1$). When the density of MTDs that share a sub-channel is low (e.g., $S = 8$), the CC-HARQ scheme does not provide an important gain compared to the ARQ scheme.

Since the derived analytical expressions and simulations match well, henceforth, we will only use the analytical expressions to analyze the performance of ARQ and CC-HARQ.

4.4.3 Energy Consumption for a Target Loss Probability of 10%

4.4.3.1 Determining the Maximum Number of Transmissions

For a given MCS level, the global success probability depends on the UE density λ_U, the maximum number of transmissions N, and the number of sub-channels S. To compare the ARQ and CC-HARQ schemes, we assume N large enough, such that the loss probability is less than 10% (i.e., a success probability higher than 90%) in both retransmission schemes. Therefore, in this section, we calculate the minimum value of N to ensures 10% loss probability for ARQ and CC-HARQ.

In this thesis, we analyse two UE density scenarios (see Section 3.4.3): low UE density with $\lambda_U = 2.5 \times 10^{-5}$ UEs/m^2 and high UE density with $\lambda_U = 14 \times 10^{-5}$ UEs/m^2. Assuming

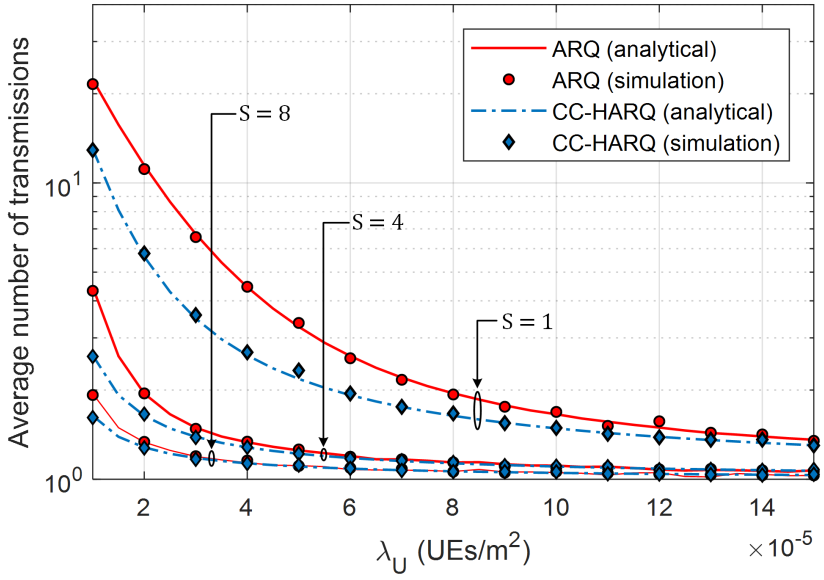

Fig. 4.5 Average number of transmissions of ARQ and CC-HARQ as a function of the UE density, considering MCS-3, maximum number of transmissions $N = 50$, and number of sub-channels $S = \{1, 4, 8\}$.

that the best relay is selected in the discovery phase, the CDF of the modified MTD-relay distance is given by equation (4.26). From this equation, we can infer that the lower the UE density, the higher the probability that the distance between the MTD and the relay is large. When the MTD-relay distance is considerable, there is a greater probability that other MTDs are close to the relay causing high interference and thus unsuccessful transmissions. Therefore, to determine the minimum value of N that ensures a certain success probability for both UE density scenarios, we need to analyze only the worst case, i.e., at low UE density ($\lambda_U = 2.5 \times 10^{-5}$ UEs/m^2).

Fig 4.6 shows the loss probability of ARQ and CC-HARQ as a function of the maximum number of transmissions N for three MCS levels. It can be seen from the figure that in both retransmission schemes, MCS-1 requires a smaller number of transmissions to achieve a certain loss probability. The reason is that the SIR threshold is lower in MCS-1 than in the other MCS levels. With a target loss probability such as 10%, CC-HARQ presents slightly better performance than the ARQ for MCS-1, but for MCS-3, the difference between both retransmission schemes is significant.

From Fig 4.6, we obtain the value of the maximum number of transmissions N, of ARQ and CC-HARQ, that guarantees 5% and 10% loss probability for MCS-1, MCS-2, and MCS-3, these values are summarized in Table 4.3. What stands out in this table is the difference between ARQ and CC-HARQ for MCS-3 and a success probability set at 5%, the maximum

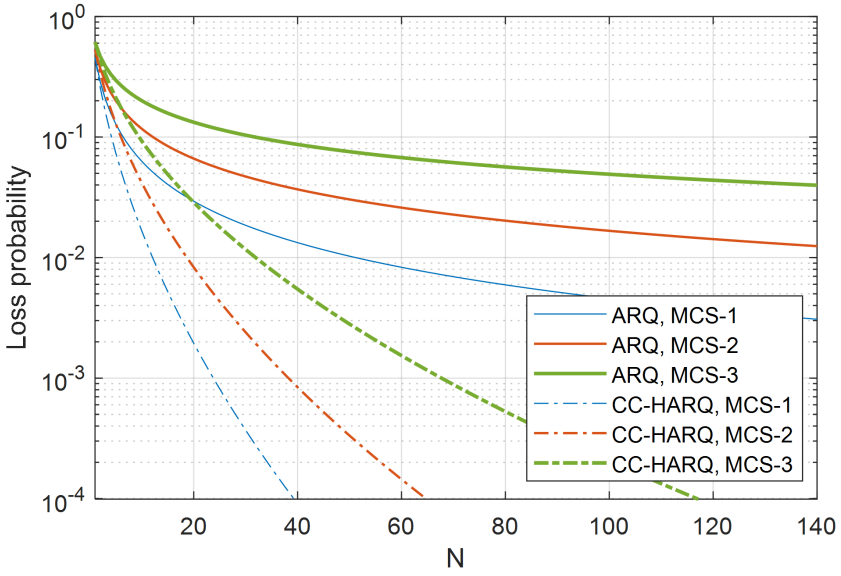

Fig. 4.6 Loss probability as a function of the maximum number of transmissions N for $\lambda_U = 2.5 \times 10^{-5}$ UEs/m^2, considering only one sub-channel ($S = 1$).

number of transmissions N is reduced from 98 to only 15. In contrast, for MCS-1 and a loss probability of 10% loss probability, N is reduced from 7 to 5.

It should be mentioned that the higher the MCS level, the lower the data transmission time (D/R_m). On the other hand, as the table shows, the higher the MCS level, the higher the number of transmissions required. Both the transmission time and the maximum number of transmissions affect energy consumption. In the next section, we compare the performance of both the ARQ and CC-HARQ schemes in terms of energy consumption, taking the target loss probability of 10%.

Table 4.3 Maximum number of transmissions N for 10% and 5% loss probability

MCS level	**MCS-1**		**MCS-2**		**MCS-3**	
Loss probability	**10%**	**5%**	**10%**	**5%**	**10%**	**5%**
ARQ	7	13	13	28	32	98
CC-HARQ	5	7	6	10	10	15

4.4.3.2 Energy Consumption Comparison

One of the main objectives of this study is to investigate the differences between ARQ and CC-HARQ in terms of energy consumption. For this comparison, the loss probability is set

as 10%, in both retransmission schemes, for UE densities greater than 2.5×10^{-5} UEs/m^2. To achieve this loss probability, we have determined the minimum value of N for each MCS level (MCS-1, MCS-2, and MCS-3) in Table 4.3. Using these values, the average MTD energy consumption as a function of the UE density λ_U for three MCS levels is represented in Fig. 4.7. The UE density λ_U varies from 1×10^{-5} UEs/m^2 to 15×10^{-5} UEs/m^2, the MTD density λ_M is fixed as 1.6×10^{-5} MTDs/m^2, parameter N is set according to Table 4.3, and only one sub-channel is used (i.e., $S = 1$).

One interesting result of the figure is that for CC-HARQ, MCS-3 offers the best performance over the entire range of UE densities analyzed. On the other hand, for ARQ, MCS-2 provides the best performance when $\lambda_U \in [1 \times 10^{-5}, 5.5 \times 10^{-5}]$ UEs/m^2 while MCS-3 offers the best performance when $\lambda_U \in [5.5 \times 10^{-5}, 15 \times 10^{-5}]$ UEs/m^2. Moreover, for a given MCS level, the CC-HARQ scheme outperforms the ARQ scheme when the UE density is low, specially for MCS-3. In contrast, when the UE density is high, energy consumption is similar in both retransmission schemes.

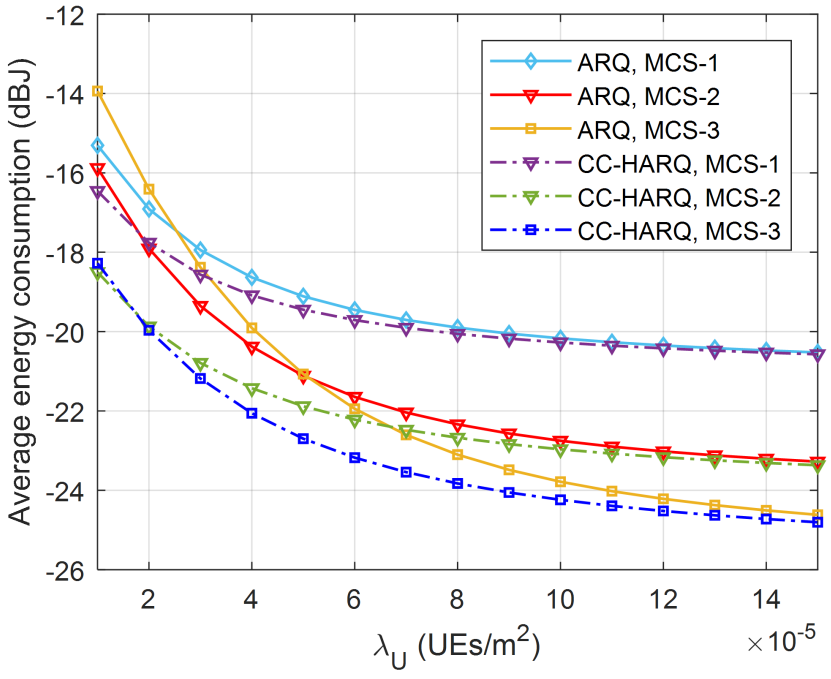

Fig. 4.7 Average energy consumption of ARQ and CC-HARQ as a function of the UE density for 10% loss probability, only one sub-channel ($S = 1$) is considered.

From Fig. 4.7, the average energy consumption (in dBJ) of ARQ and CC-HARQ for $\lambda_U = 2.5 \times 10^{-5}$ UEs/m^2 (low UE density scenario) and $\lambda_U = 14 \times 10^{-5}$ UEs/m^2 (high UE density scenario) are summarized and compared in Table 4.4. In this study, the energy reduction

factor (in dB) is defined as the difference between energy consumption of CC-HARQ (in dBJ) and energy consumption of ARQ (in dBJ). We observe that for $\lambda_U = 2.5 \times 10^{-5}$ UEs/m^2 and MCS-3, the energy reduction factor is -3.17 dB, i.e., energy consumption is divided by 2. On the other hand, for the same MCS level and high UE density ($\lambda_U = 14 \times 10^{-5}$ UEs/m^2), the energy reduction factor is -0.21 dB, i.e., the energy consumption of CC-HARQ is 0.96 times the energy consumption of ARQ.

Table 4.4 Energy reduction factor for loss probability less than 10%

UE density (UE/m^2)	$\lambda_U = 2.5 \times 10^{-5}$			$\lambda_U = 14 \times 10^{-5}$		
MCS level	**MCS-1**	**MCS-2**	**MCS-3**	**MCS-1**	**MCS-2**	**MCS-3**
ARQ (dBJ)	-17.48	-18.69	-17.45	-20.48	-23.20	-24.51
CC-HARQ (dBJ)	-18.21	-20.37	-20.62	-20.53	-23.31	-24.72
Energy Reduction (dB)	-0.73	-1.68	-3.17	-0.05	-0.11	-0.21

4.5 Conclusion

In this chapter, we have compared the performance of the ARQ and CC-HARQ schemes used in D2D communications for mMTC applications. The system model considers autonomous resource allocation and thus interference between D2D links. The propagation model takes into account the Rayleigh fading as well as the log-normal shadowing. By using stochastic geometry, we have derived analytical expressions for the transmission success probability, the average number of transmissions, and MTD energy consumption. Simulations have confirmed these analytical expressions.

The numerical results show that the CC-HARQ scheme outperforms the ARQ scheme when the UE density is low. For example, for a UE density of 2.5×10^{-5} UEs/m^2 the energy consumption is divided by 2 when CC-HARQ is used instead of ARQ. On the other hand, when the UE density is high, both retransmission schemes present almost similar performance. Moreover, the higher the MCS level is more significant is the difference between CC-HARQ and ARQ in terms of energy consumption.

In this chapter, we have analyzed the MTD energy consumption only for the data transmission phase. However, before this phase, the MTD must search and select a relay (discovery phase). Moreover, we have assumed that the MTD selects the best UE as a relay during the discovery phase. However, the selection of the best relay can lead to high energy consumption (compared to total energy consumption) in the discovery phase. In the next chapter, we will propose a relay selection strategy that allows a reduction of the total MTD energy

consumption. We will also analyze the total energy consumption (i.e., discovery and data transmission phases) when the MTD uses a D2D relaying mechanism.

Chapter 5

Energy-efficient D2D Relaying Mechanism for mMTC Applications

5.1 Introduction

In the previous chapter, we have studied the energy consumption in the data transmission phase. However, before establishing D2D communication, the MTD must select a UE using a D2D relay selection mechanism during the discovery phase.

The discovery phase is crucial since it must ensure the selection of the optimal relay. The optimal relay selection depends on various parameters, including energy consumption and the bit rate. However, in the realm of mMTC applications, energy consumption is widely considered as among the most critical parameters and hence, the best relay selection has to offer the minimum of MTD energy consumption. In other words, the best relay will be the UE that allows minimizing MTD energy consumption. It is well established that the better the MTD-relay channel quality (i.e., SNR), the lower the energy consumption in the data transmission phase. Nevertheless, finding the UE with the best channel quality can imply an increase in energy consumption during the discovery phase. Unlike eMMB applications where the energy consumption of the discovery phase is negligible compared to the consumption during the D2D communication (big data flows) in mMTC applications the energy consumption during the discovery phase is comparable or may even be greater than the energy consumption during the D2D communication, especially when the data packet size is lower than 200 bytes.

In this chapter, we propose an energy-efficient D2D relaying mechanism, offering a reduction of the total MTD energy consumption (i.e., the energy consumed in the discovery phase and the data transmission phase). Using stochastic geometry, we analyze the performance of

our proposal and draw a comparison between the analytical and simulation results to verify the model accuracy. A part of the content of this chapter has been published in [52], [98].

5.1.1 Related Work

There has been extensive research work investigating the energy-efficient relay selection in the literature and mostly focusing on wireless sensor networks. The widely considered scenario for existing studies is that all devices including those serving as relays have strict energy consumption constraints (i.e., all devices are MTDs). As a consequence, the energy consumed by the relay has been taken into account in the majority of proposed relaying mechanisms. On the other hand, recent studies have started to demonstrate benefits in terms of MTD energy consumption associated with D2D relaying, where UEs act as relays. Therefore, our survey on related work is divided into two groups, namely, the studies related to wireless sensor networks and studies related to cellular networks.

In the wireless sensor networks context, the authors of [99] of ADOPNET research team[1] proposed a relay selection mechanism. In this mechanism, the node with the smallest path loss with respect to the sink has a higher probability for being selected as the next-hop node (i.e., the relay). The authors extended their research by adding the residual energy of the nodes relay as a parameter of the next-hop node selection in [62]. They showed that their protocol extends the network lifetime, reduces the average number of hops and the average end-to-end delay. Our relay selection protocol is based on the same idea but adapted to the reduction of MTD energy consumption. Unlike both previous studies where the results are obtained only by simulation, in my thesis work, I derive analytical results, which are then confirmed by simulations. The authors of [65] proposed two relay selection schemes: (i) to minimize the overall energy consumption and (ii) to maximize the network lifetime. Both schemes have a first phase where the nodes use the Request-to-Send and Clear-to-Send (RTS/CTS) handshake to obtain the channel gains. Based on this information, the relay candidates compete and only one candidate is selected in a second phase. In their protocol, the relay candidate that reduces the total energy consumption has the highest priority to win the contention process. However, the authors have not considered the extra energy consumption due to the RTS/CTS phase and the relay competition. The authors of [100] proposed a Medium Access Control (MAC) protocol called Sift. This protocol uses a truncated increasing geometric distribution function to pick a time slot within a fixed-size contention window. The main idea is to increase the transmission probability in case no device has transmitted in the previous slot. For large packet sizes, the authors proposed the

[1] I was a member of the ADOPNET research team during my PhD thesis.

use of Sift with RTS/CTS protocol, where the competition occurs in the transmission of the RTS packet.

The relay selection protocol of our D2D relaying mechanism is based on the RTS/CTS protocol, like all these previous studies. Unlike these authors, we focus only on reducing MTD energy consumption. Our relay selection protocol selects a relay from the set of UEs (e.g., smartphones) available on the network. These devices have less stringent energy constraints than MTDs since users frequently recharge their batteries. Moreover, our protocol takes into account the channel quality of the MTD-UE links as a key parameter to select the best relay.

In a cellular network context where the UEs act as relays, the authors of [76] analytically determined a region between the transmitter and the receiver, called energy-saving zone. The relay candidates located inside this region allow a reduction of the total energy consumption and thus can be used as relays. One drawback of this approach is that the devices are required to be aware of their location, which is often a complicated task for MTDs. The authors in [101] derived the optimal relay selection range, the achievable transmission capacity of relay-assisted transmission, and the optimal transmission power ratio of cellular and D2D systems. However, the authors of these previous studies have not considered the extra cost of the relay selection protocol in their analysis. In [102], the authors studied the discovery probability of two devices, exploiting the existing knowledge of the network layout. They provided the optimal base station density that maximizes the D2D discovery probability. The issue of energy-efficient relay selection process for mMTC applications has been analyzed in some studies [77, 61, 53, 52]. The authors of [77] proposed a reduction of energy consumption through an optimization approach. They analyzed the relay selection, channel allocation, and power control as a joint optimization problem. In [53], the authors suggested an energy-efficient relay selection by using the double auction theory in cooperative cellular networks. They considered that the base station acts as auctioneer matching buyers represented by source users with sellers represented by relays. Another approach different from the previous ones is to consider that the operator deploys the relays as in [61]. In this study, the authors analyzed the relay positioning issue to minimize the global energy consumption (i.e., the energy consumed by all devices) while satisfying the QoS constraints of IoT devices.

To the best of our knowledge, the existing work in the literature have adopted the centralized approach (i.e., network-assisted) based on a central entity such as the base station which is responsible for the selection of the optimal relay. As opposed to this approach, we propose an energy-efficient D2D relaying mechanism in a distributed manner (i.e., without the participation of the BS). Our approach offers the merit of avoiding the

signaling overhead between the MTDs and the base station during the discovery phase, a major problem especially for mMTC applications.

5.1.2 Key Contributions and Organization

The energy-efficient relay selection is one of the main challenges of the discovery phase in mMTC applications. As pointed out in the related studies, the majority of existing studies exploiting the use of UEs as relays were focused only on energy consumption in the data transmission phase while ignoring the discovery phase. In contrast, the studies considering the energy consumption in both phases (i.e., in a wireless network approach) missed the opportunity offered by the UEs distributed in the cell.

As one of the key objectives of my thesis is to demonstrate the advantages of D2D relaying for mMTC applications, we thus analyze the total MTD energy consumption in an approach where the UEs are used as relays. The main contributions of our studies in this chapter can be summarized as follows:

1. We propose a D2D relaying mechanism suitable for mMTC applications thanks to the ease of implementation and the merit of saving total MTD energy consumption. Our proposal adopts a distributed approach and prioritizes the relay selection to the UEs with the best channel qualities. The results demonstrate that our proposed mechanism offers an almost constant energy consumption for an extensive range of UE densities and MTD-BS distances while not having access to the location information of the MTD or the exact UE density, which is differentiated itself from existing studies.

2. Our mechanism uses a random choice of time-slot based on a truncated geometric distribution. We derive analytical expressions for the relay discovery probability, the average number of time slots used in the contention process, the PDF of the MTD-relay distance, and the total MTD energy consumption in the D2D mode. These derived analytical expressions are then confirmed by simulations.

3. We present the uniform random choice of time slot as a special case of our mechanism. For this approach, we derive the optimal contention window size and the optimal radius of the discovery area.

4. We compare the total MTD energy consumption in cellular mode and D2D mode (using our D2D relaying mechanism). In order to determine the scenarios in which our mechanism allows a reduction of energy consumption, different scenarios are evaluated by varying the UE density, the data packet size, and the MTD-BS distance.

The rest of this chapter is organized as follows: Section 5.2 describes the system model for a single base station. Our D2D relaying mechanism is described in Section 5.3. In Section 5.4 and Section 5.5, the analysis of our mechanism is conducted and the numerical results are presented in Section 5.6. The conclusions of this chapter are presented in Section 5.7.

5.2 System Model

5.2.1 Network Model

We consider a single base station, which provides connectivity to the UEs and MTDs located within the coverage area, as illustrated in Fig. 5.1. The UEs and the MTDs are randomly distributed in $\mathbb{R}^2$ forming two independent H-PPPs with densities λ_u and λ_m, respectively. The UEs establish direct communication with the base station as in traditional

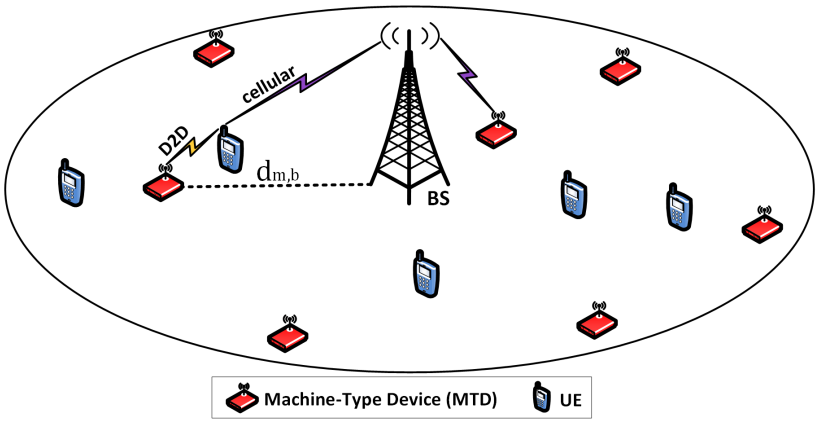

Fig. 5.1 Network model where MTDs and UEs are randomly distributed in a single cell network.

cellular communications. The MTDs can choose between transmitting directly to the base station (cellular mode) and using a nearby UE as a relay (D2D mode). They will select the communication mode that consumes the minimum amount of energy.

As mentioned in Chapter 2, the D2D relaying consists of three phases: synchronization, discovery, and data transmission. In this work, we adopt an assumption that the UEs and MTDs are synchronized with the base station and hence, our work is focused on analyzing the discovery and data transmission phases. Recalling briefly the activities that the MTD performs in these phases:

- **Discovery phase:** In this phase, the MTD searches and selects a UE that can be used as a relay to transmit its data to the base station.

- **Data transmission phase:** If the MTD selects a relay, it transmits its data to the relay via a D2D link, then the relay re-transmits the MTD data to the BS. Otherwise, the MTD transmits its data directly to the base station via a cellular link.

We assume that the base station allocates dedicated resources for D2D communications, i.e., there is no interference between D2D links and cellular links.

5.2.2 Propagation Model

We use the same propagation model given in Section 4.2.2. Nevertheless, to keep the analytical tractability of this study, we assume that the fading is averaged out. Thus, we have a log-normal shadowing propagation model [103, 99], where the received power P_{rx} can be obtained as follows:

$$P_{rx} = P_{tx} K r_g^{-\alpha} \exp(\chi), \tag{5.1}$$

where P_{tx} is the transmission power, r_g is the Euclidean distance between transmitter and receiver, K and α are the path-loss factor and the path-loss exponent, respectively, and χ is a zero-mean Gaussian random variable with variance σ^2. We assume that the channel between two devices remains constant during the discovery phase, and each communication mode (cellular and D2D) has specific K and α values.

Without loss of generality, we consider that the MTD under study is located at the origin of coordinates, and the base station is located at a distance $d_{m,b}$ from the MTD. Similar to Section 4.2.2, we use the displacement theorem to transform the initial homogeneous PPP Φ_u with shadowing into a homogeneous PPP Φ'_u with density $\lambda'_u = \lambda_u e^{2\sigma^2/\alpha^2}$ without shadowing. Thus, we can rewrite (5.1) as follows:

$$P_{rx} = P_{tx} K r^{-\alpha}, \tag{5.2}$$

where $r = \exp(-\chi/\alpha) r_g$ represents the modified distance, it combines the path loss due to the distance and the shadowing effects. In the rest of this chapter, the performance analysis of D2D links will be based on this modified distance.

From (5.2), the propagation model of the D2D link becomes a distance-based path loss model. Thus, the path loss between the MTD and a UE as a function of the modified distance r is:

$$L_{m,u} = r^{\alpha_d} / K_d. \tag{5.3}$$

where K_d and α_d are respectively the path loss factor and path loss exponent of D2D links.

5.3 D2D Relaying Protocol Description

5.3.1 Assumptions

Before introducing our D2D relaying mechanism, the following assumptions are made:

- MTDs and UEs transmit at a fixed transmission power, i.e., they do not use power control.
- The channel is reciprocal, i.e., the channel from point A to B is the same as the channel from B to A.
- The MTD determines the MTD-BS path loss $L_{m,b}$ by measuring the signal strength of downlink reference transmitted by the BS.
- UE$_i$ determines the MTD-UE$_i$ path loss L_{m,u_i} by measuring the signal strength transmitted by the MTD over the D2D link.
- It will not be worth using a relay when the MTD is under good channel conditions, for example, when it is close to the base station. For this reason, the cellular operator should define a path loss threshold $L_{th,\text{cell}}$, which determines the transmission mode that the MTD will use to transmit its data.
- UE$_i$ is a relay candidate if and only if $L_{m,u_i} < L_{th}$, where L_{th} is the D2D path loss threshold. The value of L_{th} can be preconfigured in advance by the cellular operator or indicated by the base station. In the transformed PPP Φ'_u, the condition $L_{m,u_i} < L_{th}$ is equivalent to considering that UE$_i$ is a relay candidate if and only if it is located inside a circular area of radius R_d centered around the MTD as shown in Fig. 5.2. This area is called the discovery area in this study. From (5.3), L_{th} is related to R_d by equation: $R_d = (K_d L_{th})^{1/\alpha_d}$.
- When multiple relay candidates transmit in the same time slot, we assume that a destructive collision occurs.
- We assume half-duplex operations.

5.3.2 D2D Relaying Mechanism

In this section, we first describe the overall communication process of an MTD, from the moment it wakes up to transmit some data to the station base until it returns to the idle state. We then describe in more details the choice of time slot by the relay candidate.

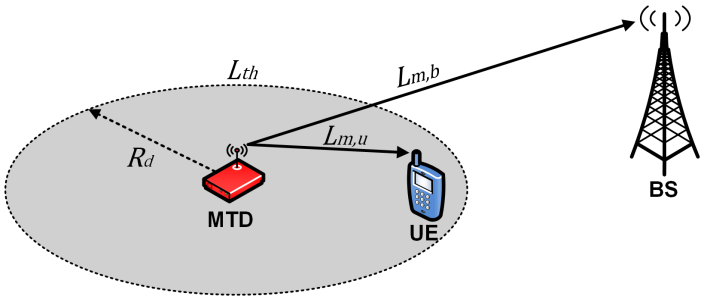

Fig. 5.2 Discovery area.

Fig. 5.3 illustrates the D2D relaying procedures for the MTD and the nearby UEs. These procedures consist of the following steps:

1. *Synchronization and network configuration:* The MTD synchronizes with the base station and then reads the configuration messages sent by the base station. The MTD measures the path loss $L_{m,b}$ between itself and the base station, and starts the discovery phase if $L_{m,b} > L_{th,\text{cell}}$; otherwise, it transmits its data directly to the base station.

2. *RR packet transmission:* The MTD broadcasts a Request-for-Relay (RR) packet that carries its ID and optionally the parameters L_{th} and W. Then, it listens to the channel waiting for a response (RC packet) from a nearby UE.

3. *Contention process:* A UE that receives an RR packet measures the path loss $L_{m,u}$ between the MTD and itself and checks if it satisfies the condition $L_{m,u} < L_{th}$. The UEs that satisfy this condition (relay candidates) participate in the contention process. Let W be the contention window size, which is previously defined by the cellular operator or sent by the MTD within the RR packet. Each relay candidate chooses randomly a time-slot $s \in [1, W]$ and responds with a Relay-Candidate (RC) packet in that time-slot. The RC packet carries the ID of the relay candidate.

4. *Feedback transmission:* The MTD broadcasts the feedback packet as soon as it successfully receives an RC packet. In other words, the first relay candidate that transmits an RC packet without collision wins the contention process. The feedback packet carries the selected relay ID and the MCS level to be used during the data transmission phase. After reading the feedback packet, only the selected relay remains active (i.e., in Rx state), the other relay candidates stop contending and thus switch to the idle state.

5. *Data transmission:* If the MTD selects a relay, it establishes a D2D link with the selected relay to transmit its data. Otherwise, the MTD transmits its data directly to the base station. In both cases, the MTD uses a dynamic data rate adaptation.

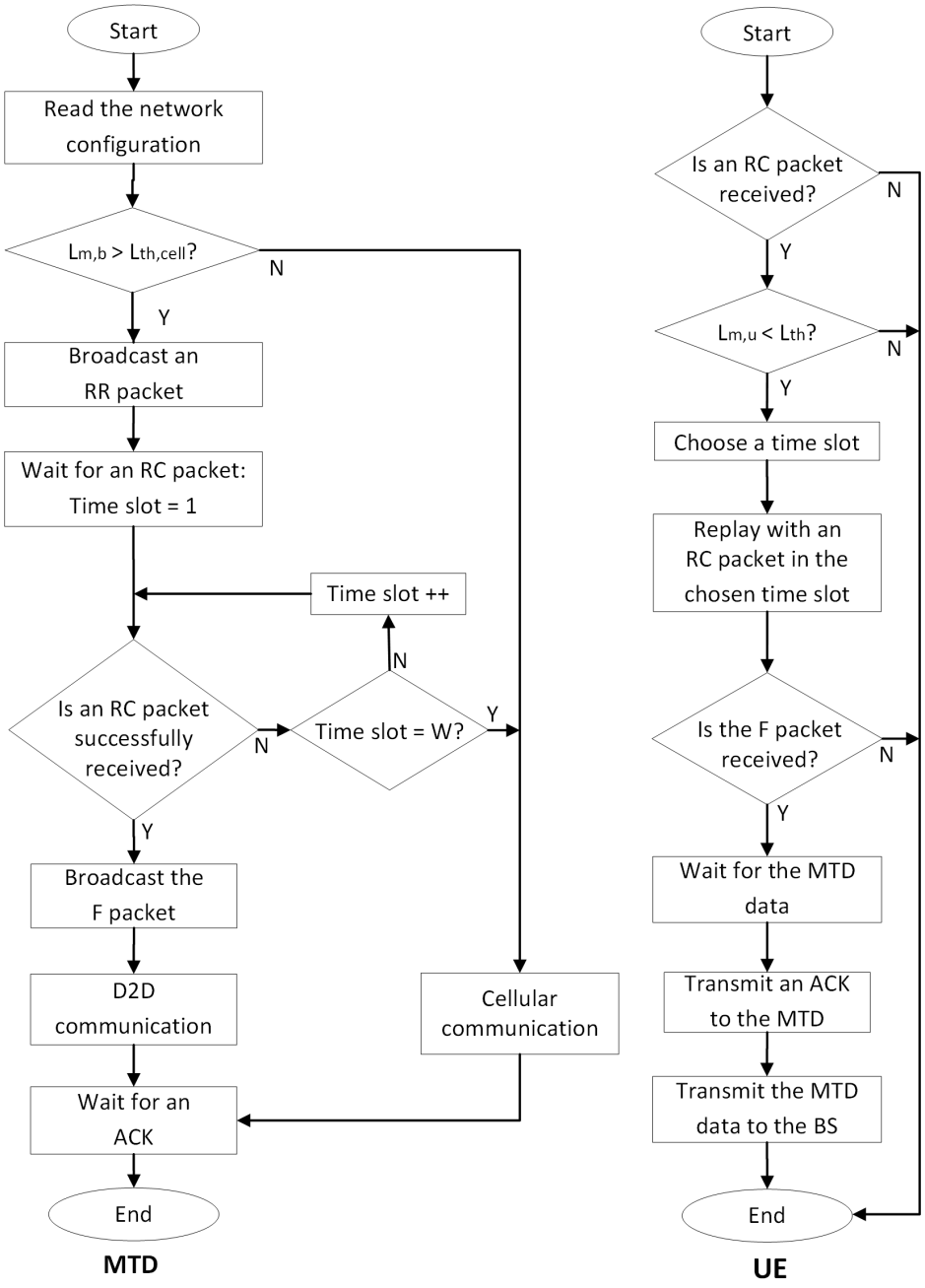

Fig. 5.3 D2D relaying procedure.

In order to avoid collisions between the feedback packet transmitted by the MTD and the RC packets sent by the relay candidates, the MTD is the only one that can transmit from the beginning of the time slot. The relay candidates that have an RC packet to transmit remain in the Rx state if the MTD is transmitting.

Fig. 5.4 illustrates two packet exchange sequences: (a) when the MTD selects a relay and (b) when it does not select a relay during the discovery phase. In both examples, we assume a network with $W = 6$ time slots. In Fig. 5.4 (a), there are five relay candidates. While UE-1 and UE-3 respectively choose time slot 4 and 6, UE-2 and UE-4 select time slot 2. In time slot 1, no relay candidate responds; the MTD thus waits for the next time slot. In time slot 2, a collision occurs; thus, the MTD waits for the next time slot. In time slot 3, only UE-5 transmits an RC packet (i.e., single-slot) and thus wins the contention process. Therefore, the MTD broadcasts the feedback packet in the next time slot (slot 4). When the relay candidates read the feedback packet, only UE-5 waits for the transmission of the MTD data, while the other candidates stop the contention process. UE-1 does not transmit an RC packet since it hears that the MTD is transmitting the feedback packet in time slot 4. In Fig. 5.4 (b), there are two relay candidates. Since both relay candidates select the same time slot, a collision occurs in time slot 2. The MTD waits for an RC packet until the maximum number of time slots (i.e., $W = 6$) is reached. Since no RC packet is received, it transmits its data directly to the base station.

5.3.3 Random Choice of Time-slot

On the basis of our relaying protocol introduced before, each relay candidate selects randomly and independently one time slot between 1 and W to send an RC packet. Therefore, the selected time slot can be modeled as a discrete random variable. In this section, we present two probability distributions for this random variable: truncated geometric and uniform.

According to the relay selection criteria, the first relay candidate to transmit an RC packet in a time slot without collisions is chosen as a relay. Therefore, the relay candidate that selects the first time-slots has a higher probability to be selected as a relay.

When the uniform random choice of time-slot is considered, all the relay candidates have the same probability to be selected as relay regardless of their locations with respect to the MTD. For example, assuming that in a network there are only two relay candidates UE-1 and UE-2 located respectively 100 and 200 meters from the MTD. UE-1 selects time slot 2, while UE-2 selects time slot 1. Even if UE-2 is located twice as far from the MTD as UE-1, it will win the contention process and will be selected as the relay because it is the first candidate to respond. To solve this problem, an alternative is the use of a time-slot choice so that the

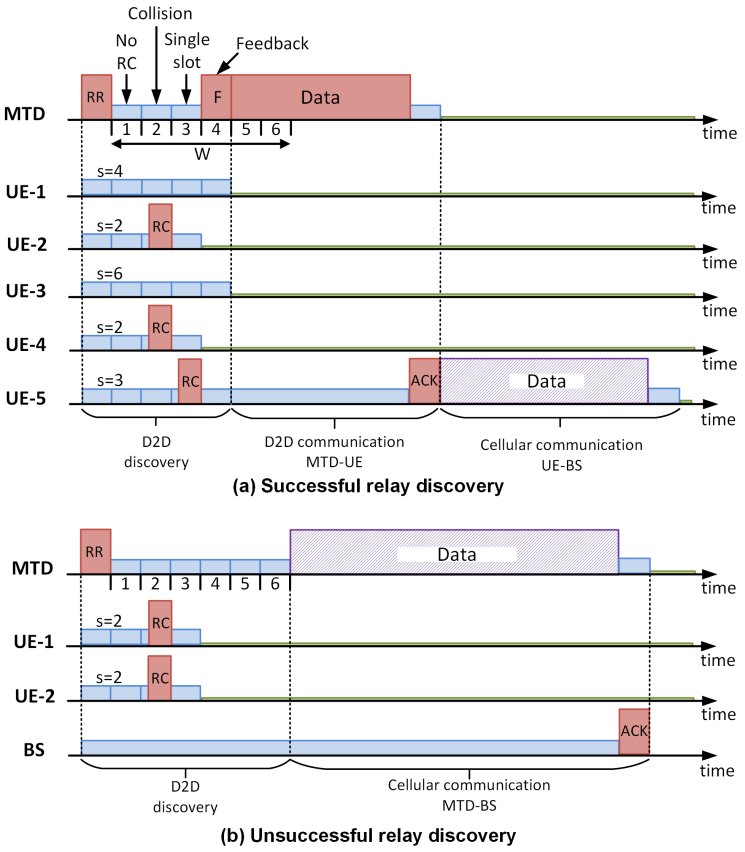

Fig. 5.4 Packet exchange sequence in our D2D relaying mechanism.

closer the relay candidate is to the MTD, the higher is the probability of responding in the first time slots.

5.3.3.1 Truncated Geometric Random Choice

In a multihop wireless sensor network context, the authors in [99] propose a random choice of time-slot based on a truncated geometric distribution that takes into account the path loss between the relay and the sink as a parameter to select the time slot. In their protocol, the relay candidates close to the sink have a higher probability of choosing the first time slots and thus win the contention process. In our discovery mechanism, the random choice of time-slot is also based on a truncated geometric distribution. However, as a opposed to their protocol, in our mechanism, the relay candidates close to the MTD have a higher probability of transmitting in the first time slots.

The relay candidates choose one time-slot $s \in [1,W]$ with a probability $\rho(s,r)$, where W is the contention window size and r the modified MTD-UE distance. The probability of transmitting in time slot s depends on r as [99]:

$$\rho(s,r) = \frac{g(r)^{s-1}(1-g(r))}{1-g(r)^{W}}, s \in [1,W], \tag{5.4}$$

where

$$g(r) = b + \frac{1-b^2}{b}\left(\frac{r}{R_d}\right), \tag{5.5}$$

where the parameter $0 < b < 1$ is constant and tunable to allow a relay candidate closer to the MTD to have a higher probability of sending an RC packet.

Each relay candidate has a particular probability mass function (PMF) of the time slot choice depending on its location with respect to the MTD. For example, Fig. 5.5 shows the PMFs of the time slot choice in a scenario where there are four relay candidates. UE-1, UE-2, UE-3, and UE-4 are located 30, 120, 210, and 300 meters from the MTD, respectively. In this example, we assume $R_d = 300$, $b = 0.6$, $W = 8$ time-slots, and shadowing $\sigma_{dB} = 8$ dB.

5.3.3.2 Uniform Random Choice

We can show that the uniform random choice of time-slot is a particular case of the truncated geometric random choice. When $b \to 1$, from (5.5) we get $g(r) \to 1$ and thus in (5.4) we have

$$\lim_{g(r)\to 1} \rho(s,r) = \lim_{g(r)\to 1} \frac{g(r)^{s-1}}{\sum_{k=1}^{W} g(r)^{k-1}} = \frac{1}{W}. \tag{5.6}$$

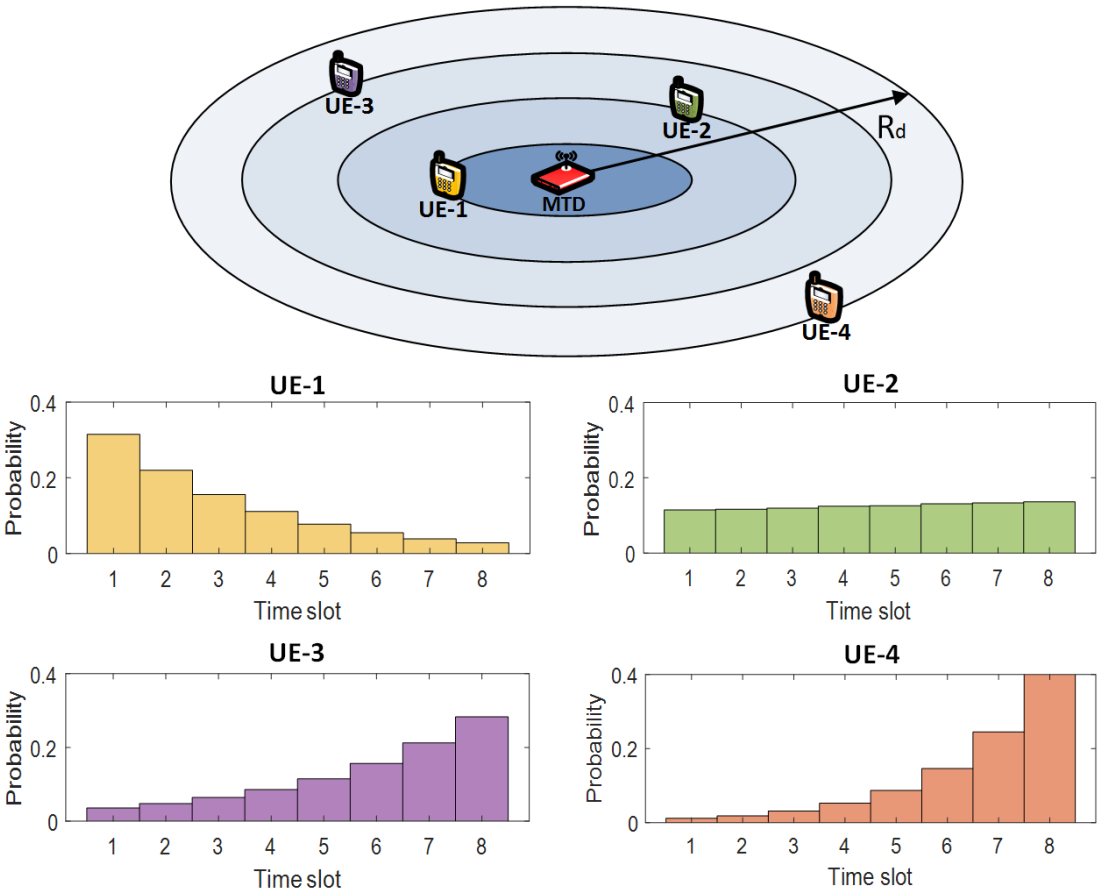

Fig. 5.5 PMFs of the time slot choice in a network with four relay candidates, $R_d = 300$, $b = 0.6$, shadowing $\sigma_{dB} = 8$ dB, and $W = 8$ time-slots. UE-1, UE-2, UE-3, and UE-4 are located 30, 120, 210, and 300 meters from the MTD, respectively.

The probability of choosing time slot $s \in [1, W]$ is $1/W$ is thus independent of the MTD-UE distance.

5.4 Analytical Model

We now provide the analytical expressions for the different performance metrics such as the relay discovery probability in Section 5.4.1, the number of time slots used in the contention process in Section 5.4.2, and the PDF of the MTD-relay distance in Section 5.4.3. We analyze the truncated geometric random choice of time slot and the uniform random choice as a particular case.

5.4.1 Relay Discovery Probability

The relay discovery probability refers to the probability that the MTD selects a relay during the contention process. This probability depends on parameters λ_u and W. On one hand, if there is no relay candidate in the discovery area, the relay discovery probability will always be zero. On the other hand, if there are many more relay candidates than time slots available, the number of collisions will be high. Therefore, there will be a low relay discovery probability. In this section, we provide the analytical expression for this probability.

5.4.1.1 Truncated geometric case

At a given time slot s, all the relay candidates located at distance r from the MTD have the same probability $\rho(s,r)$ of transmitting an RC packet. Therefore, the relay candidates form an I-PPP (see Appendix A.1.1) centered around the MTD and with isotropic intensity function $\lambda(r) = \rho(s,r)\lambda'_u = \rho(s,r)\lambda_u e^{2\sigma^2/\alpha^2}$, where r is the radius in polar coordinates, and $\rho(s,r)$ is given in (5.4). Based on the definition (A.1.4) of the I-PPP, the probability that n RC packets are transmitted in time slot s is given by:

$$\mathbb{P}(N = n) = \frac{(\Lambda_s)^n}{n!} \exp(-\Lambda_s), \tag{5.7}$$

where Λ_s is the intensity measure, which is given by:

$$\Lambda_s = 2\pi \int_0^{R_d} \lambda(r) r dr = 2\pi\lambda_u e^{2\sigma^2/\alpha^2} \int_0^{R_d} \rho(s,r) r dr. \tag{5.8}$$

The MTD successfully receives an RC packet in a certain time slot if and only if a unique relay candidate transmits in that time slot. From (5.7) we can derive the probability that only

one relay candidate transmits in time slot s:

$$P_1(s) = \mathbb{P}(N = 1) = \Lambda_s \exp(-\Lambda_s). \tag{5.9}$$

Since in each time slot s the relay candidates form an independent thinning PPP, thus the relay discovery probability can be obtained as

$$P_{\text{disc}} = 1 - \prod_{s=1}^{W}(1 - P_1(s)) = 1 - \prod_{s=1}^{W}(1 - \Lambda_s \exp(-\Lambda_s)), \tag{5.10}$$

where $\Lambda_s = 2\pi\lambda_u e^{2\sigma^2/\alpha^2} \int_0^{R_d} \rho(s,r) r dr$.

5.4.1.2 Uniform Case

The relay discovery probability in the case of a uniform random choice of the time slot is deduced as follows: let $P_{1,\text{uni}}$ and $P_{\text{disc,uni}}$ respectively be the probability that only one relay candidate transmits in time slot s and relay discovery probability for the uniform random choice. With the substitution of (5.6) into (5.8), we have $\Lambda_s = \pi R_d^2 \lambda_u e^{2\sigma^2/\alpha^2}/W$ and thus

$$P_{1,\text{uni}} = A R_d^2 \exp(-A R_d^2), \tag{5.11}$$

where $A = \pi\lambda_u \exp(2\sigma^2/\alpha^2)/W$.

Note that $P_{1,\text{uni}}$ is independent of s, thus the relay discovery probability defined in (5.10) can be simplified as follows:

$$P_{\text{disc,uni}} = 1 - \left(1 - A R_d^2 \exp(-A R_d^2)\right)^W. \tag{5.12}$$

Taking the first derivative of $P_{\text{disc,uni}}$ with respect to R_d:

$$\frac{dP_{\text{disc,uni}}}{dR_d} = 2AW R_d \exp(-A R_d^2)(1 - A R_d^2)\left(1 - A R_d^2 \exp(-A R_d^2)\right)^{W-1}. \tag{5.13}$$

We show that $P_{\text{disc,uni}}$ is maximized when $R_d = (1/A)^{1/2} = (\pi\lambda_u \exp(2\sigma^2/\alpha^2)/W)^{-1/2}$. By substituting this value into (5.12), we derive the maximum relay discovery probability in the uniform random choice case:

$$P_{\text{disc,uni}}^{\max}(W) = 1 - (1 - e^{-1})^W \approx 1 - (0.63)^W. \tag{5.14}$$

We can infer from (5.14) that when the value of W is large, $P_{\text{disc,uni}}^{\max} \approx 1$, for example, $P_{\text{disc,uni}}^{\max}(W = 8) = 0.974$, and $P_{\text{disc,uni}}^{\max}(W = 16) = 0.999$.

5.4.2 Number of Slots Used in the Contention Process

The number of time slots used by the MTD in the contention process is directly related to energy consumption in the discovery phase.

5.4.2.1 Truncated Geometric Case

According to our D2D relaying protocol, the contention process ends as soon as an RC packet is successfully received by the MTD (i.e., at the first single time-slot) or when the maximum number of time slots W is reached.

Let S be a discrete random variable that represents the number of time slots used in the contention process. The average number of time slots used in the contention process is:

$$\overline{S} = \sum_{s=1}^{W} s\mathbb{P}(S=s), \tag{5.15}$$

where $\mathbb{P}(S=s)$ is the probability that the contention process ends in time slot s.

For $S = 1,2,...,W-1$, $\mathbb{P}(S=s)$ is equivalent to the probability of a reception failure in the 1st, 2nd, ...,$(s-1)$th time slots and a successful reception at the sth time slot. Thus, we have:

$$\mathbb{P}(S=s) = P_1(s)\prod_{j=1}^{s-1}(1-P_1(j)),\ s \in [1,W-1], \tag{5.16}$$

where $P_1(s)$ is given by (5.9).

The number of time slots used in the contention process is W when an RC packet is successfully received in time slot W (the first $W-1$ time slots fail) or when all receptions fail. Therefore, the probability $\mathbb{P}(S=W)$ is equivalent to the probability of a reception failure in the 1st, 2nd,...,$(W-1)$th time slots, i.e.,

$$\mathbb{P}(S=W) = \prod_{j=1}^{W-1}(1-P_1(j)). \tag{5.17}$$

Substituting (5.16) and (5.17) into (5.15), we have:

$$\overline{S} = \sum_{s=1}^{W-1} sP_1(s)\prod_{j=1}^{s-1}(1-P_1(j)) + W\prod_{j=1}^{W-1}(1-P_1(j)). \tag{5.18}$$

5.4.2.2 Uniform Case

In the case of a uniform random choice of time slot, the average number of time slots used in the contention process $\overline{S}_{\text{uni}}$ can be derived with the substitution of (5.11) into (5.18):

$$\overline{S}_{\text{uni}} = \frac{1-(1-P_{1,\text{uni}})^W}{P_{1,\text{uni}}}, \tag{5.19}$$

where $P_{1,\text{uni}}$ is given by (5.11).

Taking the first derivative of $\overline{S}_{\text{uni}}$ with respect to R_d, we can show that $\overline{S}_{\text{uni}}$ is minimized when $R_d = (1/A)^{-1/2} = (\pi\lambda_u \exp(2\sigma^2/\alpha^2)/W)^{-1/2}$. Note that this value of R_d is the same value that maximizes the relay discovery probability in the case of uniform random choice. By substituting $R_d = (\pi\lambda_u \exp(2\sigma^2/\alpha^2)/W)^{-1/2}$ into (5.19), we have $P_{1,\text{uni}} = e^{-1}$ and thus the minimum number of time slots used in the contention process is:

$$\overline{S}^{\min}_{\text{uni}}(W) = e(1-(1-e^{-1})^W) \approx e(1-(0.63)^W). \tag{5.20}$$

Note that when the value of W is large, $\overline{S}^{\min}_{\text{uni}} \approx e$.

5.4.3 PDF of the MTD-Relay Distance

The MTD-relay distance is an important parameter to calculate the energy consumption in the data transmission phase since, as a function of this distance, the MTD adapts the MCS of the D2D link. In this section, we derive the PDF of the MTD-relay distance, i.e., when the MTD selects a relay.

5.4.3.1 Truncated Geometric Case

Let R be the distance between the MTD and the relay. Recall that the relay is always located within the discovery area (i.e., $R < R_d$). The CDF of R can be derived as:

$$F_R(r) = \mathbb{P}(R<r) = \sum_{s=1}^{W} \mathbb{P}(R<r|s)\mathbb{P}(S=s),\ 0<r\leq R_d, \tag{5.21}$$

where $\mathbb{P}(S=s)$ is the probability that an RC packet is successfully received in time slot s, which is defined in (5.16). $\mathbb{P}(R<r|s)$ is the probability that the selected relay is located inside a disk of radius r given that an RC packet is successfully received in time slot s. This probability can be deduced as follows:

$$\mathbb{P}(R < r|s) = \frac{\int_0^r 2\pi\lambda'_u \rho(s,x)xdx}{\int_0^{R_d} 2\pi\lambda'_u \rho(s,x)xdx} = \frac{\int_0^r \rho(s,x)xdx}{I_s}, \tag{5.22}$$

where $I_s = \int_0^{R_d} \rho(s,x)xdx$.

Substituting (5.16) and (5.22) into (5.21), we have

$$F_R(r) = \sum_{s=1}^{W} \frac{\int_0^r \rho(s,x)xdx}{I_s} P_1(s) \prod_{j=1}^{s-1}(1 - P_1(j)). \tag{5.23}$$

We find the PDF of the MTD-relay distance by taking the derivative of the CDF:

$$f_R(r) = \frac{dF_R(r)}{dr} = r\sum_{s=1}^{W} \frac{\rho(s,r)}{I_s} P_1(s) \prod_{j=1}^{s-1}(1 - P_1(j)),\ 0 < r \leq R_d, \tag{5.24}$$

where $P_1(s)$ and $\rho(s,r)$ are given by (5.9) and (5.4), respectively.

5.4.3.2 Uniform Case

In the case of a uniform random choice of time slot in the contention process, the PDF of the MTD-relay distance is obtained by substituting (5.6) and (5.11) into (5.24):

$$f_{R,\text{uni}}(r) = \frac{2r}{R_d^2}(1 - (1 - P_{1,\text{uni}})^W),\ 0 < r \leq R_d, \tag{5.25}$$

where $P_{1,\text{uni}}$ is given by (5.11). Note that in this case, the $f_{R,\text{uni}}(r)$ is an increasing linear function.

5.5 Analysis of the Total Energy Consumption

In this section, we provide the analytical expressions for the total energy consumed by the MTD in cellular mode and D2D mode. These expressions allow us to compare the energy consumption in both transmission modes. We use the MTD energy consumption model given in Section 2.5.1, but without taking into account the energy consumption in the synchronization phase since we assume that in both modes the MTD is synchronized with the base station and thus it consumes the same amount of energy.

5.5.1 Energy Consumption in Cellular Mode

In cellular mode, an MTD that has data to transmit uses traditional uplink communications using a dynamic data rate adaptation.

The MTD power consumption in Tx state $P_{m,T}$ is constant since we assume that the MTD transmits at a fixed transmission power P_m. The energy consumed by the MTD can be computed as $E_{\text{cell}} = P_{m,T} t_{m,b}$, where $t_{m,b}$ is the transmission time (the time that the MTD remains in Tx state). Assuming that the MTD has to send one data packet of D bits, thus $t_{m,b} = D/C_{m,b}$, where $C_{m,b}$ is the data rate (bits per second) over the MTD-BS link. Thus, we have:

$$E_{\text{cell}} = P_{m,T} \frac{D}{C_{m,b}}. \tag{5.26}$$

Let $\theta_{m,b}$ be the received signal-to-noise ratio (SNR) at the BS. The received power at the BS is given in (5.1). Thus, the SNR of the MTD-BS link is:

$$\theta_{m,b} = \frac{P_m K_c \exp(\chi)}{N_0 B_w (d_{m,b})^{\alpha_c}}, \tag{5.27}$$

where K_c and α_c are respectively the path loss factor and path loss exponent for cellular links, B_w is the transmission bandwidth, and N_0 is the noise power spectral density, $d_{m,b}$ is the Euclidean distance between the MTD and the BS. Recall that χ is a zero-mean Gaussian random variable.

We define the transmission constraint as a predefined SNR threshold $\theta_{\min}$ which controls whether or not the MTD transmits its data ($\theta_{\min} = -10$ dB [104]). In other words, the MTD transmits if and only if $\theta_{m,b} \geq \theta_{\min}$, otherwise it assumes that the BS is not reachable via a direct link. By using (5.27), the transmission constraint is satisfied when:

$$\frac{P_m K_c \exp(\chi)}{N_0 B_w (d_{m,b})^{\alpha_c}} \geq \theta_{\min}. \tag{5.28}$$

From (5.28), the transmission condition may be expressed in terms of χ for a given MTD-BS distance $d_{m,b}$:

$$\chi \geq \chi_{\min}, \tag{5.29}$$

where $\chi_{\min} = \ln\left(\frac{\theta_{\min} N_0 B_w}{P_m K_c}\right) + \alpha_c \ln(d_{m,b})$.

As we mentioned before, in the cellular mode, we consider that the MTD can dynamically adjust the data rate depending on the channel conditions. We use a modified Shannon capacity formula proposed in [105] to compute the data rate when the transmission condition

is satisfied. Thus, we have:

$$C_{m,b} = B_{\text{eff}} B_w \log_2\left(1+\frac{\theta_{m,b}}{\theta_{\text{eff}}}\right) = B_{\text{eff}} B_w \log_2\left(1+\frac{P_m K_c \exp(\chi)}{\theta_{\text{eff}} N_0 B_w (d_{m,b})^{\alpha_c}}\right),\ \chi_{m,b} \geq \chi_{\min}, \tag{5.30}$$

where B_{eff} adjusts for the system bandwidth efficiency of LTE, θ_{eff} adjusts for the SNR implementation efficiency of LTE. If $\chi < \chi_{\min}$, the MTD does not transmit anything and therefore it does not consume energy. MTD energy consumption in cellular mode is obtained by substituting (5.30) into (5.26):

$$E_{\text{cell}}(\chi) = \begin{cases} 0, & \chi < \chi_{\min}, \\ \dfrac{P_{m,T} D}{B_{\text{eff}} B_w \log_2\left(1+\frac{P_m K_c \exp(\chi)}{\theta_{\text{eff}} N_0 B_w (d_{m,b})^{\alpha_c}}\right)}, & \chi \geq \chi_{\min}. \end{cases} \tag{5.31}$$

Thus, the average MTD energy consumption for a given $d_{m,b}$ is

$$\overline{E}_{\text{cell}}(d_{m,b}) = \mathbb{P}(\chi \geq \chi_{\min}) \int_{\chi_{\min}}^{+\infty} E_{\text{cell}}(x) f_\chi(x) dx, \tag{5.32}$$

where $\mathbb{P}(\chi \geq \chi_{\min})$ is the transmission probability, and $f_\chi(x)$ is the PDF of χ. Recall that χ is a zero-mean Gaussian random variable with variance σ^2, thus:

$$f_\chi(x) = \frac{1}{\sqrt{2\pi\sigma^2}} \exp\left(\frac{-x^2}{2\sigma^2}\right). \tag{5.33}$$

Moreover, we note that $\mathbb{P}(\chi \geq \chi_{\min})$ is the complementary cumulative distribution function (CCDF) of χ. Thus, it can be expressed as:

$$\mathbb{P}(\chi \geq \chi_{\min}) = \frac{1}{2} - \frac{1}{2}\text{erf}\left(\frac{\chi_{\min}}{\sigma\sqrt{2}}\right), \tag{5.34}$$

where $\text{erf}(x) = \frac{2}{\sqrt{\pi}} \int_0^{x^2} \exp(-t^2) dt$ refers to the error function.

5.5.2 Total Energy Consumption in D2D Mode

The total energy consumed by the MTD when it uses our D2D relaying mechanism is computed as the sum of the energy consumption in the discovery and transmission phases. Thus, we have:

$$\overline{E}_{\text{D2D,total}} = \overline{E}_{\text{D2D,disc}} + \overline{E}_{\text{dataTx}}, \tag{5.35}$$

where $\overline{E}_{\text{D2D,disc}}$ and $\overline{E}_{\text{dataTx}}$ are the average energy consumption in the discovery and data transmission phases, respectively.

5.5.2.1 Energy Consumption in the Discovery Phase

In the discovery phase, the MTD is in Tx state when it transmits the RR and feedback packets while it is in Rx state during the contention process. Thus, the average energy consumption during this phase can be expressed as follows:

$$\overline{E}_{\text{D2D,disc}} = T_s(2P_{m,T} + \overline{S}P_{m,R}), \tag{5.36}$$

where T_s is the time slot duration, and $\overline{S}$ is the average number of slots used in the contention process, which is given by (5.18) and (5.19) for truncated geometric and uniform, respectively.

5.5.2.2 Energy Consumption in the Data Transmission Phase

Based on our D2D relaying mechanism, if the MTD selects a relay in the discovery phase, both devices establish D2D communication in the data transmission phase; otherwise, the MTD establishes cellular communication with the base station. Thus, the average energy consumption during the data transmission phase can be derived as:

$$\overline{E}_{\text{dataTx}} = P_{\text{disc}}\overline{E}_{\text{D2D,comm}} + (1 - P_{\text{disc}})\overline{E}_{\text{cell}}, \tag{5.37}$$

where P_{disc} is the relay discovery probability, which is given by (5.10) and (5.12) for truncated geometric and uniform, respectively; $\overline{E}_{\text{D2D,comm}}$ is the average energy consumption in the D2D communication; and $\overline{E}_{\text{cell}}$ is the average energy consumption in cellular mode, which is defined in (5.32).

Similar to (5.26), MTD energy consumption in D2D communication can be expressed as $E_{\text{D2D,comm}} = P_{m,T}D/C_{m,u}$, where D is the data packet size and $C_{m,u}$ is the data rate over the MTD-relay link. As explained in Section 5.2.2, the location of the relay candidates can be modeled as a PPP without shadowing Φ'_u but considering the modified distances. Thus, we have:

$$E_{\text{D2D,comm}} = \frac{P_{m,T}D}{B_{\text{eff}}B_w \log_2\left(1 + \frac{P_m K_d}{\theta_{\text{eff}} N_0 B_w r^{\alpha_d}}\right)}, \tag{5.38}$$

where r is the modified MTD-relay distance, K_d and α_d are respectively the path loss factor and path loss exponent for D2D links. The parameter r is a random variable whose PDF $f_R(r)$ given by (5.24) and (5.25) for truncated geometric and uniform, respectively. Thus, the

average energy consumption in the D2D communication is computed as follows:

$$\overline{E}_{\text{D2D,comm}} = \int_0^{Rd} \frac{P_{m,T} D}{B_{\text{eff}} B_w \log_2\left(1 + \frac{P_m K_d r^{-\alpha_d}}{N_0 B_w \theta_{\text{eff}}}\right)} f_R(r) dr. \tag{5.39}$$

5.6 Numerical Results and Discussion

In this section, we numerically analyze the performance of our D2D relaying protocol. Firstly, in Section 5.6.1, we determine the radius of the discovery area. In Section 5.6.2, a MATLAB-based simulation approach is adopted to validate our analytical results obtained in Section 5.4 and Section 5.5. Simulations are based on a Monte Carlo approach, where each point corresponds to the average value of 2000 iterations. In each iteration, the UEs are distributed independently according to H-PPP in a circular area of radius 1.5 km centered around the MTD. Table 5.1 summarizes the simulation parameters, as described in Section 4.4, these parameters are chosen according to the 3GPP specifications.

After the validation of the analytical model, in Section 5.6.3, Section 5.6.4, and Section 5.6.5, we only use the analytical expressions to analyze our protocol since they require less computation time than simulations. In Section 5.6.3, we investigate the impact of parameter b on the relay discovery probability, on the number of time slots used in the contention process, and on MTD energy consumption. In Section 5.6.4, we look for the optimal values of the parameters so that the energy consumption is minimized. Finally, in Section 5.6.5, we compare MTD energy consumption in cellular and D2D modes to show the benefits of our D2D relaying mechanism.

5.6.1 Determining the Radius of the Discovery Area

It is essential to correctly determine the discovery area since it is strongly related to the relay discovery probability. When the discovery area is small, the probability of finding a relay candidate inside this area is low, or it could even be zero. All relay discovery protocols work whenever there is at least one relay candidate inside the discovery area. In order to avoid an empty discovery area, we determine the minimum value of the radius of the discovery area R_d so that the probability of finding at least one UE in this area is greater than 98%:

In the transformed PPP Φ'_u, the number of UEs N inside the discovery area has a Poisson distribution with mean $\pi R_d^2 \lambda_u e^{2\sigma^2/\alpha^2}$, i.e.,

$$\mathbb{P}(N = n) = \frac{(\pi R_d^2 \lambda_u e^{2\sigma^2/\alpha^2})^n}{n!} \exp(-\pi R_d^2 \lambda_u e^{2\sigma^2/\alpha^2}). \tag{5.40}$$

Table 5.1 Simulation parameters

Parameter	Value
MTD transmission power (P_m)	23 dBm
MTD power consumption in Tx state ($P_{m,T}$)	545 mW
MTD power consumption in Rx state ($P_{m,R}$)	90 mW
MTD Bandwidth (B_w)	180 kHz
Noise Power Spectrum Density (N_0)	-174 dBm/Hz
Carrier Frequency (f_c)	900 MHz
Cellular path-loss exponent (α_c)	3.67
Cellular path-loss factor for a distance in meters (K_c)	0.0070
D2D path-loss exponent (α_d)	4
D2D path-loss factor for a distance in meters (K_d)	0.0173
Shadowing standard deviation (σ_{dB})	8 dB
Time slot duration (T_s)	0.5 ms
Bandwidth efficiency (B_{eff})	0.56
SNR efficiency (θ_{eff})	2
SNR threshold (θ_{min})	-10 dB

Thus, the probability of finding at least one UE is:

$$\mathbb{P}(N \geq 1) = 1 - \mathbb{P}(N = 0) = 1 - \exp(-\pi R_d^2 \lambda_u e^{2\sigma^2/\alpha^2}). \tag{5.41}$$

Fig 5.6 provides the probability of finding at least one UE inside the discovery area as a function of R_d for three UE density scenarios. From the figure, we can see that R_d must be greater than 286 meters if the UE density is low ($\lambda_u = 0.1 \times 10^{-4}$ UEs/m^2) while R_d has to be greater than 65 meters if the UE density is high ($\lambda_u = 2 \times 10^{-4}$ UEs/m^2). In this work, we consider $R_d \geq 300$ since this value ensures $\mathbb{P}(N \geq 1) \geq 0.98$ for UE densities greater than $\lambda_u = 0.1 \times 10^{-4}$ UEs/m^2.

5.6.2 Analytical Model Validation

Fig. 5.7 (a) and Fig. 5.7 (b) show the relay discovery probability as a function of the UE density for a truncated geometric random choice with $b = 0.6$ and a uniform random choice, respectively. From the figures, we can see that the analytical and simulation results match well, this confirms the correctness of (5.10) and (5.12). In both figures, we can see that as the

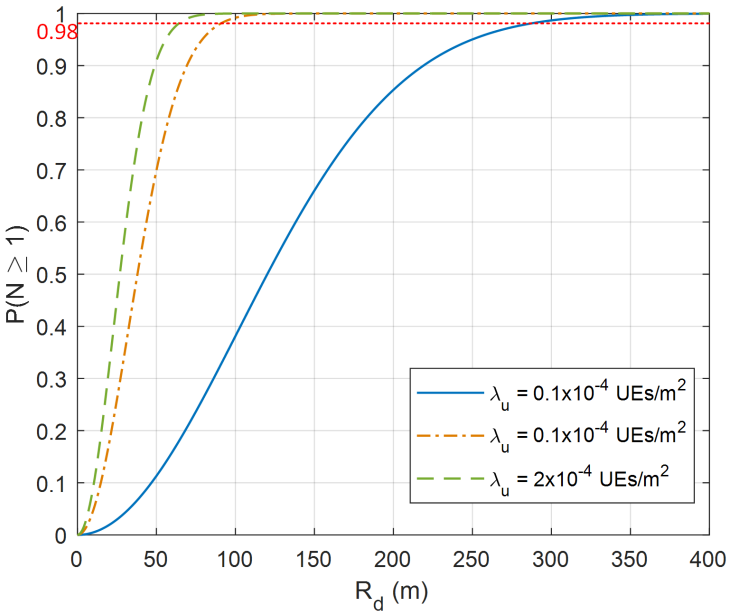

Fig. 5.6 Probability of finding at least one UE inside the discovery area, shadowing $\sigma_{dB} = 8$ dB and $\alpha = 4$.

UE density increases the relay discovery probability increases until it reaches a maximum and then it decreases. These results may be explained by the fact that when the UE density increases, the number of collisions also increases due to the limited number of time slots (W). Therefore, the impact of collisions can be reduced by increasing the contention window size. We also observe that when the UE density increases, the relay discovery probability decreases faster in the uniform case than in the truncated geometric with $b = 0.6$ case.

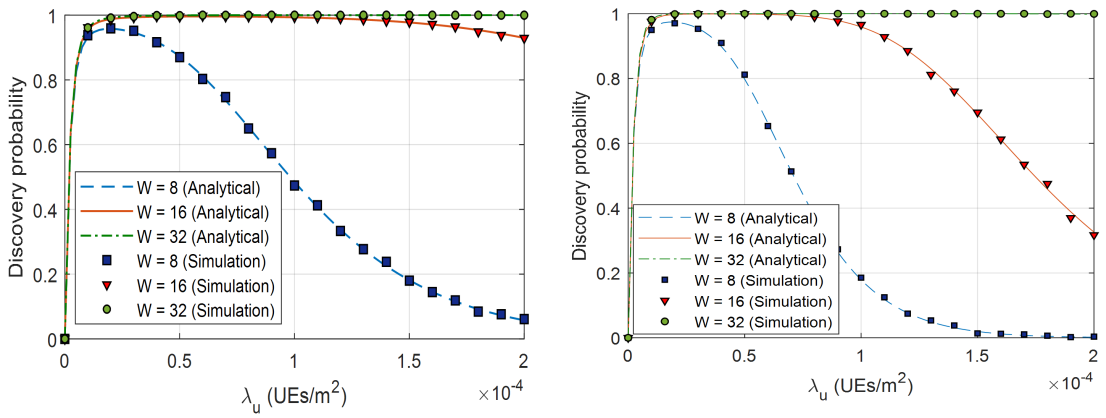

Fig. 5.7 Relay discovery probability as function of the UE density for $R_d = 300$.

Fig. 5.8 (a) and Fig. 5.8 (b) display the average number of time slots used in the contention process as a function of the UE density for a truncated geometric random choice with $b = 0.6$ and a uniform random choice, respectively. We can see that the analytical and simulation results match well, this confirms the correctness of (5.18) and (5.19). These figures show that, when the UE density is low, the MTD uses a significant number of time slots waiting for the response of a relay candidate. When the UE density increases, the number of time slots decreases and reaches a minimum value, then it increases due to the increase in the number of collisions. Recall that the maximum number of time slots that the MTD can wait to receive a successful response is W even if it does not find a relay. We can observe that when the UE density increases, the number of time slots used increases faster in the uniform case than in the truncated geometric with $b = 0.6$ case.

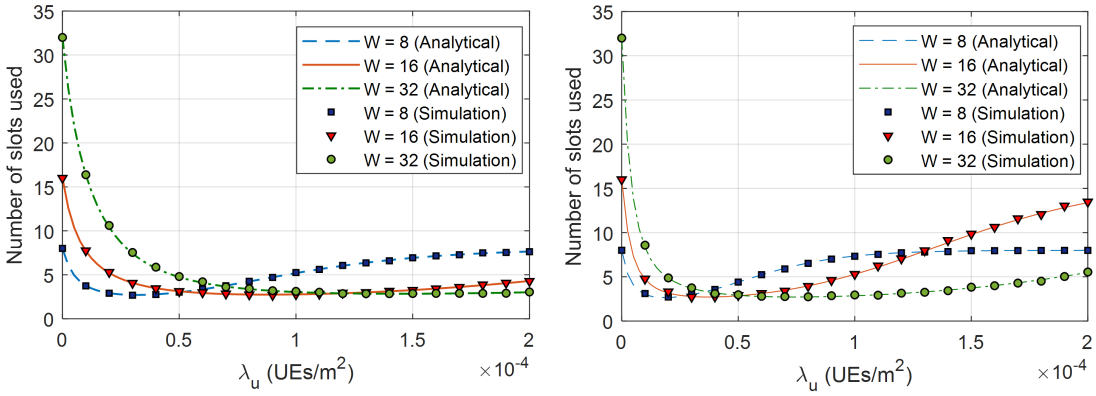

Fig. 5.8 Average number of time slots used in the contention process as function of the UE density for $R_d = 300$.

Fig. 5.9 shows the PDF of the MTD-relay distance for a truncated geometric random choice with $b = 0.6$, considering $\lambda_u = 1 \times 10^{-4}$ UEs/m^2 and $W = \{8, 16, 32\}$. The comparison between analytical and simulation results confirms the correctness of (5.24). From the figure, the larger is the size of the contention window (e.g., $W = 32$), the higher is the probability of selecting a relay near to the MTD.

The average energy consumed by the MTD in the discovery and data transmission phases can be seen in Fig. 5.10. The comparison between analytical and simulation results confirms the accuracy of our analytical models. In this figure, we consider a scenario where the MTD is located 1000 meters from the BS, and it transmits 200 bytes of data. As can be seen from the figure, the energy consumption in the discovery phase is not very sensitive to the UE density, especially when $\lambda_u \in [0.1 \times 10^{-4}, 2 \times 10^{-4}]$ UEs/m^2. The reason is that, in the discovery phase, the MTD always remains two time-slots in Tx state (RR packet

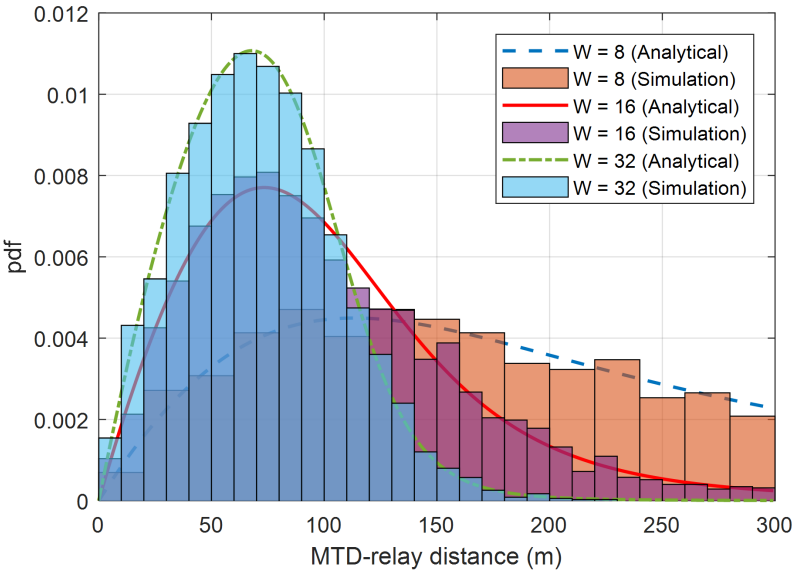

Fig. 5.9 PDF of the MTD-relay distance for $R_d = 300$, $b = 0.6$, and $\lambda_u = 1 \times 10^{-4}$ UEs/m^2.

and feedback packet), while it remains between 3 and 5 time-slots in the Rx state in this UE density range for $W = 16$ (see Fig. 5.8 (a)). The power consumption in the Rx state is approximately one-ninth of the power consumption in the Tx state (see Table 5.1). Therefore, most of the energy consumed by the MTD during the discovery phase occurs when it is in Tx state.

Since the analytical and simulation results match well, in the next sections, we will only use the derived analytical expressions to analyze the performance of our D2D relaying mechanism.

5.6.3 Impact of Parameter b

In this section, we analyze how the parameter b affects the relay discovery probability, the average number of time slots used in the contention process, and the PDF of the MTD-relay distance. The radius of the discovery area R_d in the transformed PPP Φ'_u and the contention window size W are fixed to 300 meters and 16 time slots, respectively.

In Section 3.4.3, we have defined two UE density reference scenarios: low UE density scenario with $\lambda_u = 0.25 \times 10^{-4}$ UEs/m^2 and high UE density scenario with $\lambda_u = 1.4 \times 10^{-4}$ UEs/m^2. However, the exact UE density value is difficult to determine in real scenarios due to user mobility. Therefore, we do not evaluate the performance of our D2D relaying mechanism for a specific UE density value, but we evaluate the performance for a wide range

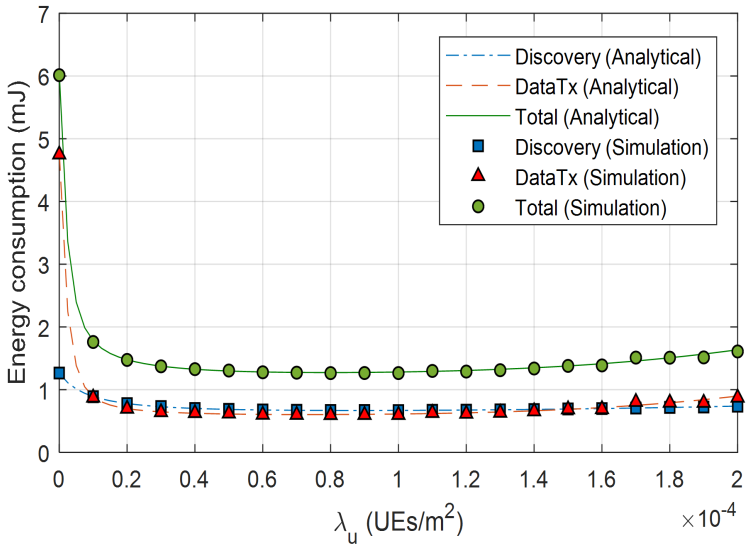

Fig. 5.10 Average energy consumption in the discovery phase, data transmission phase, and total in D2D mode as function of the UE density, for $R_d = 300$, $b = 0.6$, $W = 16$, $D = 200$ bytes, and $d_{m,b} = 1000$ meters.

of UE densities. We analyse the performance of our mechanism for $\lambda_u \in [0, 1.6 \times 10^{-4}]$ UEs/m^2, this range is called target UE densities range.

Fig. 5.11, Fig. 5.12, and Fig. 5.13 show respectively the relay discovery probability, the average number of time slots used in the contention process, and the PDF of the MTD-relay distance. In these three figures, we compare the performance of our D2D relaying mechanism with different values of $b = \{0.2, 0.4, 0.6, 0.8\}$ as well as when $b \approx 1$, which represents the uniform random choice of time slot.

As shown in Fig. 5.11, for low UE densities ($\lambda_u < 0.8 \times 10^{-4}$ UEs/m^2) it is better the use of high values of b (e.g., $b = 0.8$ and $b \approx 1$) while for high UE densities ($\lambda_u > 0.8 \times 10^{-4}$ UEs/m^2) it is better the use of $b = 0.4$ to obtain a high relay discovery probability. From the figure, we determine the range of UE densities that satisfies a relay discovery probability higher than 95%. These values are summarized in Table 5.2. In addition, in the table we show the percentage that represents these ranges with respect to the target range. The wider range of UE densities is obtained when $b = 0.6$. In contrast, the worst performance in the UE density range studied is obtained when $b = 0.2$.

Fig. 5.12 displays that for low UE densities ($\lambda_u < 0.8 \times 10^{-4}$ UEs/m^2), fewer time slots are used when the value of b is high (e.g., $b = 0.8$ and $b \approx 1$). On the other hand, when the UE density is high ($\lambda_u > 0.8 \times 10^{-4}$ UEs/m^2), fewer time slots are used when $b = 0.4$ and

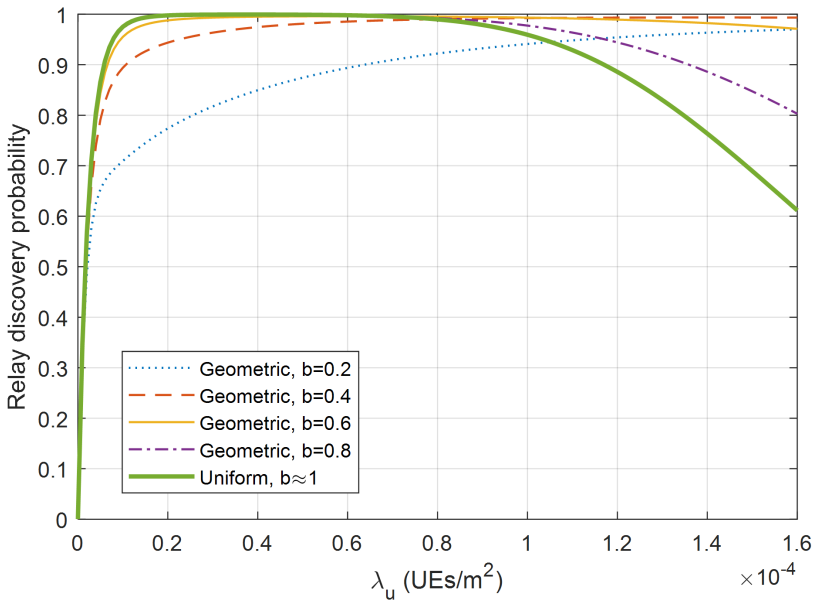

Fig. 5.11 Relay discovery probability as function of the UE density for $b = \{0.2, 0.4, 0.6, 0.8, 1\}$, considering $R_d = 300$ and $W = 16$.

Table 5.2 Ranges of UE densities for relay discovery probability greater than 95%

b	Range (UEs/m^2)$\times 10^{-4}$	Percentage of the target range
0.2	[1.13, 1.60]	29.4%
0.4	[0.23, 1.60]	85.6%
0.6	[0.10, 1.60]	93.7%
0.8	[0.08, 1.17]	68.1%
1	[0.08, 1.03]	59.4%

$b = 0.6$. Moreover, we can see that when the value of b is high, the average number of time slots used in the contention process considerably increases when the UE density increases.

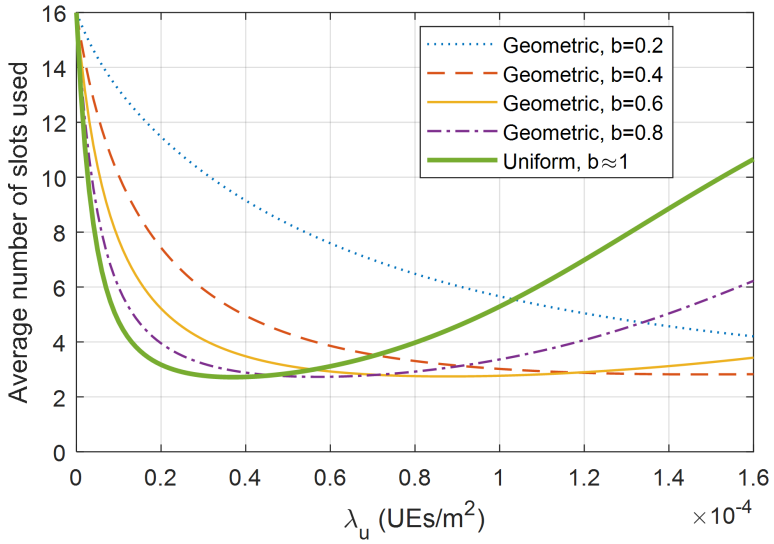

Fig. 5.12 Average number of time slots used during contention process as function of the UE density for $b = \{0.2, 0.4, 0.6, 0.8, 1\}$, considering $R_d = 300$ and $W = 16$.

From Fig. 5.12, we find the range of UE densities within which the average number of time slots used in the contention process is less than 4 time-slots for each b value. These ranges are shown in Table 5.3. The wider range of UE densities is achieved when $b = 0.6$. In contrast, the worst performance is obtained when $b = 0.2$, for this value, the average number of time slots is greater than 4 over the entire target UE densities range.

Table 5.3 Ranges of UE densities for less than 4 time-slots

b	Range (UEs/m^2)$\times 10^{-4}$	Percentage of the target range
0.2	-	0%
0.4	[0.56, 1.60]	65.0%
0.6	[0.31, 1.60]	80.3%
0.8	[0.20, 1.18]	61.2%
1	[0.13, 0.80]	41.8%

Fig. 5.13 shows the PDF of the MTD-relay distance for different values of the parameter b, $\lambda_u = 1.4 \times 10^{-4}$ UEs/m^2, $R_d = 300$, and $W = 16$. As shown in the figure, the probability that the selected relay is near to the MTD is greater when the parameter b is a small value (e.g., $b = 0.2$) than when it is a large value. The MTD-relay distance is directly related to

energy consumption in D2D communication. In other words, the energy consumption in the D2D communication will be lower if we use a small value of b than if we use a large value. But on the other hand, when b is small and the UE density is low, we have a low relay discovery probability and high consumption of time slots which increases the energy consumption in the discovery phase.

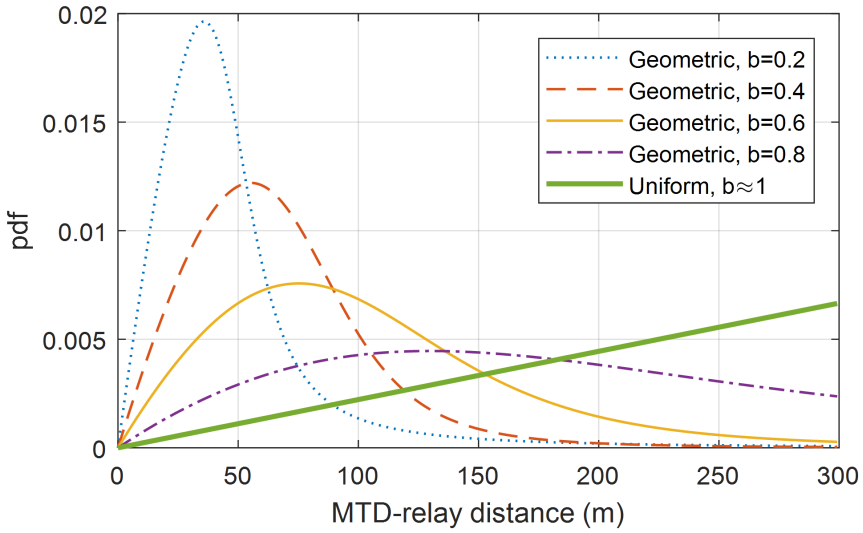

Fig. 5.13 PDF of the MTD-relay distance, for $R_d = 300$, $b = \{0.2, 0.4, 0.6, 0.8, 1\}$, $W = 16$, and $\lambda_u = 1.4 \times 10^{-4}$ UEs/m^2.

We have seen the impact of b on the relay discovery probability, the number of time slots used in the contention process, and the PDF of the MTD-relay distance. We also know that total energy consumption depends on these three parameters. In Fig. 5.14, we illustrate the impact of parameter b on the total MTD energy consumption for $D = 200$ bytes and $d_{m,b} = 1000$ meters. It can be seen in the figure a significant difference in terms of energy consumption between our D2D relaying mechanism and cellular communication. Moreover, when the UE density is low ($\lambda_u < 0.8 \times 10^{-4}$ UEs/m^2), energy consumption is not significantly affected if we choose b between 0.4 and 1. However, when the UE density increases, the difference in terms of total energy consumption between $b = 0.4$ and $b \approx 1$ grows considerably. When the UE density is high ($\lambda_u > 0.8 \times 10^{-4}$ UEs/m^2), the minimum energy consumption is obtained when $b = 0.4$.

From Fig. 5.14, we determine for each b value, the range of UE densities within which the total energy consumption is less than 1.6 mJ ($\approx$ 2 dBJ). These ranges are shown in Table 5.4. We can see that the most extended range is achieved when $b = 0.6$, and the second wider range is achieved when $b = 0.4$. The worst performance is obtained when $b = 1$. However

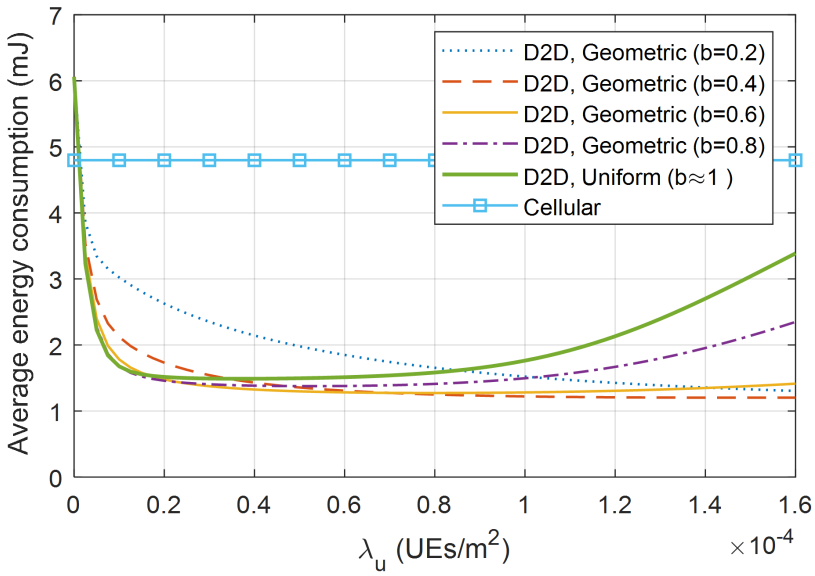

Fig. 5.14 Total MTD energy consumption in D2D and cellular modes, for $R_d = 300$, $b = \{0.2, 0.4, 0.6, 0.8, 1\}$, $W = 16$, shadowing $\sigma_{dB} = 8$ dB, $D = 200$ bytes, and $d_{m,b} = 1000$ meters.

for low densities ($\lambda_u < 0.8 \times 10^{-4}$ UEs/m^2), this value of b offers an acceptable energy consumption.

Table 5.4 Ranges of UE densities for energy consumption less than 1.6 mJ

b	Range (UEs/m^2) $\times 10^{-4}$	Percentage of the target range
0.2	[0.87, 1.60]	45.6%
0.4	[0.26, 1.60]	83.8%
0.6	[0.14, 1.60]	91.3%
0.8	[0.12, 1.13]	63.1%
1	[0.12, 0.83]	44.4%

Table 5.5 summarizes the impact of parameter b on performance metrics: the relay discovery probability, the average number of time slots, the probability to select a close relay, and MTD energy consumption. From Table 5.2, Table 5.3, and Table 5.4, the performance metrics are qualified as follows:

- Very bad (--): if the density range covers less than 20% of the target range.
- Bad (-): if the range covers between 20% and 40% of the target range.

- Not good (0): if the range covers between 40% and 60% of the target range.
- Good (+): if the range covers between 60% and 80% of the target range.
- Very good (++): if the range covers more than 80% of the target range.

The probability to select a close relay is qualified from the PDF of the distance between the MTD and the relay given in Fig. 5.13. As can be seen from the table, in general, the best performance of our D2D relaying mechanism within the target UE densities range is achieved when using b between 0.4 and 0.6. The worst performance is obtained when $b = 1$. However, as previously mentioned for low UE densities, $b = 1$ offers acceptable performance.

Table 5.5 Qualitative comparison for different values of b

Performance metric	$b = 0.2$	$b = 0.4$	$b = 0.6$	$b = 0.8$	$b = 1$
Relay discovery probability	-	++	++	+	0
Average number of time slots	--	+	++	+	0
Probability to select a close relay	++	+	0	-	--
MTD energy consumption	0	++	++	+	0

Legend: -- very bad, - bad, 0 not good, + good, ++ very good.

5.6.4 Minimization of the Total MTD Energy Consumption

5.6.4.1 Optimization in the Uniform Random Choice

In the uniform case, for a given UE density λ_u, the total MTD energy consumption $\overline{E}_{\text{D2D,total}}$ depends on three variables: R_d, W, and $d_{m,b}$. We look for the optimal values of these three variables in order to minimize energy consumption in D2D mode. It has been demonstrated in Section 5.4.1.2 and Section 5.4.2.2 respectively that P_{disc} is maximized and $\overline{E}_{\text{D2D,disc}}$ is minimized when $R_d = (\pi\lambda_u \exp(2\sigma^2/\alpha^2)/W)^{-1/2}$ and thus $\overline{E}_{\text{D2D,total}}$ is also minimized. Replacing W by $\pi R_d^2 \lambda_u \exp(2\sigma^2/\alpha^2)$, $\overline{E}_{\text{D2D,total}}$ depends only on two variables (R_d and $d_{m,b}$) and thus we can find the optimal radius of the discovery area R_d^* as a function of $d_{m,b}$. However, it is not possible to get this value analytically so we use numerical computation. Once the value R_d^* is found, the value of the optimal contention window size can be obtained as $W^* = \lceil \pi\lambda_u \exp(2\sigma^2/\alpha^2) R_d^2 \rceil$, where $\lceil \cdot \rceil$ is the ceiling operator.

Fig. 5.15 shows the optimal normalized radius of the discovery area $R_d^*/d_{m,b}$ as a function of the MTD-BS distance for $\lambda_u = \{0.25 \times 10^{-4}, 1.4 \times 10^{-4}\}$ UEs/m^2 and $D = 200$ bytes. From the figure, we can see that for each $d_{m,b}$ there is a value of R_d^* that minimizes the total

MTD energy consumption. When the MTD is near the base station ($d_{m,b} < 50$ meters), the optimal radius of the discovery area is similar in both scenarios. However, when the MTD-BS distance is greater than 300 meters, the radius of the discovery area for $\lambda_u = 0.25 \times 10^{-4}$ UEs/m^2 is 1.7 times greater than the size of the radius when $\lambda_u = 1.4 \times 10^{-4}$ UEs/m^2. This suggests that the UE density has a significant impact on the optimal discovery area. For example, from the figure we obtain the optimal value of R_d for three MTD-BS distances and from these values we calculate the optimal values of W, these optimal values are shown in Table 5.6. Both R_d^* and W^* should be sent by the MTD within the RR packet.

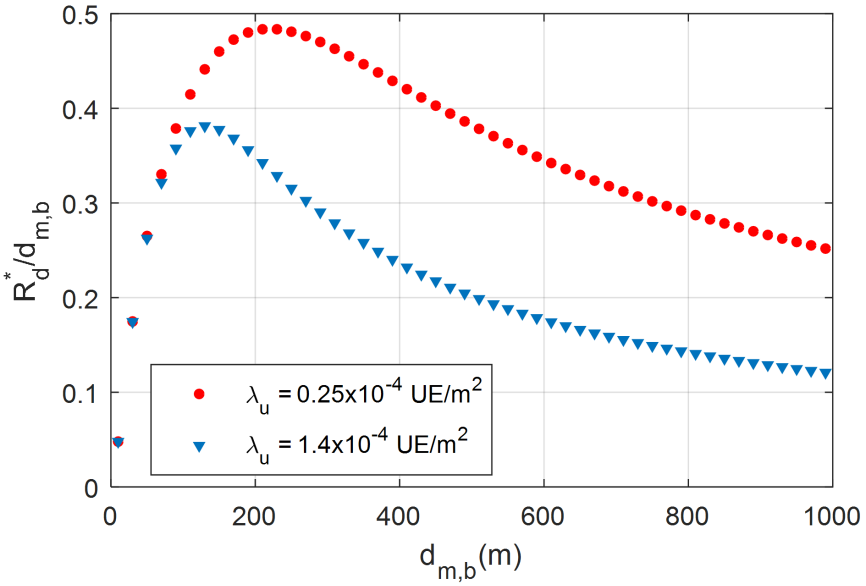

Fig. 5.15 Optimal normalized radius of the discovery area $R_d^*/d_{m,b}$ as a function of the MTD-BS distance, considering $D = 200$ bytes and $\lambda_u = \{0.25 \times 10^{-4}, 1.4 \times 10^{-4}\}$ UEs/m^2.

Table 5.6 Optimal R_d and W parameters

	$\lambda_u = 0.25 \times 10^{-4}$ UEs/m^2			$\lambda_u = 1.4 \times 10^{-4}$ UEs/m^2		
$d_{m,b}$ (m)	$R_d^*/d_{m,b}$	R_d^* (m)	W^*	$R_d^*/d_{m,b}$	R_d^* (m)	W^*
100	0.4	40	1	0.37	37	1
500	0.38	190	5	0.20	100	7
1000	0.25	250	8	0.12	120	10

5.6.4.2 Optimization in the Truncated Geometric Random Choice

Unlike the uniform case, in the truncated geometric random choice case, there is an additional variable (i.e., parameter b) to take into account to minimize energy consumption in D2D mode. The only method to determine the optimal values of W, R_d, and b is through numerical computation due to the complexity of the analytical expressions. However, this method is relatively complex for a simple MTD. Besides, the optimization depends strongly on the MTD-BS distance and the UE density. This last parameter being difficult or even impossible to determine in realistic scenarios. A simple but effective solution is to choose the value of b that minimizes energy consumption in the greater UE density range of the target range $[0.1 \times 10^{-4}, 1.6 \times 10^{-4}]$ UEs/m^2.

The radius of the discovery area R_d is set as 300 (see the analysis in Section 5.6.1), this value should ensure with a probability higher than 98% that there is at least one relay candidate inside the discovery area for UE densities greater than 0.1×10^{-4} UEs/m^2. By choosing the value of b properly, it is possible a reduction of the number of relay candidates contending in the first time slots and thus the number of collisions.

We numerically evaluate the energy consumption for $b = \{0.1, 0.2, ..., 1\}$ in order to determine the optimal value of the parameter b, i.e., the value that minimizes the total MTD energy consumption. Fig. 5.16 presents these optimal values as a function of the UE density for $d_{m,b} = \{250, 500, 750, 1000\}$ meters. From this figure, we observe that when the UE density is very low (i.e., $\lambda_u < 0.2 \times 10^{-4}$ UEs/m^2), it is better the use of highest values (in this case, $b > 0.7$) while when the UE density is very high (i.e., $\lambda_u > 1.4 \times 10^{-4}$ UEs/m^2), $b = 0.3$ is the most appropriate value. In the target UE density range, energy consumption is never minimal when using $b = 0.1$ and $b = 0.2$.

From Fig. 5.16, for each value of b, we estimate the percentage of the target UE density range where the total MTD energy consumption is minimal. These percentages are resumed in Table 5.7. From the table, we observe that for all the analyzed MTD-BS distances, the highest percentage is obtained when $b = 0.4$. This value of b allows a minimization of the energy consumption in almost a third of the target range. Therefore, we choose $b = 0.4$ as the parameter of our D2D relaying mechanism since it allows a reduction of energy consumption in most of the range of UE densities analyzed in this work, especially for high UE densities. Moreover, as shown in Fig. 5.14 for low UE densities, the energy consumption when $b = 0.4$ is almost similar to the energy consumption obtained when the optimal value of b is used.

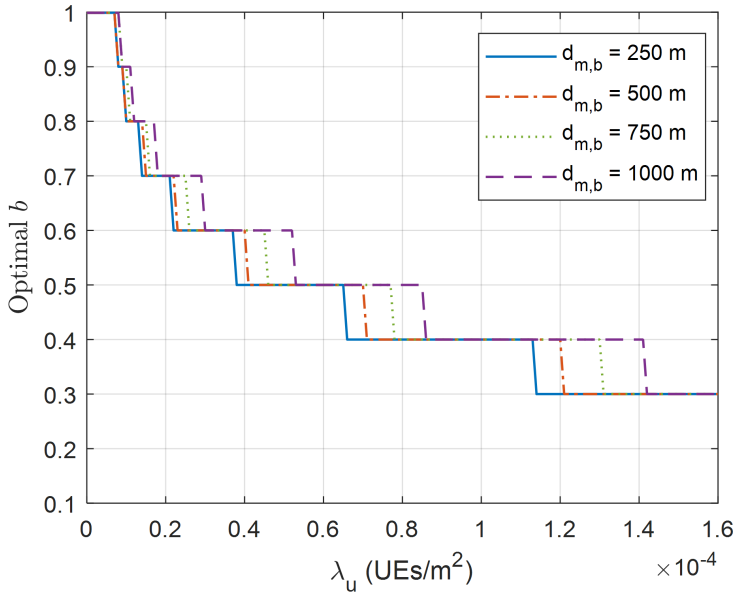

Fig. 5.16 Optimal b, for $R_d = 300$, $W = 16$, shadowing $\sigma_{dB} = 8$ dB, $D = 200$ bytes, and $d_{m,b} = \{250, 500, 750, 1000\}$ meters.

Table 5.7 Percentage of the target UE density range where MTD energy consumption is minimal.

b	$d_{m,b} = 250$ m	$d_{m,b} = 500$ m	$d_{m,b} = 750$ m	$d_{m,b} = 1000$ m
0.3	29.2%	24.8%	18.6%	11.8%
0.4	29.8%	31.1%	32.9%	34.8%
0.5	17.4%	18.6%	19.9%	20.5%
0.6	9.9%	11.2%	12.4%	14.3%
0.7	5.0%	5.0%	6.2%	7.5%
0.8	2.5%	3.1%	3.1%	3.7%
0.9	1.2%	1.2%	1.2%	1.9%
1	5.0%	5.0%	5.6%	5.6%

5.6.5 Comparison of MTD Energy Consumption in Cellular Mode and D2D Mode

One of the purposes of this study is to determine in which scenarios it is convenient the use of D2D mode instead of the cellular mode in terms of energy consumption. In Fig. 5.17 and Fig. 5.18, we compare the energy consumed by the MTD when it uses cellular communication (cellular mode) and when it uses our relaying mechanism (D2D mode) with $b = 0.4$, $R_d = 300$, and $W = 16$.

Fig. 5.17 shows the total MTD energy consumption (in cellular mode and D2D mode) as a function of the UE density (λ_u) and the Euclidean distance between the MTD and the base station ($d_{m,b}$). We consider a scenario where the data packet size D is 200 bytes, the UE density varies in the interval of $[0, 2 \times 10^{-4}]$ UEs/m^2, and $d_{m,b}$ varies from 50 to 1000 meters.

It can be seen from the figure that our proposed mechanism allows a reduction of the total MTD energy consumption in scenarios where $\lambda_u \in [0.2 \times 10^{-4}, 1.6 \times 10^{-4}]$ UEs/m^2 and $d_{m,b} > 500$ meters. The difference between cellular mode and D2D mode is significant when the MTD is far from the base station. The most interesting characteristic of this figure is that when the UE density is within the range $[0.2 \times 10^{-4}, 1.6 \times 10^{-4}]$ UEs/m^2, the UE density and the MTD-BS distance have little influence on MTD energy consumption in D2D mode, i.e., the energy consumption is almost constant and does not depend on λ_u, a parameter that as mentioned before is difficult to estimate in real scenarios.

The energy reduction factor is defined as the ratio between MTD energy consumption in D2D mode (using our proposed relaying mechanism) and the energy consumption in cellular mode. In Table 5.8, we present the energy reduction factor for different values of λ_u and $d_{m,b} = \{500, 1000\}$ meters. For example, for $\lambda_u = 0.25 \times 10^{-4}$ UEs/m^2 and $d_{m,b} = 500$ meters, the energy reduction factor is 0.95, i.e., the energy consumption in D2D mode is almost the same as in cellular mode. The energy reduction factor is 0.34 for $\lambda_u = 0.25 \times 10^{-4}$ UEs/m^2 and $d_{m,b} = 1000$ meters, this means that in D2D mode the MTD consumes 66% less energy than in cellular mode. For $\lambda_u = 1 \times 10^{-4}$ UEs/m^2 and $d_{m,b} = 1000$ meters, the energy reduction factor is 0.25, i.e., in D2D mode the MTD consumes 75% less energy than in cellular mode.

Fig. 5.18 compares the total MTD energy consumption in cellular and D2D modes, as a function of the data packet size (D) and the Euclidean distance between the MTD and the BS ($d_{m,b}$). We consider two scenarios: (a) low UE density with $\lambda_u = 0.25 \times 10^{-4}$ UEs/m^2 and (b) high UE density with $\lambda_u = 1.4 \times 10^{-4}$ UEs/m^2. In both scenarios, the data packet size varies from 50 to 200 bytes, and the MTD-BS distance $d_{m,b}$ varies from 50 to 1000 meters. As can be seen from these two figures, the energy consumption in D2D mode is slightly lower when

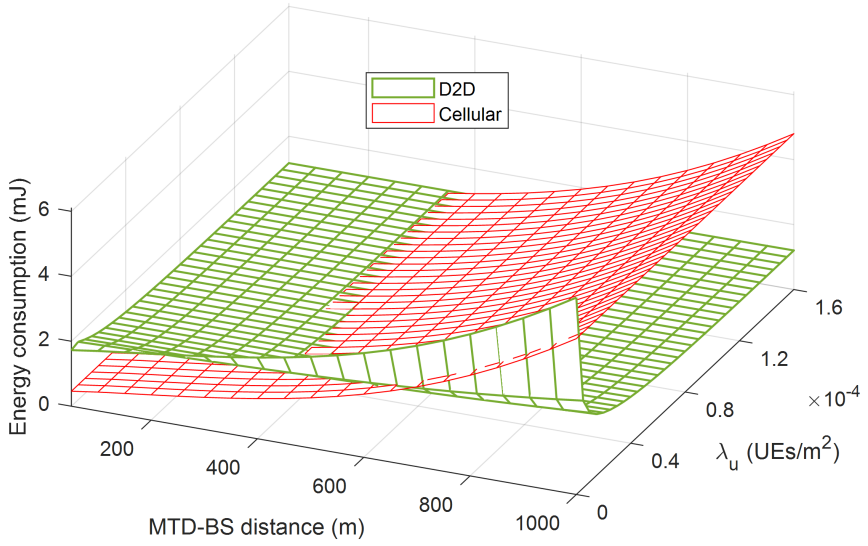

Fig. 5.17 Total MTD energy consumption in cellular mode and D2D mode ($R_d = 300$, $b = 0.4$, and $W = 16$) as a function of the UE density and the MTD-BS distance, for $D = 200$ bytes.

Table 5.8 Energy reduction factor as a function of the UE density

UE density (UEs/m^2)	$\mathbf{0.25 \times 10^{-4}}$		$\mathbf{0.6 \times 10^{-4}}$		$\mathbf{1 \times 10^{-4}}$		$\mathbf{1.4 \times 10^{-4}}$	
MTD-BS distance (m)	**500**	**1000**	**500**	**1000**	**500**	**1000**	**500**	**1000**
Energy cons. D2D (mJ)	1.48	1.63	1.26	1.31	1.20	1.22	1.18	1.20
Energy cons. Cellular (mJ)	1.55	4.80	1.55	4.80	1.55	4.80	1.55	4.80
Energy reduction factor	0.95	0.34	0.81	0.27	0.98	0.25	0.76	0.25

the UE density is high. We can also observe that, for a given $d_{m,b}$, the energy consumption, in cellular mode and D2D mode, grows linearly as a function of the data packet size. These results may be explained by the fact that in cellular mode $\overline{E}_{\text{cell}}$ is directly proportional to D. On the other hand, in D2D mode $\overline{E}_{\text{D2D,total}}$ is the sum of two terms $\overline{E}_{\text{D2D,disc}}$ and $\overline{E}_{\text{dataTx}}$. For a given λ_u, the energy consumption in the discovery phase ($\overline{E}_{\text{D2D,disc}}$) is independent of D, while it is directly proportional to D in the data transmission phase ($\overline{E}_{\text{dataTx}}$). When the data packet size is greater than 150 bytes, in case of low UE density ($\lambda_u = 0.25 \times 10^{-4}$ UEs/m^2), our D2D relaying mechanism allows a significant reduction (more than 50%) of the total energy consumption when the MTD is located more than 900 meters from the base station. In case of high UE density ($\lambda_u = 1.4 \times 10^{-4}$ UEs/m^2), our mechanism allows a significant reduction when the MTD is located more than 750 meters from the base station.

Table 5.9 and Table 5.10, respectively obtained from Fig. 5.18 (a) and Fig. 5.18 (b), present the energy reduction factor for $d_{m,b} = \{500, 1000\}$ meters and data packets of different sizes. As the tables show, there are significant reductions when $d_{m,b}$ = 1000 meters. For example, at low UE density ($\lambda_u = 0.25 \times 10^{-4}$ UEs/m^2), the MTD in D2D mode consumes 23%, 49%, and 66% less energy than in cellular mode for $D = 50$, $D = 100$, and $D = 200$ bytes, respectively. At high UE density ($\lambda_u = 1.4 \times 10^{-4}$ UEs/m^2), the MTD in D2D mode consumes 32%, 60%, and 75% less energy than in cellular mode for $D = 50$, $D = 100$, and $D = 200$ bytes, respectively. We observe in both tables that for a packet of data of 50 bytes and a distance between the MTD and the base station of 500 meters, the D2D mode can double the energy consumption compared to the direct cellular transmission. For this reason, it should be well defined in which cases the use of this D2D relaying mechanism is beneficial.

Table 5.9 Energy reduction factor versus the data packet size for $\lambda_u = 0.25 \times 10^{-4}$ UEs/m^2

Data size (bytes)	**50**		**100**		**200**	
MTD-BS distance (m)	**500**	**1000**	**500**	**1000**	**500**	**1000**
Energy consumption D2D (mJ)	1.00	1.04	1.16	1.23	1.48	1.63
Energy consumption Cellular (mJ)	0.39	1.20	0.77	2.40	1.55	4.80
Energy Reduction Factor	2.56	0.87	1.51	0.51	0.95	0.34

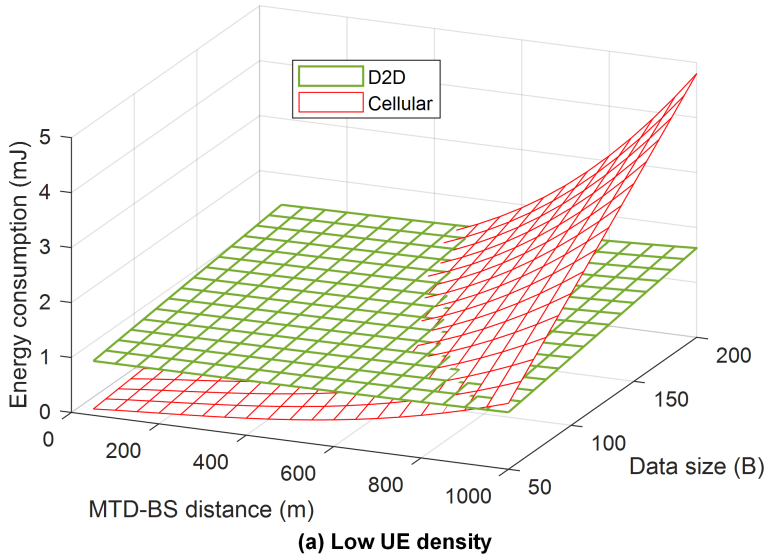

(a) Low UE density

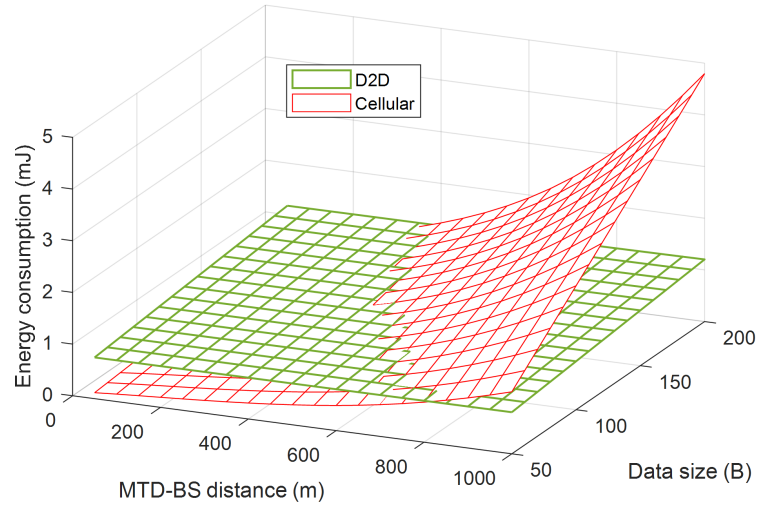

(b) High UE density

Fig. 5.18 Total MTD energy consumption in cellular mode and D2D mode ($R_d = 300$, $b = 0.4$, and $W = 16$) as a function of the UE density and the data packet size, for (a) $\lambda_u = 0.25 \times 10^{-4}$ UEs/m^2 and (b) $\lambda_u = 1.4 \times 10^{-4}$ UEs/m^2.

Table 5.10 Energy reduction factor versus the data packet size for $\lambda_u = 1.4 \times 10^{-4}$ UEs/m^2

Data size (bytes)	**50**		**100**		**200**	
MTD-BS distance (m)	**500**	**1000**	**500**	**1000**	**500**	**1000**
Energy consumption D2D (mJ)	0.81	0.82	0.94	0.95	1.20	1.22
Energy consumption Cellular (mJ)	0.39	1.20	0.77	2.40	1.55	4.80
Energy Reduction Factor	2.08	0.68	1.22	0.40	0.77	0.25

5.7 Conclusion

In this chapter, we have proposed a simple and distributed D2D relaying mechanism, which is suitable for mMTC applications since it allows a reduction of the energy consumed by the MTDs, especially when they have an unfavorable link budget.

The key idea of our protocol is the use of a contention process that gives priority to UEs close to the MTD to be selected as relays. Using stochastic geometry, we derived analytical expressions for the relay discovery probability, the average number of time slots used in the contention process, the PDF of the MTD-relay distance, and the total energy consumed by the MTD. The analytical results are then validated by simulations.

Numerical results show that our D2D relaying mechanism allows a reduction of the total MTD energy consumption (up to 75% compared to a direct cellular transmission) when they have an unfavorable link budget. Moreover, our mechanism achieves almost constant energy consumption for a large range of UE densities and distances between the MTD and the base station. The results shown in this chapter allow determining the scenarios where D2D mode is more favorable than the cellular mode in terms of energy consumption.

Chapter 6

Conclusion and Perspective

6.1 Conclusion

D2D communication is considered one of the enablers of the 5G cellular networks since it permits more efficient communication taking advantage of the proximity between the communicating devices. In this thesis, we focus on the use of D2D communications as an alternative to traditional cellular communications for the connectivity of mMTC devices. As it was seen in Chapter 2, mMTC applications have specific constraints, different from human-communications. Currently, there are new cellular technologies proposed by the 3GPP and specially designed for this type of application. However, in some scenarios, these technologies fail to satisfy all mMTC requirements; for example, extending the coverage implies the increase of MTD energy consumption. In this study, we show that the battery life of a device located at the cell border that transmits 200-byte reports is less than ten years when the device transmits more than one daily report.

In Chapter 3, we show how D2D technology allows not only a reduction of MTD energy consumption but also the global energy consumption, i.e., the sum of energy consumed by the MTD and the relay. In this case, we find that the relay should be located midway between the device and the base station to minimize the global energy consumption. Using a simple model, we derive mathematical formulas to determine when it is more convenient to use a relay rather than a direct transmission to the base station.

In Chapter 4, we consider that the UEs act as a relay, and thus the priority is to reduce the MTD energy consumption whose battery cannot be recharged, unlike the UE. We analyze the energy consumed by an MTD that use D2D communication with the ARQ and CC-HARQ retransmission schemes. In this study, we consider that the MTDs independently select the resources from a pool (i.e., autonomous mode). Using stochastic geometry, we derive analytical expressions for the transmission success probability, the average number

of transmission, and the MTD energy consumption. The results of this study show that CC-HARQ has a better performance than ARQ, especially when the UE density is low or when the MTD density is much higher than the number of resources available for D2D communications. In some cases, MTD energy consumption using CC-HARQ can be half of the consumption using ARQ.

In Chapter 5, we propose a distributed relay mechanism that allows a reduction of the total MTD energy consumption, i.e., the energy consumed during the discovery phase and the data transmission phase. Unlike other mechanisms that select the best UE as a relay, either centrally or by exchanging messages between the MTD and nearby UEs, our mechanism selects the first UE that responds to a discovery message sent by the MTD. The key idea of our mechanism is the fact that it gives a higher chance of responding quickly to UEs that have a better MTD-UE channel. Using stochastic geometry, we provide an analytical framework to analyze the performance of our D2D relaying mechanism. We derive analytical expressions for the relay discovery probability, the average number of time slots used in the contention process, the PDF of the MTD-relay distance, and the total energy consumed by the MTD. Numerical results show that an MTD using our mechanism can consume only a quarter of the energy consumed in cellular communication. Another interesting aspect of our mechanism is that energy consumption is almost constant for an extensive range of UE densities.

6.2 Perspective

The energy consumption model proposed in Chapter 3 considers the same weighting to the energy consumption of the UE and MTD. An extension of this work could be to consider different weighting, where a particular case would be when only the MTD energy consumption is taken into account.

The work in Chapter 4 can be extended considering the autonomous selection of sub-channels in a non-uniform way, for example, by considering the distance between the MTD and the relay as a sub-channel selection parameter. The links whose MTD-relay distance is large are the most vulnerable to interference and consequently have a low probability of successful transmission. To solve this problem, the resources pool can be divided into two unequal subgroups, the subgroup containing the least number of sub-channels is used by the MTDs that are close to their relays. In contrast, the MTDs whose relays are at a considerable distance use the subgroup with the highest number of resources. The higher is the number of sub-channels available, the smaller is the number of devices sharing a sub-channel, and the lower is the interference.

The work in Chapter 5 can be extended considering the choice of time slot different from the uniform or the truncated geometric distribution considered in this work, i.e., the optimal distribution could be found. In our protocol, if two relay candidates respond at the same time-slot a collision occurs and consequently, the RC packets and the UEs that sent those packets are discarded. Thus, our relay selection mechanism could be extended so that if there is a collision, colliding UEs could return to participate in the contention process. Another line of investigation would be to consider the capture effect instead of a destructive collision considered in our study.

Beyond the possible tracks that can be followed to extend this thesis, there are still many open research questions so that D2D relaying technology can be used as an alternative to the traditional cellular networks for mMTC applications. In particular, aspects related to communication security should be investigated in depth since all the information would pass through the relay, which could be a weak security point. D2D communication for mMTC is a still attracts the attention of researchers; it was not only one of the study topics of the European ONE5G project [20], but also standardization organizations such as 3GPP, in Release 14 [70], presents a new study item related to LTE D2D technology applied to the IoT. Therefore, it is expected that in future user equipment such as smartphones can become part of the cellular network playing the role of relays and thus contribute to better connectivity of IoT devices as well as energy savings.

Publications Made during the Thesis

Conference Papers

- C. V. Anamuro, N. Varsier, J. Schwoerer and X. Lagrange, "Simple modeling of energy consumption for D2D relay mechanism," 2018 IEEE Wireless Communications and Networking Conference Workshops (WCNCW), Barcelona, 2018, pp. 231-236.
- C. V. Anamuro, N. Varsier, J. Schwoerer and X. Lagrange, "Modeling of MTC Energy Consumption for D2D Communications with Chase Combining HARQ Scheme," 2018 IEEE Globecom Workshops (GC Wkshps), Abu Dhabi, United Arab Emirates, 2018, pp. 1-6.
- C. V. Anamuro, N. Varsier, J. Schwoerer and X. Lagrange, "Energy-efficient discovery process for mMTC applications," 2019 12th IFIP Wireless and Mobile Networking Conference (WMNC), Paris, France, 2019, pp. 79-86.

Patent

- Cesar Vargas Anamuro and Nadège Varsier, "Une stratégie de sélection distribuée de relais économe en énergie pour le relayage D2D dans un réseau cellulaire IoT, " Patent submitted to INPI N° FR 1913960, France, December 2019.

Contribution to deliverables

- ONE5G project, deliverable D3.1 "Preliminary Multi-Service Performance Optimization Solutions for Improved E2E Performance," 2018.
- ONE5G project, deliverable D3.2 "Recommended Multi-Service Performance Optimization Solutions for Improved E2E Performance," 2019.

References

[1] Ericsson. Cellular networks for massive iot. *White Paper*, January 2020.

[2] Rashmi Sharan Sinha, Yiqiao Wei, and Seung-Hoon Hwang. A survey on lpwa technology: Lora and nb-iot. *Ict Express*, 3(1):14–21, 2017.

[3] 3GPP. Cellular system support for ultra low complexity and low throughput internet of things. Technical Report (TR) 45.820, 3rd Generation Partnership Project (3GPP), 2015. Version 13.1.0.

[4] Luca Feltrin, Galini Tsoukaneri, Massimo Condoluci, Chiara Buratti, Toktam Mahmoodi, Mischa Dohler, and Roberto Verdone. Narrowband iot: A survey on downlink and uplink perspectives. *IEEE Wireless Communications*, 26(1):78–86, 2019.

[5] Qualcomm Techn. Inc. Leading the lte iot evolution to connect the massive internet of things. *Whitepaper*, 2017.

[6] Daquan Feng, Lu Lu, Yi Yuan-Wu, Geoffrey Ye Li, Shaoqian Li, and Gang Feng. Device-to-device communications in cellular networks. *IEEE Communications Magazine*, 52(4):49–55, 2014.

[7] G Araniti, A Raschellà, A Orsino, L Militano, and M Condoluci. Device-to-device communications over 5g systems: Standardization, challenges and open issues. In *5G mobile communications*, pages 337–360. Springer, 2017.

[8] 3GPP. Proximity-Based Services (ProSe); Stage 2. Technical Specification (TS) 23.303, 3rd Generation Partnership Project (3GPP), 2015.

[9] J Schlienz and A Roessler. Device to device communication in lte whitepaper. *ROHDE & SCHWARZ: Munich, Germany*, 2015.

[10] M Series. IMT Vision–Framework and overall objectives of the future development of IMT for 2020 and beyond. *Recommendation ITU*, pages 2083–0, 2015.

[11] Cisco. Cisco visual networking index: Forecast and trends, 2018–2023. *White Paper*, February 2020.

[12] Kuor-Hsin Chang. Bluetooth: a viable solution for iot?[industry perspectives]. *IEEE Wireless Communications*, 21(6):6–7, 2014.

[13] ZigBee Alliance. Zigbee specification version 1.0, 2005.

[14] Serbulent Tozlu, Murat Senel, Wei Mao, and Abtin Keshavarzian. Wi-fi enabled sensors for internet of things: A practical approach. *IEEE Communications Magazine*, 50(6):134–143, 2012.

[15] LoRa Alliance. Wide area networks for iot. *Recovered of: https://www. lora-alliance. org*, 2015.

[16] SA Sigfox. Sigfox technology overview, 2018.

[17] Carsten Bockelmann, Nuno K Pratas, Gerhard Wunder, Stephan Saur, Monica Navarro, David Gregoratti, Guillaume Vivier, Elisabeth De Carvalho, Yalei Ji, Čedomir Stefanović, et al. Towards massive connectivity support for scalable mmtc communications in 5g networks. *IEEE access*, 6:28969–28992, 2018.

[18] Rapeepat Ratasuk, Nitin Mangalvedhe, David Bhatoolaul, and Amitava Ghosh. Lte-m evolution towards 5g massive mtc. In *2017 IEEE Globecom Workshops (GC Wkshps)*, pages 1–6. IEEE, 2017.

[19] Gábor Fodor, Sandra Roger, Nandana Rajatheva, Slimane Ben Slimane, Tommy Svensson, Petar Popovski, José Mairton B Da Silva, and Samad Ali. An overview of device-to-device communications technology components in metis. *Ieee Access*, 4:3288–3299, 2016.

[20] E2e-aware optimizations and advancements for network edge of 5g new radio (one5g). https://one5g.eu.

[21] 3GPP. Study on Facilitating Machine to Machine Communication in 3GPP Systems. Technical Report (TR) 22.868, 3rd Generation Partnership Project (3GPP), 2016. Version 8.0.0.

[22] 3GPP. Service requirements for Machine-Type Communications (MTC); Stage 1. Technical Report (TR) 22.368, 3rd Generation Partnership Project (3GPP), 2014. Version 13.0.0.

[23] P Popovski, G Mange, D Gozalvez-Serrano, T Rosowski, G Zimmermann, P Agyapong, M Fallgren, A Höglund, O Queseth, H Tullberg, et al. Final report on the metis 5g system concept and technology roadmap. *METIS Document ICT-317669-METIS/D6. 6*, 2015.

[24] Olof Liberg, Marten Sundberg, Eric Wang, Johan Bergman, and Joachim Sachs. *Cellular Internet of Things: Technologies, Standards, and Performance*. Academic Press, 2017.

[25] Ericsson Altair SONY Virtuosys ATT Verizon Sequans KDDI Nokia NTT DOCOMO KT Sierra Wireless, ORANGE. Evaluation of LTE-M towards 5G IoT requirements. *White paper*, 2017.

[26] 3GPP. Study on Scenarios and Requirements for Next Generation Access Technologies; (Release 14). Technical Report (TR) 38.913, 3rd Generation Partnership Project (3GPP), 2017. Version 14.2.0.

[27] Maria Rita Palattella, Mischa Dohler, Alfredo Grieco, Gianluca Rizzo, Johan Torsner, Thomas Engel, and Latif Ladid. Internet of things in the 5g era: Enablers, architecture, and business models. *IEEE Journal on Selected Areas in Communications*, 34(3):510–527, 2016.

[28] 3GPP. Architecture Enhancements to Facilitate Communications with Packet Data Networks and Applications. Technical Specification (TS) 23.682, 3rd Generation Partnership Project (3GPP), 2016. Version 14.0.0.

[29] C. Bockelmann, N. Pratas, H. Nikopour, K. Au, T. Svensson, C. Stefanovic, P. Popovski, and A. Dekorsy. Massive machine-type communications in 5g: physical and mac-layer solutions. *IEEE Communications Magazine*, 54(9):59–65, Sep. 2016.

[30] Rapeepat Ratasuk, Jun Tan, and Amitava Ghosh. Coverage and capacity analysis for machine type communications in lte. In *2012 IEEE 75th Vehicular Technology Conference (VTC Spring)*, pages 1–5. IEEE, 2012.

[31] Rapeepat Ratasuk, Nitin Mangalvedhe, and Amitava Ghosh. Overview of lte enhancements for cellular iot. In *2015 IEEE 26th annual international symposium on personal, indoor, and mobile radio communications (PIMRC)*, pages 2293–2297. IEEE, 2015.

[32] Mei Ling Huang, Vincenzo Coia, and Percy Brill. A cluster truncated pareto distribution and its applications. *ISRN Probability and Statistics*, 2013, 2013.

[33] 3GPP. GERAN Study on Power Saving for MTC Devices. Technical Report (TR) 43.869, 3rd Generation Partnership Project (3GPP), 2016.

[34] Naveen Mysore Balasubramanya, Lutz Lampe, Gustav Vos, and Steve Bennett. On timing reacquisition and enhanced primary synchronization signal (epss) design for energy efficient 3gpp lte mtc. *IEEE Transactions on Mobile Computing*, 16(8):2292–2305, 2016.

[35] Seonghwa Yun, Kyeongmin Lee, Sangdon Park, and Jun Kyun Choi. Energy efficient relay selection scheme with drx mechanism in 3gpp lte network. In *2013 International Conference on ICT Convergence (ICTC)*, pages 6–11. IEEE, 2013.

[36] Rothna Pec, Mohammed Saquib Khan, Chang-Hwan Park, and Yong-Soo Cho. A detection for synchronization signal in lte-based machine-type communication. In *2016 International Conference on Information and Communication Technology Convergence (ICTC)*, pages 1–3. IEEE, 2016.

[37] Leila Nasraoui, Leila Najjar Atallah, and Mohamed Siala. Performance analysis of low-complexity simply-differential time synchronization approach for mtc over lte systems. In *2016 IEEE 84th Vehicular Technology Conference (VTC-Fall)*, pages 1–5. IEEE, 2016.

[38] 3GPP. Evolved Universal Terrestrial Radio Access (E-UTRA); Radio Resource Control (RRC); Protocol Specification. Technical Specification (TS) 36.331, 3rd Generation Partnership Project (3GPP), 2016. Version 14.0.0.

[39] Qipeng Song, Xavier Lagrange, and Loutfi Nuaymi. An efficient m2m-oriented network-integrated multiple-period polling service in lte network. In *2015 IEEE 82nd Vehicular Technology Conference (VTC2015-Fall)*, pages 1–6. IEEE, 2015.

[40] Kaijie Zhou and Navid Nikaein. Packet aggregation for machine type communications in lte with random access channel. In *2013 IEEE Wireless Communications and Networking Conference (WCNC)*, pages 262–267. IEEE, 2013.

[41] Kaijie Zhou and Navid Nikaein. Low latency random access with tti bundling in lte/lte-a. In *2015 IEEE International Conference on Communications (ICC)*, pages 2257–2263. IEEE, 2015.

[42] Furqan Jameel, Zara Hamid, Farhana Jabeen, Sherali Zeadally, and Muhammad Awais Javed. A survey of device-to-device communications: Research issues and challenges. *IEEE Communications Surveys & Tutorials*, 20(3):2133–2168, 2018.

[43] Shao-Yu Lien, Chun-Che Chien, Fan-Min Tseng, and Tien-Chen Ho. 3gpp device-to-device communications for beyond 4g cellular networks. *IEEE Communications Magazine*, 54(3):29–35, 2016.

[44] Pavel Mach, Zdenek Becvar, and Tomas Vanek. In-band device-to-device communication in ofdma cellular networks: A survey and challenges. *IEEE Communications Surveys & Tutorials*, 17(4):1885–1922, 2015.

[45] 3GPP. Feasibility study for Proximity Services (ProSe). Technical Report (TR) 23.803, 3rd Generation Partnership Project (3GPP), 2013.

[46] Kiran Vanganuru, Steven Ferrante, and Gregory Sternberg. System capacity and coverage of a cellular network with d2d mobile relays. In *MILCOM 2012-2012 IEEE Military Communications Conference*, pages 1–6. IEEE, 2012.

[47] Guogang Zhao, Sheng Chen, Lin Qi, Liqiang Zhao, and Lajos Hanzo. Mobile-traffic-aware offloading for energy-and spectral-efficient large-scale d2d-enabled cellular networks. *IEEE Transactions on Wireless Communications*, 2019.

[48] Sergey Andreev, Alexander Pyattaev, Kerstin Johnsson, Olga Galinina, and Yevgeni Koucheryavy. Cellular traffic offloading onto network-assisted device-to-device connections. *IEEE Communications Magazine*, 52(4):20–31, 2014.

[49] Kae Won Choi and Zhu Han. Device-to-device discovery for proximity-based service in lte-advanced system. *IEEE Journal on Selected Areas in Communications*, 33(1):55–66, 2014.

[50] Utku Tefek and Teng Joon Lim. Relaying and radio resource partitioning for machine-type communications in cellular networks. *IEEE Transactions on Wireless Communications*, 16(2):1344–1356, 2016.

[51] Ruofei Ma, Yao-Jen Chang, Hsiao-Hwa Chen, and Chun-Yuan Chiu. On relay selection schemes for relay-assisted d2d communications in lte-a systems. *IEEE Transactions on Vehicular Technology*, 66(9):8303–8314, 2017.

[52] C. V. Anamuro, N. Varsier, J. Schwoerer, and X. Lagrange. Energy-efficient discovery process for mmtc applications. In *2019 12th IFIP Wireless and Mobile Networking Conference (WMNC)*, pages 79–86, Sep. 2019.

[53] Yun Li, Chao Liao, Yong Wang, and Chonggang Wang. Energy-efficient optimal relay selection in cooperative cellular networks based on double auction. *IEEE Transactions on Wireless Communications*, 14(8):4093–4104, 2015.

[54] Wantanee Viriyasitavat, Mate Boban, Hsin-Mu Tsai, and Athanasios Vasilakos. Vehicular communications: Survey and challenges of channel and propagation models. *IEEE Vehicular Technology Magazine*, 10(2):55–66, 2015.

[55] Bin Zhou, Honglin Hu, Sheng-Qiang Huang, and Hsiao-Hwa Chen. Intracluster device-to-device relay algorithm with optimal resource utilization. *IEEE transactions on vehicular technology*, 62(5):2315–2326, 2013.

[56] Cesar Vargas Anamuro, Nadège Varsier, Jean Schwoerer, and Xavier Lagrange. Simple modeling of energy consumption for d2d relay mechanism. In *2018 IEEE Wireless Communications and Networking Conference Workshops (WCNCW)*, pages 231–236. IEEE, 2018.

[57] ONE5G project. Preliminary multi-service performance optimization solutions for improved e2e performance. *Deliverable D3.1*, 2018.

[58] Arash Asadi, Qing Wang, and Vincenzo Mancuso. A survey on device-to-device communication in cellular networks. *IEEE Communications Surveys & Tutorials*, 16(4):1801–1819, 2014.

[59] Mohsen Nader Tehrani, Murat Uysal, and Halim Yanikomeroglu. Device-to-device communication in 5g cellular networks: challenges, solutions, and future directions. *IEEE Communications Magazine*, 52(5):86–92, 2014.

[60] Fengchen Ouyang, Jianhua Ge, Fengkui Gong, and Jun Hou. Collision resolving relay selection in large-scale blind relay networks. *Wireless Networks*, 23(6):1793–1807, 2017.

[61] Ahmad Alsharoa, Xiaoyun Zhang, Daji Qiao, and Ahmed Kamal. An energy-efficient relaying scheme for internet of things communications. In *2018 IEEE International Conference on Communications (ICC)*, pages 1–6. IEEE, 2018.

[62] Azlan Awang, Xavier Lagrange, and David Ros. Toward an analysis of energy consumption in multihop wireless sensor networks. In *2010 International Conference on Intelligent and Advanced Systems*, pages 1–6. IEEE, 2010.

[63] Mehdi Seyfi, Sami Muhaidat, Jie Liang, and Mehrdad Dianati. Effect of feedback delay on the performance of cooperative networks with relay selection. *IEEE Transactions on Wireless Communications*, 10(12):4161–4171, 2011.

[64] Diomidis S Michalopoulos, Himal A Suraweera, George K Karagiannidis, and Robert Schober. Amplify-and-forward relay selection with outdated channel estimates. *IEEE Transactions on Communications*, 60(5):1278–1290, 2012.

[65] Zhong Zhou, Shengli Zhou, Jun-Hong Cui, and Shuguang Cui. Energy-efficient cooperative communication based on power control and selective single-relay in wireless sensor networks. *IEEE transactions on wireless communications*, 7(8):3066–3078, 2008.

[66] Aggelos Bletsas, Hyundong Shin, and Moe Z Win. Cooperative communications with outage-optimal opportunistic relaying. *IEEE Transactions on Wireless Communications*, 6(9):3450–3460, 2007.

[67] Hao Feng, Yao Xiao, and Leonard J Cimini. Net throughput of centralized and decentralized cooperative networks with relay selection. *IEEE Wireless Communications Letters*, 3(5):477–480, 2014.

[68] Shuanshuan Wu, Rachad Atat, Nicholas Mastronarde, and Lingjia Liu. Coverage analysis of d2d relay-assisted millimeter-wave cellular networks. In *2017 IEEE Wireless Communications and Networking Conference (WCNC)*, pages 1–6. IEEE, 2017.

[69] Haichao Wei, Na Deng, Ming Zhao, Wuyang Zhou, and Peng Dong. Station density effect on energy efficiency of relay-assisted cellular networks. In *2012 1st IEEE International Conference on Communications in China (ICCC)*, pages 411–415. IEEE, 2012.

[70] 3GPP. Study on further enhancements to LTE Device to Device (D2D), User Equipment (UE) to network relays for Internet of Things (IoT) and wearables. Technical Report (TR) 36.746, 3rd Generation Partnership Project (3GPP), 2017.

[71] Giovanni Rigazzi, Francesco Chiti, Romano Fantacci, and Camillo Carlini. Multi-hop d2d networking and resource management scheme for m2m communications over lte-a systems. In *2014 international wireless communications and mobile computing conference (IWCMC)*, pages 973–978. IEEE, 2014.

[72] Nuno K Pratas and Petar Popovski. Underlay of low-rate machine-type d2d links on downlink cellular links. In *2014 IEEE International Conference on Communications Workshops (ICC)*, pages 423–428. IEEE, 2014.

[73] Miloud Bagaa, Adlen Ksentini, Tarik Taleb, Riku Jantti, Ali Chelli, and Ilangko Balasingham. An efficient d2d-based strategies for machine type communications in 5g mobile systems. In *2016 IEEE Wireless Communications and Networking Conference*, pages 1–6. IEEE, 2016.

[74] Giovanni Rigazzi, Nuno K Pratas, Petar Popovski, and Romano Fantacci. Aggregation and trunking of m2m traffic via d2d connections. In *2015 IEEE international conference on communications (ICC)*, pages 2973–2978. IEEE, 2015.

[75] Guowang Miao, Amin Azari, and Taewon Hwang. E2 mac: Energy efficient medium access for massive m2m communications. *IEEE Transactions on communications*, 64(11):4720–4735, 2016.

[76] Akram Al-Hourani, Sithamparanathan Kandeepan, and Ekram Hossain. Relay-assisted device-to-device communication: A stochastic analysis of energy saving. *IEEE Transactions on Mobile Computing*, 15(12):3129–3141, 2016.

[77] Jinlong Chai, Lei Feng, Fanqin Zhou, Pan Zhao, Peng Yu, and Wenjing Li. Energy-efficient resource allocation based on hypergraph 3d matching for d2d-assisted mmtc networks. In *2018 IEEE Global Communications Conference (GLOBECOM)*, pages 1–7. IEEE, 2018.

[78] Chih-Yuan Tu, Chieh-Yuan Ho, and Ching-Yao Huang. Energy-efficient algorithms and evaluations for massive access management in cellular based machine to machine communications. In *2011 IEEE Vehicular Technology Conference (VTC Fall)*, pages 1–5. IEEE, 2011.

[79] David Chase. Code combining-a maximum-likelihood decoding approach for combining an arbitrary number of noisy packets. *IEEE transactions on communications*, 33(5):385–393, 1985.

[80] David Mandelbaum. An adaptive-feedback coding scheme using incremental redundancy (corresp.). *IEEE Transactions on Information Theory*, 20(3):388–389, 1974.

[81] Pal Frenger, Stefan Parkvall, and Erik Dahlman. Performance comparison of harq with chase combining and incremental redundancy for hsdpa. In *IEEE 54th Vehicular Technology Conference. VTC Fall 2001. Proceedings (Cat. No. 01CH37211)*, volume 3, pages 1829–1833. IEEE, 2001.

[82] Cesar Vargas Anamuro, Nadège Varsier, Jean Schwoerer, and Xavier Lagrange. Modeling of mtc energy consumption for d2d communications with chase combining harq scheme. In *2018 IEEE Globecom Workshops (GC Wkshps)*, pages 1–6. IEEE, 2018.

[83] Xavier Leturc, Philippe Ciblat, and Christophe J Le Martret. Energy-efficient resource allocation for harq with statistical csi. *IEEE Transactions on Vehicular Technology*, 67(12):11936–11949, 2018.

[84] Marco Centenaro, Giulio Ministeri, and Lorenzo Vangelista. A comparison of energy-efficient harq protocols for m2m communication in the finite block-length regime. In *2015 IEEE International Conference on Ubiquitous Wireless Broadband (ICUWB)*, pages 1–6. IEEE, 2015.

[85] Songhu Ge, Yong Xi, Haitao Zhao, Shengchun Huang, and Jibo Wei. Energy efficient optimization for cc-harq over block rayleigh fading channels. *IEEE Communications Letters*, 19(10):1854–1857, 2015.

[86] Elieser B Manhas, Marcelo E Pellenz, Glauber Brante, Richard D Souza, and Fernando Rosas. Energy efficiency analysis of harq with chase combining in multi-hop wireless sensor networks. In *2014 IEEE Symposium on Computers and Communications (ISCC)*, pages 1–6. IEEE, 2014.

[87] Harpreet S Dhillon and Jeffrey G Andrews. Downlink rate distribution in heterogeneous cellular networks under generalized cell selection. *IEEE Wireless Communications Letters*, 3(1):42–45, 2013.

[88] Qipeng Song, Loutfi Nuaymi, and Xavier Lagrange. Analysis of macro diversity based on maximum ratio combining in long range aloha networks. *Telecommunication Systems*, pages 1–12, 2019.

[89] Martin Haenggi, Radha Krishna Ganti, et al. Interference in large wireless networks. *Foundations and Trends® in Networking*, 3(2):127–248, 2009.

[90] Leonard R Kahn. Ratio squarer. *Proceedings of the Institute of Radio Engineers*, 42(11):1704–1704, 1954.

[91] John G Proakis and Masoud Salehi. *Digital communications*, volume 4. McGraw-hill New York, 2001.

[92] Abdelmajid Bessate and Faissal El Bouanani. A very tight approximate results of mrc receivers over independent weibull fading channels. *Physical Communication*, 21:30–40, 2016.

[93] Xavier Lagrange. Performance analysis of harq protocols with link adaptation on fading channels. *annals of telecommunications-annales des télécommunications*, 66(11-12):695–705, 2011.

[94] Qipeng Song, Xavier Lagrange, and Loutfi Nuaymi. Evaluation of macro diversity gain in long range aloha networks. *IEEE Communications Letters*, 21(11):2472–2475, 2017.

[95] Jeffrey G Andrews, François Baccelli, and Radha Krishna Ganti. A tractable approach to coverage and rate in cellular networks. *IEEE Transactions on communications*, 59(11):3122–3134, 2011.

[96] Hongnian Xing and Sami Hakola. The investigation of power control schemes for a device-to-device communication integrated into ofdma cellular system. In *21st Annual IEEE International Symposium on Personal, Indoor and Mobile Radio Communications*, pages 1775–1780. IEEE, 2010.

[97] Qingwen Liu, Shengli Zhou, and Georgios B Giannakis. Cross-layer combining of adaptive modulation and coding with truncated arq over wireless links. *IEEE Transactions on wireless communications*, 3(5):1746–1755, 2004.

[98] ONE5G project. Recommended multi-service performance optimization solutions for improved e2e performance. *Deliverable D3.2*, 2019.

[99] Azlan Awang, Xavier Lagrange, and David Ros. Rssi-based forwarding for multihop wireless sensor networks. In *Meeting of the European Network of Universities and Companies in Information and Communication Engineering*, pages 138–147. Springer, 2009.

[100] Kyle Jamieson, Hari Balakrishnan, and YC Tay. Sift: A mac protocol for event-driven wireless sensor networks. In *European workshop on wireless sensor networks*, pages 260–275. Springer, 2006.

[101] Zhesheng Lin, Yuancao Li, Si Wen, Yuehong Gao, Xin Zhang, and Dacheng Yang. Stochastic geometry analysis of achievable transmission capacity for relay-assisted device-to-device networks. In *2014 IEEE international conference on communications (ICC)*, pages 2251–2256. IEEE, 2014.

[102] Dionysis Xenakis, Marios Kountouris, Lazaros Merakos, Nikos Passas, and Christos Verikoukis. Performance analysis of network-assisted d2d discovery in random spatial networks. *IEEE Transactions on Wireless Communications*, 15(8):5695–5707, 2016.

[103] Jiuqiang Xu, Wei Liu, Fenggao Lang, Yuanyuan Zhang, and Chenglong Wang. Distance measurement model based on rssi in wsn. *Wireless Sensor Network*, 2(08):606, 2010.

[104] 3GPP. Evolved Universal Terrestrial Radio Access (E-UTRA); Radio Frequency (RF) system scenarios. Technical Report (TR) 36.942, 3rd Generation Partnership Project (3GPP), 06 2018. Version 15.0.0.

[105] Preben Mogensen, Wei Na, István Z Kovács, Frank Frederiksen, Akhilesh Pokhariyal, Klaus I Pedersen, Troels Kolding, Klaus Hugl, and Markku Kuusela. Lte capacity compared to the shannon bound. In *2007 IEEE 65th vehicular technology conference-VTC2007-Spring*, pages 1234–1238. IEEE, 2007.

[106] Roy L Streit. *Poisson point processes: imaging, tracking, and sensing*. Springer Science & Business Media, 2010.

[107] Sung Nok Chiu, Dietrich Stoyan, Wilfrid S Kendall, and Joseph Mecke. *Stochastic geometry and its applications*. John Wiley & Sons, 2013.

[108] Eric W Weisstein. Incomplete gamma function. *MathWorld, A Wolfram Web Resource.,[Online]. Available: http://mathworld. wolfram. com/Incomplete Gamma-Function. html*, 2006.

[109] Izrail Solomonovich Gradshteyn and Iosif Moiseevich Ryzhik. *Table of integrals, series, and products*. Academic press, 2014.

Appendix A

Fundamental Concepts of Stochastic Geometry

In recent years, stochastic geometry has received considerable attention as a useful tool for modeling the locations of nodes (e.g., UEs, MTDs, etc) in wireless networks. Stochastic geometric approaches offer a tractable mathematical analysis of the key performance metrics of cellular networks [106, 89].

The theory of geometry stochastic is expounded in detail in [106, 107]. The following is a summary of the basic concepts necessary to understand the mathematical analysis of this thesis.

A.1 Spatial Point Process

A spatial point process is a random pattern of points $\Phi = \{x_n\}$ in d-dimensional space ($d \geq 2$), where the number of points and their locations are random. The point process satisfy the following two conditions:

(i) Any bounded set $A \subset \mathbb{R}^d$ must contain only a finite number of points ($N(A) < \infty$) with probability 1,

(ii) At most one point of the process is observed at any location (i.e., $x_i \neq x_j$ if $i \neq j$).

These conditions are called (i) *locally finite*, and (ii) *simple*. In this thesis we assume that the locations of the UEs, and MTDs constitute two different random point patterns in two dimensions (i.e., $d = 2$);

Definition A.1.1. *A point process is called stationary if its characteristics are invariant under translation, i.e., the point processes $\Phi = \{x_n\}$ and $\Phi = \{x_n + x\}$ have the same distribution for all x in $\mathbb{R}^2$.*

Definition A.1.2. *The density of a stationary point process $\Phi = \{x_n\}$ is defined as follows:*

$$\frac{\mathbb{E}[N(A)]}{|A|},\ A \subset \mathbb{R}^2, \tag{A.1}$$

where $N(A)$ and $|A|$ denote the number of points inside A and the area of A, respectively.

A.1.1 General Poisson Point Process (PPP)

Definition A.1.3. *A general Poison point process Φ in $\mathbb{R}^2$ with intensity measure Λ is characterized by the two following properties:*

(i) For any set $A \subset \mathbb{R}^2$, the number of points inside A follows a Poisson distribution with mean $\Lambda(A)$, i.e.,

$$\mathbb{P}(N(A) = n) = \frac{(\Lambda(A))^n}{n!}\exp(-\Lambda(A)),\ n = 0,1,2,... \tag{A.2}$$

(ii) For any disjoint $A_1,...,A_m \subset \mathbb{R}^2$ sets, $N(A_1),...,N(A_m)$ are independent random variables, where $N(A_i)$ represents the number of points falling inside A_i.

Definition A.1.4. *The intensity measure Λ of a general Poisson point process is given by*

$$\Lambda(A) = \int_A \lambda(u)du,\ for A \subset \mathbb{R}^2, \tag{A.3}$$

where $\lambda(u)$ is called intensity function of the general Poisson point process.

If $\lambda(u) = k \geq 0$, where k is a constant, the PPP is called homogeneous (H-PPP); otherwise, it is called nonhomogeneous or inhomogeneous (I-PPP). Figure A.1 (a) shows a realization of a H-PPP with intensity $\lambda = 0.01$ points per m^2. The homogeneity of the point pattern can be noticed in the figure. A realization of an I-PPP with intensity function in polar coordinates $\lambda(r) = 1/r$ points per m^2 is shown in Figure A.1 (b). Note that the density of points is greater near to the origin of coordinates.

Definition A.1.5. *Let $f(x)$: $\mathbb{R}^2 \to [0,1]$ be a measurable function. For a point process Φ the probability generating functional (PGFL) is defined as*

$$\mathcal{G}[f] = \mathbb{E}\left[\prod_{x\in\Phi} f(x)\right]. \tag{A.4}$$

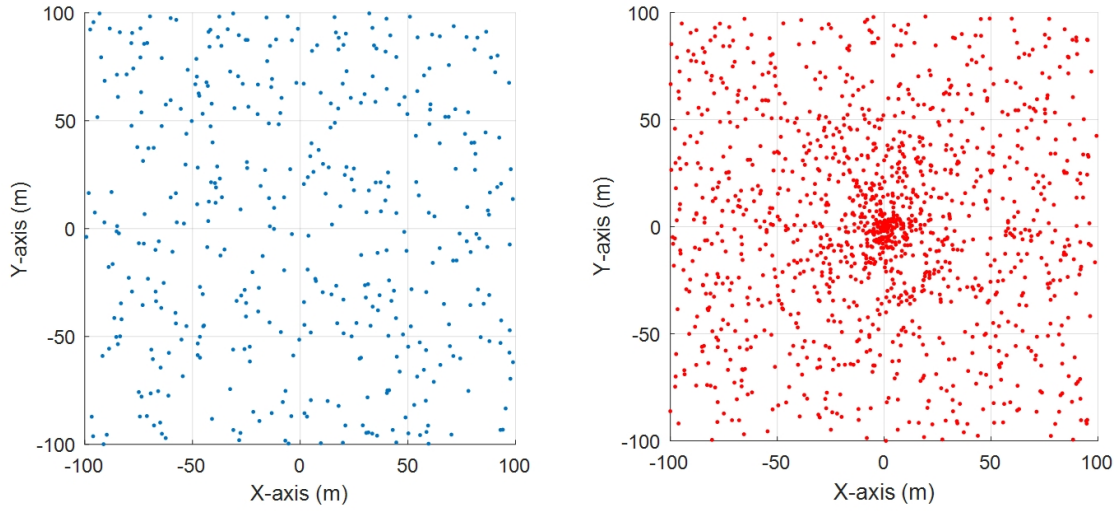

Fig. A.1 Realizations of : (a) a homogeneous PPP with intensity $\lambda = 0.01$ points per m^2; and (b) an inhomogeneous PPP with intensity function $\lambda(r) = 1/r$ points per m^2 (r refers to the radial coordinate).

Theorem A.1.1. *Let Φ be a H-PPP with density λ and $f(x)$: $\mathbb{R}^2 \to [0,1]$ be a real valued function. The PGFL of Φ is given by*

$$\mathscr{G}[f] = \mathbb{E}\left[\prod_{x\in\Phi} f(x)\right] = \exp\left(-\lambda \int_{\mathbb{R}^2} (1-f(x))dx\right). \tag{A.5}$$

Theorem A.1.2 (Campbell's theorem)**.** *Let Φ be a H-PPP with density λ and $f(x)$: $\mathbb{R}^2 \to \mathbb{R}^+$.*

$$\mathbb{E}\left[\sum_{x\in\Phi} f(x)\right] = \lambda \int_{\mathbb{R}^2} f(x)dx. \tag{A.6}$$

A.1.2 Operations on Poisson Point Processes

There are three fundamental operations on point processes, which generate new processes from other basic processes: thinning, clustering, and superposition. The thinning operation is the process of removing certain points of a basic process Φ_b, thus generating the thinned point process Φ is a subset of Φ_b. In the clustering operation, each point of a point process Φ_b is replaced by a cluster of points. In the superposition operation a new point process Φ is generated by the superposition of two independent point processes Φ_1 and Φ_2 (i.e., $\Phi = \Phi_1 \cup \Phi_2$).

Definition A.1.6. *A thinning is called independent if the deletion of each point is independent of locations and possible deletions of any other point of Φ_b [107].*

Theorem A.1.3 (Independent thinning of a PPP)**.** *Let Φ_b be a H-PPP with intensity λ_b and let $p \in [0,1]$ be a constant. A thinned point process Φ is generated by removing each point of Φ_b with probability $1-p$, independently of all other points. Thus Φ is also a H-PPP with intensity $\lambda = p\lambda_b$.*

Theorem A.1.4 (Superposition of PPPs)**.** *Let Φ_1 and Φ_2 be two independent H-PPP with intensities λ_1 and λ_2, respectively. The superposition of Φ_1 and Φ_2 generates a new H-PPP Φ (i.e., $\Phi = \Phi_1 \cup \Phi_2$) with intensity $\lambda = \lambda_1 + \lambda_2$.*

Appendix B

Proof of Equations used in this thesis

B.1 Performance of ARQ when the Best UE is Selected as a Relay

B.1.1 Transmission Success Probability

From (4.27) we have:

$$P_{s,\text{arq}}^{\text{best}}(\lambda_U) = \int_0^{+\infty} (1-(1-P_s(r))^N) 2\pi\lambda_U e^{2\sigma^2/\alpha^2} \exp(-\lambda_U e^{2\sigma^2/\alpha^2}\pi r^2) r dr, \tag{B.1}$$

where $P_s(r) = \exp(-\pi\lambda_M e^{2\sigma^2/\alpha^2} r^2 \theta_{th}^{2/\alpha} \Gamma(1+\frac{2}{\alpha})\Gamma(1-\frac{2}{\alpha})/S)$.

In order to simplify the analysis, let

$$A_1 = \pi\lambda_M e^{2\sigma^2/\alpha^2} \theta_{th}^{2/\alpha} \Gamma(1+2/\alpha)\Gamma(1-2/\alpha)/S \tag{B.2}$$

and

$$A_2 = \pi\lambda_U e^{2\sigma^2/\alpha^2} \tag{B.3}$$

Using A_1 and A_2 and then with substitution $r^2 = x$, we can rewrite (B.1) as follows:

$$\begin{aligned} P_{s,\text{arq}}^{\text{best}}(\lambda_U) &= \int_0^{+\infty} (1-(1-\exp(-A_1 r^2))^N) A_2 \exp(-A_2 r^2) 2r dr \\ &= A_2 \int_0^{+\infty} (1-(1-\exp(-A_1 x))^N) \exp(-A_2 x) dx. \end{aligned} \tag{B.4}$$

Applying the binomial theorem to:

$$(1-\exp(-A_1x))^N = \sum_{k=0}^{N} \binom{N}{k} (-1)^k (\exp(-A_1x))^k. \tag{B.5}$$

Substituting (B.5) into (B.4):

$$\begin{aligned} P_{s,\text{arq}}^{\text{best}}(\lambda_U) &= A_2 \int_0^{+\infty} \left(1 - \sum_{k=0}^{N} \binom{N}{k} (-1)^k (\exp(-A_1x))^k\right) \exp(-A_2x)dx \quad \text{(B.6)} \\ &= A_2 \int_0^{+\infty} \sum_{k=1}^{N} \binom{N}{k} (-1)^{k+1} \exp(-A_1kx) \exp(-A_2x)dx \\ &= A_2 \sum_{k=1}^{N} \binom{N}{k} (-1)^{k+1} \int_0^{+\infty} \exp(-(A_2+A_1k)x)dx \\ &= A_2 \sum_{k=1}^{N} \binom{N}{k} (-1)^{k+1} \frac{1}{A_2+A_1k} \\ &= \sum_{k=1}^{N} \binom{N}{k} (-1)^{k+1} \frac{1}{1+C_1k}, \end{aligned}$$

where

$$C_1 = \frac{A_1}{A_2} = \frac{\lambda_M}{S\lambda_U} \theta_{th}^{2/\alpha} \Gamma(1+2/\alpha)\Gamma(1-2/\alpha). \tag{B.7}$$

B.1.2 Average Number of Transmissions

From (4.30) we have:

$$\overline{T}_{\text{arq}}^{\text{best}}(\lambda_U) = \int_0^{+\infty} \frac{1-(1-P_s(r))^N}{P_s(r)} 2\pi\lambda_U e^{2\sigma^2/\alpha^2} \exp(-\lambda_U e^{2\sigma^2/\alpha^2} \pi r^2) r dr. \tag{B.8}$$

where $P_s(r) = \exp(-\pi\lambda_M e^{2\sigma^2/\alpha^2} r^2 \theta_{th}^{2/\alpha} \Gamma(1+\frac{2}{\alpha})\Gamma(1-\frac{2}{\alpha})/S)$.

Using A_1 and A_2, which are respectively defined in (B.2) and (B.3), in (B.8):

$$\overline{T}_{\text{arq}}^{\text{best}}(\lambda_U) = \int_0^{+\infty} \frac{1-(1-\exp(A_1r^2))^N}{\exp(A_1r^2)} A_2 \exp(-A_2r^2) 2r dr. \tag{B.9}$$

Using the binomial theorem and with substitution $r^2 = x$ into (B.9):

$$\begin{aligned}\overline{T}_{\text{arq}}^{\text{best}}(\lambda_U) &= A_2 \int_0^{+\infty} \frac{\sum_{k=1}^{N} \binom{N}{k}(-1)^{k+1}\exp(-A_1 kx)}{\exp(A_1 x)} \exp(-A_2 x)dx \qquad \text{(B.10)}\\ &= A_2 \sum_{k=1}^{N} \binom{N}{k}(-1)^{k+1} \int_0^{+\infty} \exp(-(A_2 + A_1(k-1))x)dx \\ &= \sum_{k=1}^{N} \binom{N}{k}(-1)^{k+1} \frac{1}{1+C_1(k-1)},\end{aligned}$$

where $C_1 = A_1/A_2$ is given by (B.7).

B.2 Performance of CC-HARQ when the Best UE is Selected as a Relay

B.2.1 Transmission Success Probability

From (4.32), we have:

$$P_{s,\text{harq}}^{\text{best}}(\lambda_U) = \int_0^{+\infty} \left(\frac{\Gamma(N, U_N(r))}{(N-1)!}\right) 2\pi\lambda_U e^{2\sigma^2/\alpha^2} \exp(-\lambda_U e^{2\sigma^2/\alpha^2}\pi r^2) r dr, \qquad \text{(B.11)}$$

where $U_N(r) = \pi\lambda_M e^{2\sigma^2/\alpha^2} r^2 \Gamma(1+2/\alpha)\Gamma(1-2/\alpha)/S\left(\frac{\Gamma(N+\alpha/2)\theta_{th}}{N!\Gamma(1+\alpha/2)}\right)^{2/\alpha}$.

Since N is an integer, the upper incomplete gamma function is given by [108]:

$$\Gamma(N, U_N(r)) = (N-1)!\exp(-U_N(r)) \sum_{k=0}^{N-1} \frac{(U_N(r))^k}{k!}. \qquad \text{(B.12)}$$

By substituting (B.12) into (B.11) and simplifying, we have:

$$P_{s,\text{harq}}^{\text{best}}(\lambda_U) = \int_0^{+\infty} \exp(-U_N(r)) \sum_{k=0}^{N-1} \frac{(U_N(r))^k}{k!} \pi\lambda_U e^{2\sigma^2/\alpha^2} \exp(-\lambda_U e^{2\sigma^2/\alpha^2}\pi r^2) 2r dr, \qquad \text{(B.13)}$$

In order to simplify the analysis, let

$$A_3 = \pi\lambda_M e^{2\sigma^2/\alpha^2}\Gamma(1+2/\alpha)\Gamma(1-2/\alpha)/S\left(\frac{\Gamma(N+\alpha/2)\theta_{th}}{N!\Gamma(1+\alpha/2)}\right)^{2/\alpha} \qquad \text{(B.14)}$$

and

$$A_4 = \pi\lambda_U e^{2\sigma^2/\alpha^2}. \qquad \text{(B.15)}$$

By substituting $U_N(r) = A_3 r^2$ and $\pi\lambda_U e^{2\sigma^2/\alpha^2} = A_4$ into (B.13), and then with substitution $r^2 = x$:

$$\begin{aligned} P_{s,\text{harq}}^{\text{best}}(\lambda_U) &= \int_0^{+\infty} \exp(-A_3 x) \sum_{k=0}^{N-1} \frac{(A_3 x)^k}{k!} A_4 \exp(-A_4 x) dx \\ &= A_4 \sum_{k=0}^{N-1} \frac{(A_3)^k}{k!} \int_0^{+\infty} x^k \exp(-(A_3+A_4)x) dx \end{aligned} \tag{B.16}$$

Integral in (B.16) can be written as follows [109]:

$$\int_0^{+\infty} x^k \exp(-(A_3+A_4)x) dx = \frac{\Gamma(k+1)}{(A_3+A_4)^{k+1}}. \tag{B.17}$$

Substituting (B.17) into (B.16), we have:

$$\begin{aligned} P_{s,\text{harq}}^{\text{best}}(\lambda_U) &= A_4 \sum_{k=0}^{N-1} \frac{(A_3)^k \Gamma(k+1)}{k!(A_3+A_4)^{k+1}} \\ &= A_4 \sum_{k=0}^{N-1} \frac{(A_3)^k}{(A_3+A_4)^{k+1}} \\ &= \frac{A_4}{A_3} \sum_{k=0}^{N-1} \frac{1}{(1+A_4/A_3)^{k+1}} \\ &= C_2 \sum_{k=1}^{N} \frac{1}{(1+C_2)^k} \\ &= 1 - \frac{1}{(1+C_2)^N}, \end{aligned} \tag{B.18}$$

where

$$C_2 = \frac{A_4}{A_3} = \frac{S\lambda_U (N!\Gamma(1+\alpha/2))^{2/\alpha}}{\lambda_M \Gamma(1+2/\alpha)\Gamma(1-2/\alpha)(\Gamma(N+\alpha/2)\theta_{th})^{2/\alpha}}. \tag{B.19}$$

B.2.2 Average Number of Transmissions

From (4.35), we have:

$$\overline{T}_{\text{harq}}^{\text{best}}(\lambda_U) = \int_0^{+\infty} \left(N - \sum_{n=1}^{N-1} \frac{\Gamma(n, U_n(r))}{(n-1)!} \right) 2\pi\lambda_U e^{2\sigma^2/\alpha^2} \exp(-\lambda_U e^{2\sigma^2/\alpha^2} \pi r^2) r dr. \tag{B.20}$$

where $U_n(r) = \pi\lambda_M e^{2\sigma^2/\alpha^2} r^2 \Gamma(1+2/\alpha)\Gamma(1-2/\alpha)/S \left(\frac{\Gamma(n+\alpha/2)\theta_{th}}{n!\Gamma(1+\alpha/2)} \right)^{2/\alpha}$.

The upper incomplete gamma can be replaced by using the formula (B.12). Then, by substituting $\pi\lambda_U e^{2\sigma^2/\alpha^2} = A_4$ in (B.20), we have:

$$\overline{T}_{\text{harq}}^{\text{best}}(\lambda_U) = \int_0^{+\infty} \left(N - \sum_{n=1}^{N-1} \exp(-U_n(r)) \sum_{k=0}^{n-1} \frac{(U_n(r))^k}{k!} \right) A_4 \exp(-A_4 r^2) 2rdr. \quad \text{(B.21)}$$

Let

$$A_5 = \pi\lambda_M e^{2\sigma^2/\alpha^2} \Gamma(1+2/\alpha)\Gamma(1-2/\alpha)/S \left(\frac{\Gamma(n+\alpha/2)\theta_{th}}{n!\Gamma(1+\alpha/2)} \right)^{2/\alpha}. \quad \text{(B.22)}$$

Substituting $U_n(r) = A_5 r^2$ in (B.21), we have:

$$\overline{T}_{\text{harq}}^{\text{best}}(\lambda_U) = \int_0^{+\infty} \left(N - \sum_{n=1}^{N-1} \exp(-A_5 r^2) \sum_{k=0}^{n-1} \frac{(A_5 r^2)^k}{k!} \right) A_4 \exp(-A_4 r^2) 2rdr \quad \text{(B.23)}$$

With substitution $r^2 = x$:

$$\begin{aligned} \overline{T}_{\text{harq}}^{\text{best}}(\lambda_U) &= \int_0^{+\infty} \left(N - \sum_{n=1}^{N-1} \exp(-A_5 x) \sum_{k=0}^{n-1} \frac{(A_5 x)^k}{k!} \right) A_4 \exp(-A_4 x) dx \quad \text{(B.24)} \\ &= N - \int_0^{+\infty} \sum_{n=1}^{N-1} \exp(-A_5 x) \sum_{k=0}^{n-1} \frac{(A_5 x)^k}{k!} A_4 \exp(-A_4 x) dx \\ &= N - \sum_{n=1}^{N-1} \left[A_4 \sum_{k=0}^{n-1} \frac{A_5^k}{k!} \int_0^{+\infty} x^k \exp(-(A_4 + A_5)x) dx \right]. \end{aligned}$$

The expression inside the brackets is similar to (B.16), using similar justification, we can rewrite (B.24) as follows:

$$\begin{aligned} \overline{T}_{\text{harq}}^{\text{best}}(\lambda_U) &= N - \sum_{n=1}^{N-1} \left[1 - \frac{1}{(1+C_3(n))^n} \right] \quad \text{(B.25)} \\ &= 1 + \sum_{n=1}^{N-1} \frac{1}{(1+C_3(n))^n}, \end{aligned}$$

where

$$C_3(n) = \frac{A_4}{A_5} = \frac{S\lambda_U (n!\Gamma(1+\alpha/2))^{2/\alpha}}{\lambda_M \Gamma(1+2/\alpha)\Gamma(1-2/\alpha)(\Gamma(n+\alpha/2)\theta_{th})^{2/\alpha}}. \quad \text{(B.26)}$$

Appendix C

LTE-M Link-Level Simulations

In order to evaluate the performance of LTE-M technology in terms of energy consumption, in this appendix, we present some of the results obtained during an internship conducted by a master's student and advised by me. These results were obtained through simulations carried out thanks to the LTE Toolbox of MATLAB.

The worst coverage scenario proposed by 3GPP is analyzed, i.e., 164 MCL. The first objective is to determine the number of repetitions necessary to achieve a BLER less than 10%. Then using this number of repetitions obtained, the data rate is calculated and finally the energy consumption for a 200-byte data packet. Taking into account these objectives, three physical channels are studied: PUSCH, PDSCH and PRACH.

The physical layer data rate c in bps is given by:

$$c = \frac{1000 L_{TBS}(1-\beta)}{N_{rep}}, \tag{C.1}$$

where L_{TBS} is the transport block size, β is the BLER, and N_{rep} is the number of repetitions. This data rate does not include MAC/RLC/PDCP/IP header overhead or scheduling delays.

The energy consumption is $E = P_c t$, where P_c is the power consumption for a given operation state (Tx or Rx) and t is the time that the device remains in the same state which can be calculated as follows:

$$t = \max\left\{\frac{N_{rep}}{1000}, \frac{L_{msg}}{c}\right\}, \tag{C.2}$$

where L_{msg} is the size of the message in bits.

C.1 PUSCH

It is assumed that only one device is transmitting ans thus there is no interference. The simulation parameters are given in Table C.1.

Table C.1 LTE-M PUSCH simulation parameters

Parameter	Value
Number of TB transmissions	100
SNR	-25,56 dB
TB size	328 bits
Number of PRB	2
Repetitions	32, 64, 128, 192, 256, 384, 512, 768
Nacc	4
HARQ Retransmissions	4
System Bandwidth	10 MHz
Transmission mode	Transmit Diversity
Duplexing mode	FDD
Cyclic Prefix	Normal
UE Antennas	1
eNB Antenna	2
Hopping Group	16
CE Mode	B
Modulation	QPSK
RV Sequence	[0 2 3 1]
Channel	ETU 1Hz Low Correlation
Channel Estimation	Perfect

Fig. C.1 shows the BLER as a function of the number of repetitions for PUSCH at 164 dB MCL and using a transport block size of 328 bits. We can see that the BLER target of 10% is achieved using at least 512 repetitions, in this case the BLER is 5%. By using (C.1) we find a data rate of 608 bps.

C.2 PDSCH

The simulation parameters are given in Table C.2.

Table C.2 LTE-M PDSCH simulation parameters

Parameter	**Value**
Number of TB transmissions	100
SNR	-18.54 dB
TB size	936 bits
Number of PRB	6
Repetitions	32, 64, 128, 192, 256, 384, 512, 768
Nacc	4
HARQ Retransmissions	4
System Bandwidth	10 MHz
Transmission mode	Transmit Diversity
Duplexing mode	FDD
Cyclic Prefix	Normal
UE Antennas	1
eNB Antenna	2
Hopping Group	16
CE Mode	B
Modulation	QPSK
RV Sequence	[0 2 3 1]
Channel	ETU 1Hz Low Correlation
Channel Estimation	Perfect

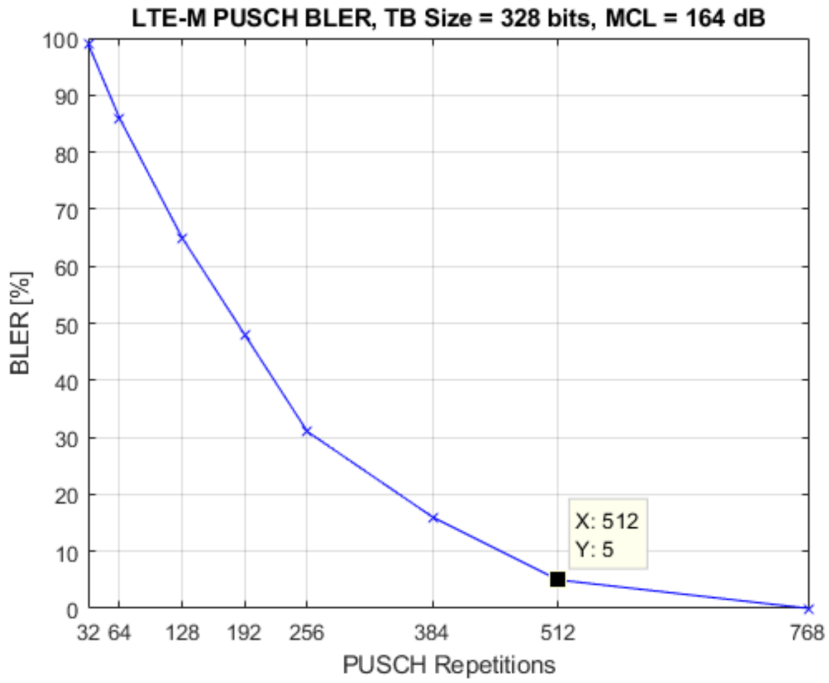

Fig. C.1 BLER versus number of repetitions for LTE-M PUSCH at 164 dB MCL.

Fig. C.2 presents the BLER versus the number of repetitions for PDSCH at 164 dB MCL and a transport block size of 936 bits. In order to achieve the BLER target, the MTD have to use 256 repetitions, in this case the BLER is 8%. Thus the data rate is 3364 bps.

C.3 PRACH

This simulation is used to determine the number of repetitions required to ensure that the PRACH preamble is detected with a 99% probability of success. In this simulation, PRACH format 0 is considered, which has a total duration of 1ms. The parameters used in this simulation are summarized in Table C.3.

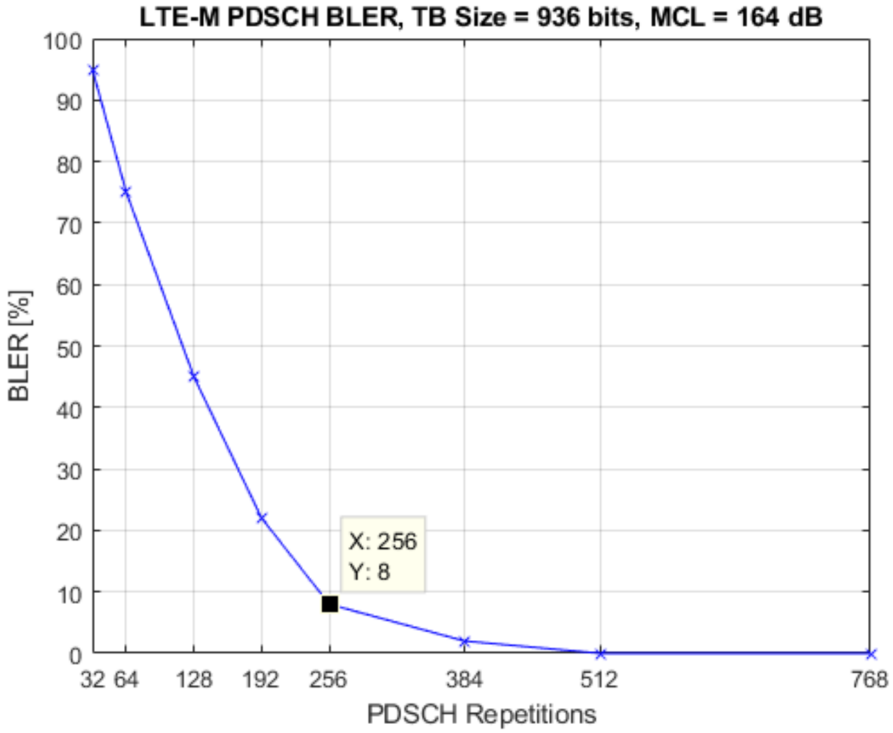

Fig. C.2 BLER versus number of repetitions for LTE-M PDSCH at 164 dB MCL.

Table C.3 LTE-M PRACH simulation parameters

Parameter	**Value**
Number of PRACH attempts	300
SNR	-30.34 dB
Number of PRB	6
Repetitions	8, 16, 32, 64, 128
Duplexing mode	FDD
Frequency Offset	270 Hz
PRACH Format	0
Logical Sequence Index	22
Preamble Index	32
PRACH Configuration	14
UE Antennas	1
eNB Antenna	2
CE Mode	B
Channel	ETU 1Hz Low Correlation

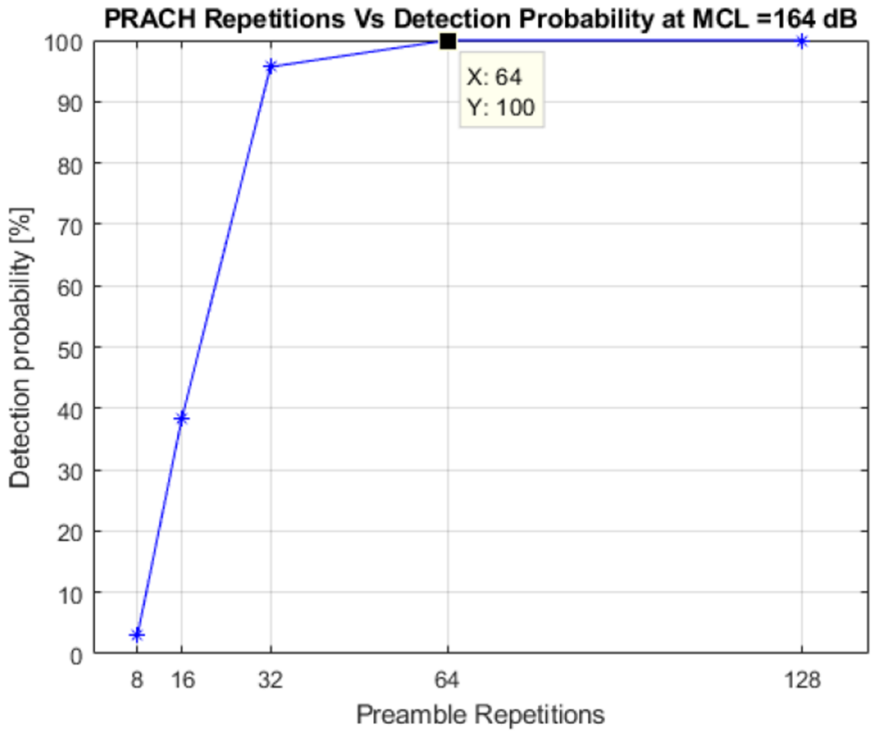

Fig. C.3 LTE-M PRACH repetitions versus detection probability.

Appendix D

Résumé en français

D.1 Contexte de la thèse

Les communications massives pour l'internet des objets, connues sous l'acronyme mMTC (massive machine-type communications), sont l'un des principaux services fournis par le réseau mobile de cinquième génération (5G). L'internet des objets (IoT) représente un défi majeur pour les réseaux cellulaires car il se caractérise par un grand nombre d'objets connectés de faible complexité qui envoient de manière sporadique de petits paquets de données. Ces objets connectés, que nous appellerons MTDs (Machine-type devices), sont souvent alimentés par une batterie. Cette batterie doit fonctionner pendant de longues périodes sans avoir besoin d'être rechargée ou remplacée car ces objets se trouvent souvent dans des endroits difficiles d'accès ou hors couverture, où il n'y a pas de source d'énergie continue. Parmi les cas d'usage des applications mMTC on peut citer la surveillance de l'environnement ou encore les compteurs intelligents. Pour faire face à ce nouveau type d'applications, l'organisation de normalisation 3GPP (3rd Generation Partnership Project) propose trois nouvelles technologies cellulaires : LTE-M (Long-Term Evolution for Machine-Type Communications), NB-IoT (Narrowband Internet of Things), EC-GSM-IoT (Extended Coverage-GSM-IoT). Ces nouvelles technologies, comme les réseaux cellulaires traditionnels, permettent la connexion d'un objet avec le réseau, en passant par la station de base, c'est à dire que l'objet va établir un lien direct avec la station de base. Ces technologies permettent l'extension de la couverture cellulaire grâce à la technique de répétition. Cependant, l'utilisation de cette technique conduit à une forte consommation d'énergie et de ressources radio. Pour résoudre ce problème, nous étudions dans cette thèse l'utilisation d'un équipement utilisateur (UE) comme relais pour transmettre les données de l'objet connecté à proximité. Ce mécanisme est appelé relayage D2D (Device-to-Device). L'objectif principal est de proposer des solutions techniques pour l'intégration des mécanismes de relayage D2D dans les applications

mMTC. Un second objectif est de déterminer dans quels cas il est plus avantageux, en termes de consommation d'énergie, d'utiliser les mécanismes de relayage D2D au lieu d'une communication cellulaire classique.

D.2 Contributions

Les principales contributions de cette thèse sont les suivantes :

- Par des simulations, nous calculons la consommation d'énergie à chaque phase du processus de communication pour un MTD à 164 dB de MCL (Maximum Coupling Loss) qui utilise la technologie LTE-M. Dans cette analyse, nous considérons les paramètres proposés par le 3GPP ainsi que le mécanisme de répétition.
- À l'aide d'un modèle simple, nous comparons la consommation d'énergie d'un MTD pour une communication cellulaire directe et la consommation d'énergie globale (c'est-à-dire l'énergie consommée à la fois par le MTD et le relais) pour une communication qui utilise un relais. Sur la base de cette analyse, nous déterminons l'emplacement optimal du relais pour minimiser la consommation d'énergie globale.
- Dans un scénario où les MTD sélectionnent de manière autonome les ressources radio à utiliser pour la communication D2D, nous analysons les performances d'une communication D2D utilisant les mécanismes de répétitions ARQ (Automatic Repeat reQuest) et CC-HARQ (Hybrid ARQ with Chase Combining) en termes de probabilité de réussite de la transmission, de nombre moyen de transmissions et de consommation d'énergie.
- En supposant que le MTD sélectionne le meilleur UE comme relais pendant la phase de découverte, nous analysons les performances des mécanismes ARQ et CC-HARQ. Ensuite, nous comparons les performances des deux schémas de retransmission en termes de consommation d'énergie pour différents niveaux de MCS (Modulation and Coding Scheme) et en considérant une probabilité de perte cible de 10%.
- Nous proposons un mécanisme de relayage D2D adapté aux applications IoT grâce à sa mise en œuvre facile et l'énergie qu'il pourrait permettre d'économiser. Ce mécanisme utilise une approche de sélection de relais distribuée (c'est-à-dire sans la participation de la station de base), qui priorise la sélection des relais bénéficiant des meilleures qualités de canal.

- Nous présentons un modèle mathématique pour évaluer les performances de notre mécanisme de relayage D2D. Nous dérivons des formules afin de calculer la probabilité de découverte de relais, le nombre moyen de time-slots utilisés dans le processus de contention, la fonction de densité de probabilité de la distance MTD-relais et la consommation totale d'énergie du MTD. Ces formules sont utiles pour déterminer les valeurs optimales des paramètres clés de notre protocole de sélection de relais.

D.3 Comparaison de la consommation d'énergie des modes cellulaire et D2D

Notre première étude a consisté à évaluer l'énergie consommée par l'objet connecté dans chaque phase du processus de communication lorsqu'il est localisé en bordure de cellule pour la technologie LTE-M. Ensuite, à l'aide d'un modèle simple, nous avons comparé la consommation d'énergie des modes de transmission cellulaire et D2D (voir Fig. D.1), et déterminé la localisation optimale du relais. La consommation d'énergie en mode D2D prend en compte à la fois la consommation d'énergie du MTD et la consommation d'énergie de l'UE.

D'après les résultats obtenus, le comportement de la consommation totale d'énergie en mode D2D dépend de l'emplacement du MTD. Lorsque le MTD est proche de la station de base, il s'agit d'une courbe concave tandis que lorsqu'il est loin de la station de base cela devient une courbe convexe. La consommation d'énergie est la plus faible lorsque le relais est situé à mi-chemin entre le MTD et la station de base.

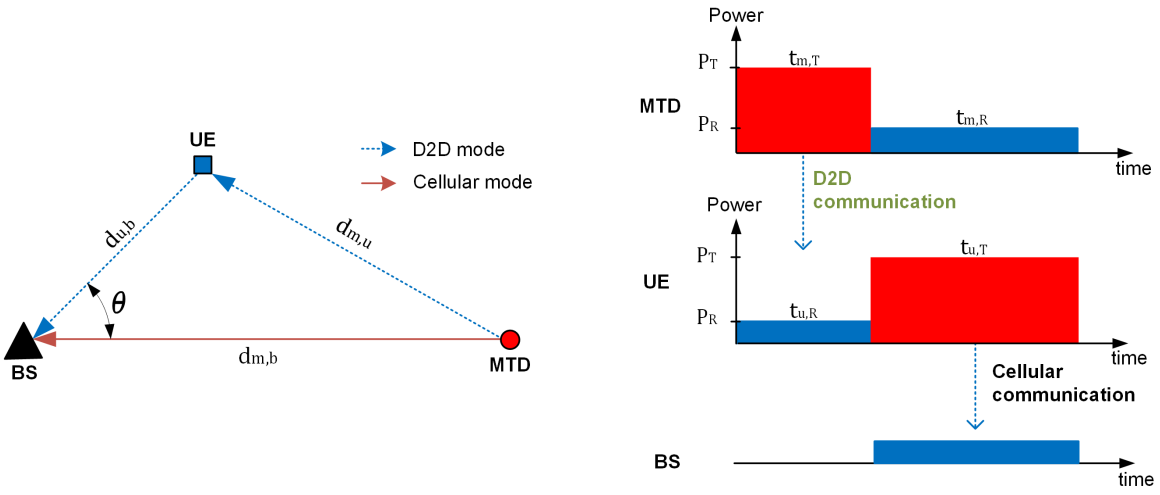

Fig. D.1 Processus de relayage D2D.

D.4 Évaluation des performances d'une communication D2D avec CC-HARQ

Dans une communication D2D, l'allocation des ressources peut être faite par le réseau via la station de base, mais l'allocation peut aussi se faire de manière autonome. Dans ce dernier cas, chaque MTD sélectionne de manière aléatoire une ressource radio d'un pool de ressources qui peut être indiqué à l'avance par la station de base. Ce mode d'allocation est avantageux pour les applications mMTC car il permet la réutilisation des ressources et réduit considérablement le nombre de messages de signalisation entre le MTD et la station de base. Cependant, un des problèmes de ce type d'allocation sont les interférences entre les dispositifs qui peuvent se produire quand deux ou plusieurs dispositifs sélectionnent la même ressource radio (voir Fig. D.2). Ces interférences peuvent entraîner une augmentation de la probabilité de perte des paquets.

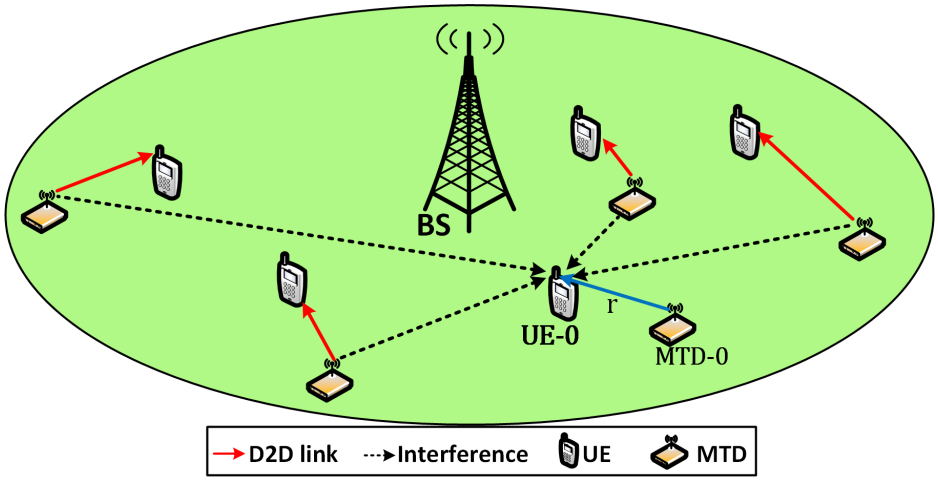

Fig. D.2 Modèle de réseau avec allocation autonome des ressources.

Dans cette étude, nous nous concentrons sur l'exploitation des schémas de retransmission ARQ et CC-HARQ pour réduire l'impact des interférences dans les communications D2D pour le scénario d'allocation de ressources autonome. L'utilisation des schémas de retransmission permet d'améliorer la fiabilité de la transmission en exploitant la diversité temporelle du canal. Nous analysons deux indicateurs de performance : la probabilité de succès, laquelle est définie comme la probabilité que le MTD puisse transmettre avec succès ses données au relais. L'autre indicateur de performance analysé est la consommation d'énergie du MTD.

Dans un premier temps, nous analysons la performance en fonction de la distance entre le MTD et l'UE. Puis, nous calculons la consommation d'énergie du MTD, en considérant que le MTD a sélectionné le meilleur relais durant la phase de découverte. Nous définissons

le meilleur relais comme l'UE qui a le plus faible affaiblissement de propagation, dans la liaison MTD-UE. Finalement, nous établissons un taux de perte de 10% et nous calculons la consommation d'énergie du MTD. Il faut mentionner que l'évaluation des performances est réalisée au moyen d'un modèle analytique basé sur la géométrie stochastique, lequel a été validé par des simulations.

D'après les résultats obtenus, nous constatons que, quel que soit le mécanisme de retransmission, plus il y a un nombre élevé de ressources radio, moins on a de retransmissions. Cela est dû au fait que dans le mode autonome, chaque MTD sélectionne de manière aléatoire une ressource et moins on aura de ressources disponibles, plus l'interférence entre les liaisons D2D sera élevée. En ce qui concerne la comparaison des deux mécanismes, on voit que, dans tous les cas, le mécanisme CC-HARQ est plus performant que le mécanisme ARQ. Cependant, nous notons que cette différence de performance augmente significativement quand la densité des UEs diminue, ou quand il y a un faible nombre de ressources radio.

Un autre résultat de cette étude est la comparaison des mécanismes ARQ et CC-HARQ en termes de consommation d'énergie du MTD. Dans le cadre de cette analyse, nous commençons par déterminer, pour chaque valeur de densité des UEs, le nombre maximum de transmissions nécessaires pour garantir une probabilité de perte de 10%. Ensuite, pour chaque valeur de densité des UEs, nous calculons le nombre moyen de transmissions et la consommation d'énergie du MTD. Les résultats montrent que le mécanisme CC-HARQ consomme moins d'énergie que le mécanisme ARQ. Cette différence de consommation d'énergie est plus importante lorsque le niveau de MCS est élevé. Par exemple, pour le MCS-3 et pour une densité de UEs de $30 \times 10^{-4}\text{UEs}/\text{m}^2$, le mécanisme ARQ consomme deux fois plus d'énergie que le mécanisme CC-HARQ. Dans cette étude, nous avons supposé que le meilleur relais avait été sélectionné lors de la phase de découverte.

D.5 Mécanisme de relayage D2D adapté aux applications IoT

La phase de découverte est cruciale car elle doit assurer la sélection du relais optimal. La sélection optimale du relais dépend de divers paramètres dont la consommation d'énergie, le débit, etc. Cependant, pour les applications mMTC, la consommation d'énergie est largement considérée comme l'un des paramètres les plus critiques et par conséquent, le meilleur relais doit être celui qui minimise la consommation totale d'énergie du MTD. Il est bien établi que plus la qualité du canal MTD-relais sera élevée, plus la consommation d'énergie sera faible dans la phase de transmission de données. Néanmoins, trouver l'UE avec la meilleure qualité

de canal peut impliquer une augmentation de la consommation d'énergie pendant la phase de découverte. Contrairement aux applications eMBB où la consommation d'énergie de la phase de découverte est négligeable par rapport à la consommation lors de la phase de transmission de données, dans les applications mMTC, la consommation d'énergie lors de la phase de découverte est comparable ou peut même être supérieure à la consommation d'énergie lors de la phase transmission de données. Cette étude a donc pour objet la proposition d'un mécanisme de relayage D2D économe en énergie et adapté aux applications IoT en termes de complexité d'implémentation et de consommation d'énergie. L'analyse de la consommation d'énergie se rapporte aussi bien à la phase de découverte qu'à la phase de transmission des données. Au cours de cette étude, nous analysons deux indicateurs de performance : la probabilité de découverte du relais et la consommation d'énergie du MTD. La probabilité de découverte est définie comme la probabilité que le MTD sélectionne un UE proche comme relais.

Notre mécanisme utilise une approche de sélection de relais distribuée, qui priorise la sélection des relais bénéficiant des meilleures qualités de canal. Si nous partons de l'hypothèse selon laquelle, plus le relais est proche du MTD, plus l'économie d'énergie est importante pendant la phase de transmission des données, alors le meilleur relais serait l'UE qui se trouve le plus proche du MTD. Cependant, la recherche de l'UE le plus proche pourrait impliquer une augmentation de la consommation d'énergie pendant la phase de découverte. Notre mécanisme ne cherche pas à sélectionner l'UE le plus proche du MTD, mais essaye de faire en sorte que les UEs les plus proches du MTD aient une probabilité élevée d'être choisis comme relais. De cette manière, la consommation d'énergie au moment de la phase de découverte est minime et le choix d'un UE proche du MTD est garanti.

Fig. D.3 montre notre protocole de relayage, lorsque le MTD a des données à transmettre, il envoie tout d'abord un message RR (request-for-relay). Dans ce message, le MTD envoie son identifiant, la taille de la fenêtre de contention W et le seuil du pathloss UE-MTD. Une fois que les UEs ont reçu le message RR, ils sélectionnent de manière aléatoire un time-slot entre 1 et W pour répondre au MTD avec un message RC (Relay Candidate). Le premier UE qui réussit à transmettre sans collision est choisi comme relais. Par conséquent, l'objectif doit être d'augmenter la probabilité de transmission des UE les plus proches du MTD pendant les premiers time-slots.

L'idée centrale de notre mécanisme réside dans la loi de sélection du time-slot. La Fig. D.4 montre un exemple de sélection du time slot proposé dans notre mécanisme. Lorsqu'un UE reçoit un message de requête envoyé par le MTD, il sélectionne de manière aléatoire un time-slot. La sélection de ce time-slot est basée sur une loi géométrique tronquée, laquelle a entre autre comme paramètre, la distance entre le MTD et l'UE. Sur le schéma, nous pouvons

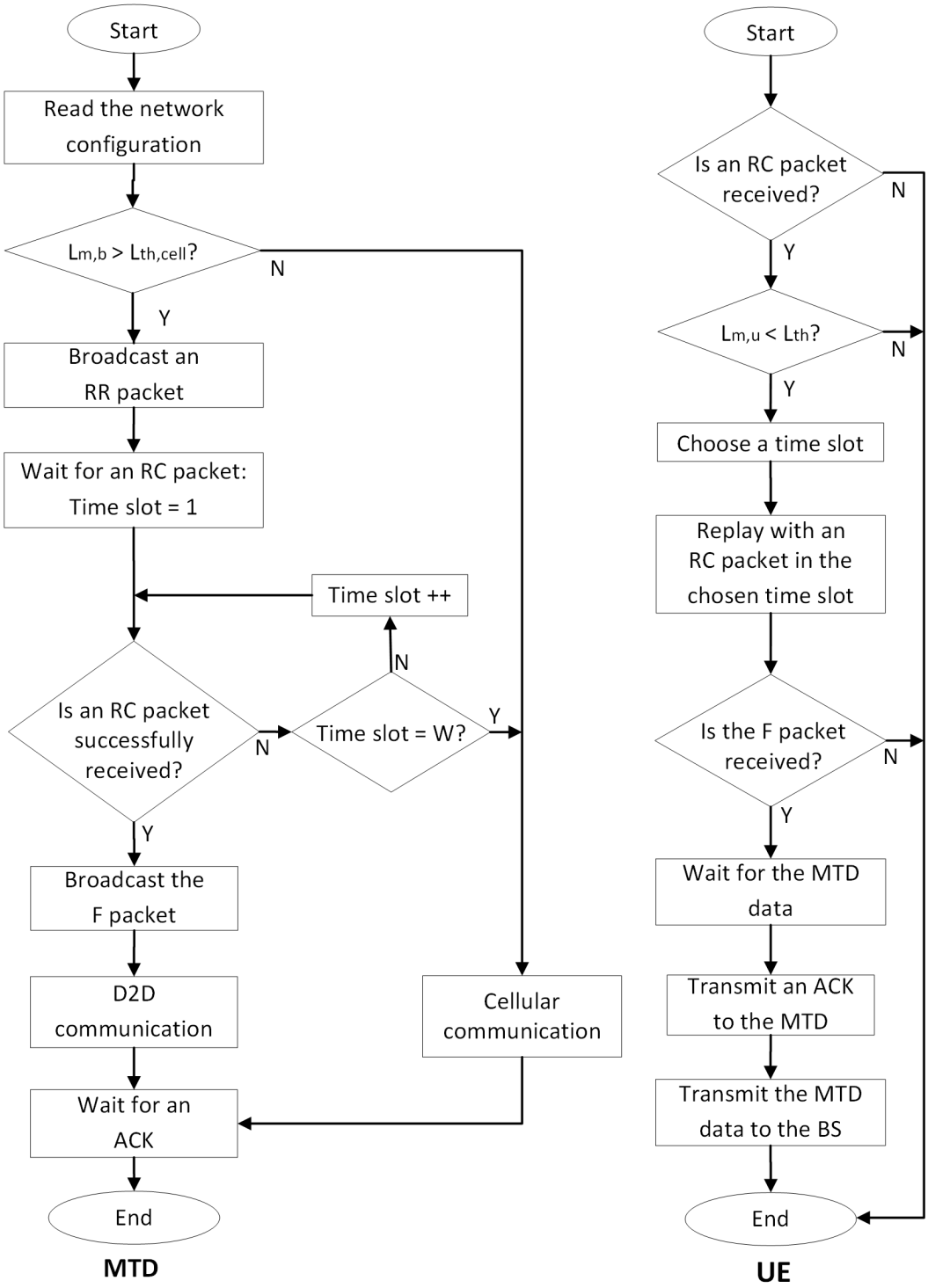

Fig. D.3 Proposition d'un protocole de relayage D2D.

voir, pour chaque UE, la fonction de masse du time-slot sélectionné. L'UE-1 qui est l'UE le plus proche du MTD, a une probabilité élevée de transmettre lors des premiers time-slots, alors que l'UE-4 qui se trouve plus éloigné du MTD a une faible probabilité de transmettre lors des premiers time-slots.

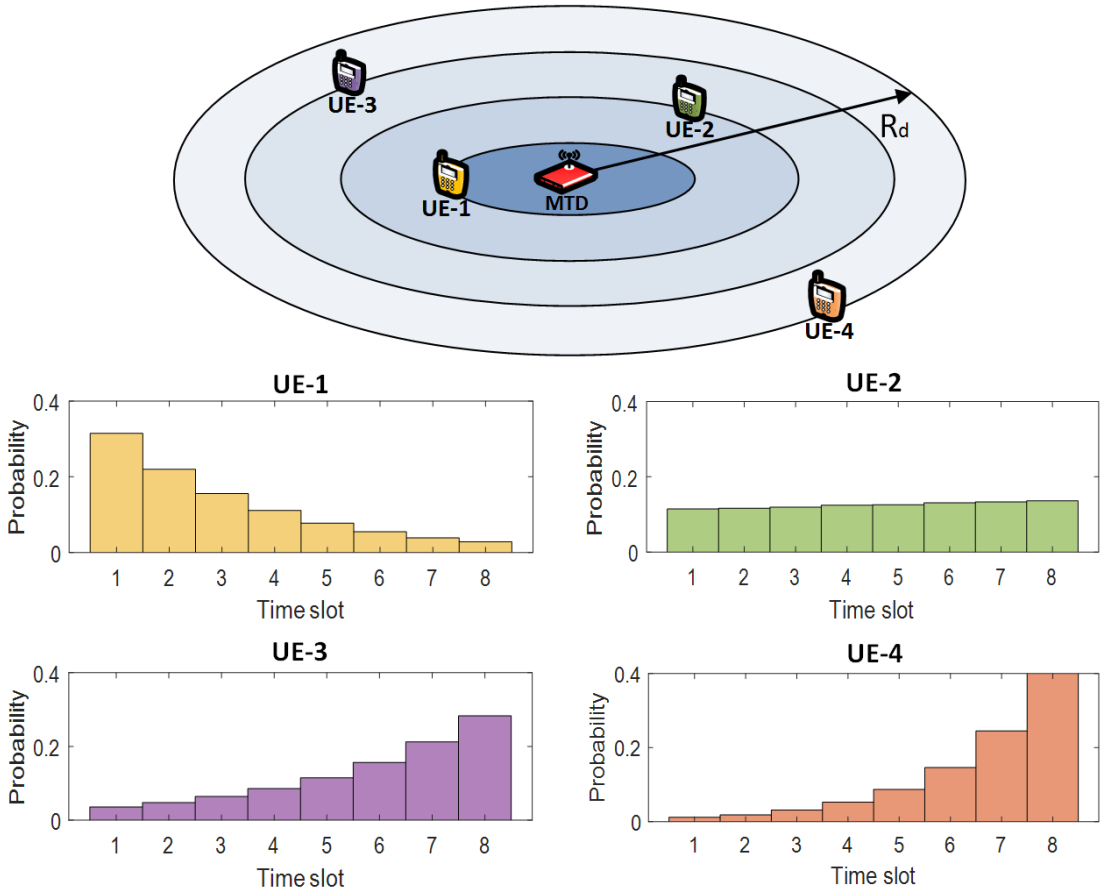

Fig. D.4 PMF du choix du time-slot dans un réseau avec quatre UEs.

D'après les résultats obtenus, nous constatons qu'il est préférable d'utiliser notre mécanisme lorsque le MTD est éloigné de la station de base, sauf quand la densité des UEs est très faible (voir Fig. D.5). Par exemple, quand la distance entre le MTD et la station de base est de 1000 mètres et que la densité des UEs est égale à $1,4 \times 10^{-4}$UEs/m^2, notre mécanisme consomme un quart de l'énergie consommée lors d'une communication cellulaire classique. Nous pouvons aussi remarquer que, ou que soit situé le MTD par rapport à la station de base, la consommation d'énergie varie peu. Une autre remarque qui est encore plus intéressante, est relative au constat suivant : pour une large gamme de densités, la consommation d'énergie varie peu. Ce dernier point est très important car, dans la littérature, la densité des UEs est considérée comme un paramètre connu ou qui peut être estimé statistiquement. Cependant,

dans un scénario réaliste, il est difficile de déterminer la densité exacte des UEs en raison de la mobilité des usagers. Notre mécanisme offre une consommation d'énergie quasi constante pour des densités supérieures à $0,1 \times 10^{-4}\text{UEs}/\text{m}^2$.

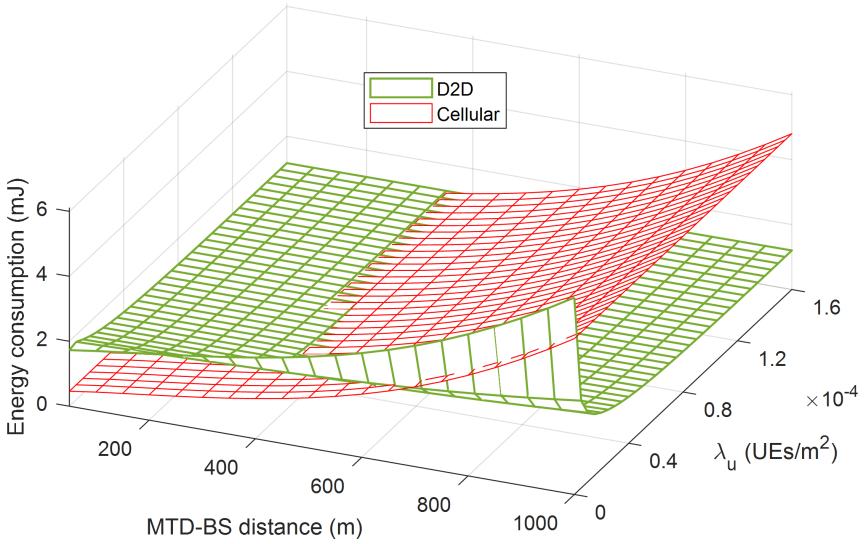

Fig. D.5 Comparaison de la consomation d'énergie entre les modes D2D et cellulaire.

DOCTORAT BRETAGNE LOIRE / MATHSTIC

IMT Atlantique
Bretagne-Pays de la Loire
École Mines-Télécom

Titre : Etude du relayage entre terminaux pour la connectivité des objets dans les réseaux 5G

Mots clés : D2D, relayage, mMTC, HARQ, géométrie stochastique, efficacité énergétique

Résumé : Les communications massives pour l'Internet des objets (IoT) sont l'un des principaux services fournis par le réseau 5G. L'IoT représente un défi majeur pour les réseaux cellulaires car il se caractérise par un grand nombre d'objets connectés de faible complexité qui envoient de petits paquets de données. Ces objets connectés sont souvent alimentés par une batterie, cette batterie devant fonctionner pendant de longues périodes. Les réseaux cellulaires traditionnels, conçus pour les communications humaines, et pas assez économes en énergie, ne sont pas adaptés à ce type de service. Pour résoudre ce problème, dans cette thèse, nous étudions l'utilisation d'un équipement utilisateur de type smartphone comme relais pour transmettre les données de l'objet connecté à proximité. Ce mécanisme est appelé relayage D2D (Device-to-Device).

Notre première étude a consisté à évaluer l'énergie consommée par l'objet connecté lorsqu'il est localisé en bordure de cellule pour la technologie LTE-M. Ensuite, nous avons comparé la consommation d'énergie des modes de transmission cellulaire et D2D, et déterminé la localisation optimale du relais. Grâce à l'utilisation de la géométrie stochastique, nous avons ensuite analysé les performances d'une communication D2D utilisant les mécanismes de répétitions ARQ et CC-HARQ en termes de consommation d'énergie. Enfin, nous avons proposé un mécanisme de relayage D2D adapté aux applications IoT, en termes de complexité d'implémentation et de consommation d'énergie. Ce mécanisme utilise une approche de sélection de relais distribuée, qui priorise la sélection des relais bénéficiant des meilleures qualités de canal.

Title: Opportunity and challenges of Device-to-Device relaying for IoT connectivity in cellular networks

Keywords: D2D, relaying, mMTC, HARQ, stochastic geometry, energy efficiency

Abstract: Massive machine-type communication (mMTC) is one of the main services delivered by the 5G mobile network. mMTC represents a major challenge for 5G network since it is characterized by a large number of low complexity devices that send small data packets. Moreover, mMTC devices are often battery-powered, and the battery is expected to operate for long periods without being recharged or replaced. Traditional cellular networks, which are designed for human communications, are not energy efficient for this type of service. To address this problem, in this thesis, we study the use of Device-to-Device (D2D) relaying as a complementary transmission. In this approach, the mMTC device can transmit its data using a nearby UE as a relay.
First, we calculate the energy consumed in each phase of the communication process for a device located at the cell border that uses LTE-M technology. Then, using a simple model, we compare the energy consumption of cellular and D2D transmission modes, and we determine the optimal relay location. Through the use of stochastic geometry, we analyze the performance of D2D communication with ARQ and CC-HARQ with regard to the transmission success probability, the average number of transmissions, and MTD energy consumption. Finally, we propose an energy-efficient D2D relaying mechanism suitable for mMTC applications thanks to its easy implementation. This mechanism uses a distributed relay selection approach, which prioritizes the selection of the user equipments (UEs) with the best channel qualities. Moreover, we present a tractable model to evaluate the performance of our mechanism.